IDENTIFICATION, STABILITY AND REACTIVITY OF NO_X ADSORBED SPECIES ON TITANIA-SUPPORTED MANGANESE CATALYSTS

A THESIS

SUBMITTED TO THE DEPARTMENT OF CHEMISTRY

AND THE INSTITUTE OF ENGINEERING AND SCIENCES

OF BILKENT UNIVERSITY

IN PARTIAL FULFILLMENT OF THE REQUIREMENTS

FOR THE DEGREE OF MASTER SCIENCE

By

MUSTAFA U. KÜÇÜKKAL

January 2001

I certify that I have read this thesis and that in my opinion it is fully adequate, in scope and in quality, as a thesis of the degree of Master of Science

_____

Dr. Margarita Kantcheva (Supervisor)

I certify that I have read this thesis and that in my opinion it is fully adequate, in scope and in quality, as a thesis of the degree of Master of Science

_____

Dr. Ömer Dağ

I certify that I have read this thesis and that in my opinion it is fully adequate, in scope and in quality, as a thesis of the degree of Master of Science

_____

Prof. Dr. Atilla Aydınlı

Approved for the Institute of Engineering and Sciences

_____

Prof. Dr. Mehmet Baray

Director of Institute of Engineering and Sciences

ABSTRACT

IDENTIFICATION, STABILITY AND REACTIVITY OF NO_x ADSORBED SPECIES ON TITANIA-SUPPORTED MANGANESE CATALYSTS

MUSTAFA U. KÜÇÜKKAL

M.S in Chemistry

Supervisor: Dr. Margarita Kantcheva

January 2001,

The needs of improved fuel economy, and lower emission of green-house gases such as CO_2, is projected to increase the demand for diesel engines through the world. These engines operate at air/fuel ratio higher than stoichiometric (lean-burn conditions). This results in relatively low hydrocarbon/NO_x ratio in the exhaust and an additional amount of reductant (typically about 2-3% of additional fuel) should be fed upstream of de-NOx catalyst. For this reason, it is important to study the interaction of NO_x species produced upon adsorption of NO/O_2 mixtures on the catalyst surface with long chain saturate hydrocarbons, which are typical for diesel fuel.

In recent years many de-NOx lean-burn catalysts have been proposed among which supported metal oxides have been taken in consideration for their potential thermal stability and large composition variability.

Subjects of this study are titania (anatase)-supported manganese catalysts, prepared by impregnation and ion-exchange from aqueous solutions of Mn^{2+} ions. TiO_2 (anatase) is stable in SO_2 containing atmosphere, typical for the exhaust gases in diesel engines.

The identification of the NO_x species formed during the adsorption of NO, NO/O_2 mixtures and NO_2 is performed by *in situ* FTIR Spectroscopy. the thermal stability and reactivity of the surface NO_x forms towards n-decane is followed by application of the same technique. It is established that adsorption of NO on the support and manganese-containing catalysts is reactive and leads to linearly adsorbed NO and formation of anionic nitrosyl, NO^- and NO_3^- species. Contrary to the impregnated catalyst, the ion-exchanged catalyst does not contain NO^- species coordinated to Ti^{4+} ions. This experimental fact is in agreement with the high dispersion of Mn^{3+} ions concluded from the CO adsorption experiments.

The NO/O_2 co-adsorption on the anatase and catalysts studied results in formation of NO_3^- species differing in the mode of their coordination. Under these conditions no NO^- species are detected. The surface nitrates formed on the manganese-containing catalysts possess lower thermal stability than those on the pure support. This difference explains the higher reactivity of the former toward the n-decane.

The nitrates formed upon NO/O_2 co-adsorption on the manganese-containing catalysts are able to activate and oxidize the hydrocarbon at temperatures as low as 373 K. The latter process gives rise to adsorbed CO_2, formic acid and isocyanate species. The NCO species is considered as an important intermediate in the formation of nitrogen. The extent of oxidation of n-decane is higher on the ion-exchanged catalyst. It is concluded that this catalyst can be promising in the selective catalytic reduction of NO by longer-chain saturated hydrocarbons.

Keywords: manganese-titania catalysts, *in situ* FTIR spectroscopy of adsorbed CO and NO_x, manganese-titania catalyst, ion-exchange, impregnation, SCR of NO_x by n-decane, mechanism

ÖZET

MANGAN DEPOLANMIŞ TİTANİA KATALİZÖRE TUTUNMUŞ NO_X MOLEKÜLLERİNİN TANIMLANMASI, KARARLILIĞI VE TEPKİMESİ

MUSTAFA U. KÜÇÜKKAL

Kimya Bölümü Yüksek Lisans

Tez Yöneticisi: Dr. Margarita Kantcheva

Ocak 2001,

Uygun yakıt ekonomisi ve daha az CO_2 sera gazlarının emisyonuna duyulan ihtiyaç tüm dünyada dizel motorlara olan talebin artmasına yoğunlaştirmıştır. Bu motorlar hava/yakıt oranının stokiometrik orandan yüksek olan durumda çalışmaktadır. Bu egzoz gazındaki hidrokarbon/NO_X oranının nispeten düşük olmasına sebep olmaktadır ve bır miktar indirgeyici (tipik olarak %2-3 ek yakıt) de- NO_X katalizörün akıntısına eklenmelidir. Bu sebeple, NO/O_2 karışımının katalizör yüzeyine tutunmasdan dolayı oluşan NO_X türlerlerinin dizel yakıtlar için tipik olan uzun zincir hidrokarbonlarıyla etkileşiminin incelenmesi önem kazanmaktadır.

Son yıllarda birçok de-NO_X katalizörler önerilmiştir ve bunların arasından metal oksit destekli olanlar potansiyel termik kararlılıklarından ve geniş komposizyon çeşitliliğinden dolayı göz önüne alınmıştır.

Bu çalışmaya konu olan katalizörler Mn^{2+} iyonlarının sulu çözeltisinden imregnasyon ve iyon değişimi yöntemiyle hazırlanan mangan depolanmiş titania katalizörleridir.

NO, NO_2 ve NO/O_2 karışımı adsorbsiyonu sonucunda oluşan NO_X teşhisi kendi ortamında (*in situ*) FTIR spektoroskopisiyle yapılmıştır. Aynı teknik kullanılarak yüzeydeki NO_x türlerinin n-dekana karsı olan termik kararlılığı ve reaktifliği takip edilmiştir. Destek ve mangan depolanmış katalizörlerinin üzerine NO tutulumunun aniyonik nitrosil, NO^- ve NO_3^- türlerinin oluşumuna sebep olan reaktif bir adsorbsiyon olduğu kanıtlanmıştır. Imregnasyonla elde edilen katalizörle karşılaştırıldığında, iyon değişimiyle elde edilen katalizör Ti^{4+} iyonuna koordine olan aniyonik nitrosil içermemektedir. Bu deneysel sonuç, CO tutulumundan çıkarılan Mn^{3+} iyonlarının yüksek dağılımıyla uyumludur.

Anatez ve çalışılan katalizörler üzerine NO/O_2 ko-adsorbsiyonu koordinasyon biçimlerinde farklılık gösteren NO_3^- türlerinin oluşumuna sebep olmaktadır. Bu şartlar altında NO^- türleri gözlemlenmemiştir. Mangan içeren katalizörlerin üzerinde oluşan yüzey nitratları detek üzerindekilerden daha düşük termik kararlılığa sahiptir. Bu fark önceki türlerin n-dekana karşı olan daha yükek tepkimesini açıklamaktadır.

Mangan içeren katalizörlerinin üzerindeki NO/O_2 birlikte tutulumuyla oluşan nitratlar hidrokarbonu 373 K gibi düşük derecede aktive edebilmektedir ve oksitleyebilmektedir. Sonraki yöntem tutulmuş CO_2, formik asit ve isosiyanat türlerinin artışına sebep olmaktadır. NCO türünün azot oluşumunda önemli bir ara ürün olduğu düşünülmektedir. N-dekanın oksitlenme miktarı iyon değişimiyle hazırlanan katalizörün üzerinde daha fazladır. Sonuç olarak bu katalizör uzun doymuş hidrokarbonlar tarafından NO'nun seçici katalitik olarak indirgenmesinde umut vermektedir.

Anahtar kelimeler: Mangan depolanmış titania katalizörler, tutulmuş CO ve NO' nun kendi ortamında (*in situ)* FTIR spectroskopisi, iyon değişimi, impregnasyon, NO'nun n-dekan tarafından seçici katalitik olarak indirgenmesi

ACKNOWLEDGEMENT

It is a pleasure for me to express my deepest gratitude to Dr. Margarita Kantcheva for her encouragement and supervision throughout my studies.

I would like to express my deepest gratitude to Özgür Birer, Olga Samarskaya, Ethem Amber, Talal Shahwan, Mehmet Bayındır, Necmi Bıyıklı, Ersin Esen, Erkan Z. Çiftlikli, Aysegül Kapucu and Şule Atahan for their encouragement and their kind help.

I would like to thank all present and former members of the Bilkent University Chemistry Department for their help.

I would like to thank my wife Tuba Gül for endless love and support.

TABLE OF CONTENTS

LIST OF TABLES

LIST OF FIGURES

1. INTRODUCTION

1.1 Nitrogen oxides (NO_x)

Nitrogen oxides (NO_x) are formed when nitrogen combines with oxygen and consist of mainly nitrogen oxide (NO) and nitrogen dioxide (NO_2). NO_x are harmful pollutants.

1.2 Effects of NO_x to environment

NO_X emissions are the components of the principle precursors to ground-level ozone, acid rain and also contribute to fine particular matter (PM10) pollution [1].

NO is a major atmospheric pollutant. It has the ability to generate secondary contaminants through its interaction with other primary pollutants (like carbonyl containing molecules, alcohol radicals, etc.)[2]. NO is very important in the photochemistry of the troposphere and stratosphere. It reacts with photochemical pollutants such as ozone, formaldehyde, organic hydroperoxides and peroxyacyl nitrates that are all very reactive and have very short lifetime [2]. This is a very fast reaction, which generates more nitrogen oxides and organic nitrates. NO_2 contributes substantially to so called acid rain. The chemical depletion of ozone an important

part due to nitrogen oxide species, is a prolonged phenomenon. Carcinogenic products are also formed during the reactions [2].

Hydrocarbons (HCs) in polluted air show a high reactivity towards intermediate species such as peroxides, RO_2. Such species react with primary pollutants, NO, NO_2, O_3 and hydrocarbon (HC) according to partially known mechanism [2]. The photochemical complex HC-NO_x-O_x is formed during the HC interactions in the photolytic cycle of NO; the mixture of products generated is called " photochemical smog" and contains O_3, CO, peroxyacyl nitrates, alkyl nitrates, ketones, etc [2].

The photochemical cycle of nitrogen oxides starts under sunlight (300-460 nm). NO_2 decomposes as follows [2]:

$NO_2 + h\nu(> 3.2\ eV) \rightarrow NO + O$

$O + O_2 + M \rightarrow O_3 + M\ (Third\ body) + 24.2\ kcal$

$O_3 + NO \rightarrow NO_2 + O_2 + 48.5\ kcal$

Until a dynamic equilibrium is reached:

$NO_2 + O_2 + h\nu \rightarrow NO + O_3$

Ozone Depletion:

$NO + O_3 \rightarrow NO_2 + O_2$

$O_3 + uv\ light \rightarrow O_2 + O$

$NO_2 + O \rightarrow NO + O_2$

Overall Reaction: $\mathbf{2O_3 \rightarrow 3O_2}$ [2]

ACID RAIN FORMATION:

Precipitation, which has a pH, value less than 5.6 and is therefore acidic in nature. Acid rain is the reason why some forests are being destroyed. Figure 1 shows the distribution of the sources of the acid rain [3].

$2NO_{x(g)} + H_2O_{(l)} \rightarrow 2\ H^+_{(aq)} + 2\ NO_3^-{}_{(aq)}$ [3]

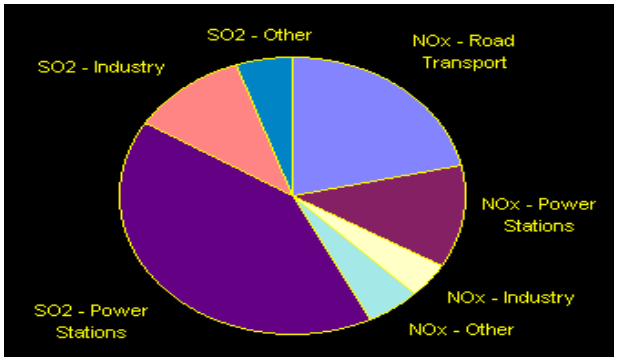

Figure 1 Sources of acid rain

1.3 Main sources of NO_x emissions

NO_x emissions are produced almost entirely by combustion. The main sources of nitrogen oxides are:

a) Industrial sources

b) Vehicle exhaust sources

c) Domestic heating sources

Due to the rapid growth of primary energy consumption, increasing traffic density and the use of low-quality fuels in households, NO_x emissions have increased rapidly in Turkey in recent years.

The source most responsible for NO_x emissions in Turkey is transportation followed by the power generation (Fig.2) [4]. The NO_x emission was 357.000 tons in 1985 which is expected to increase in to 1.2 millions tons by 2010 in Turkey [4].

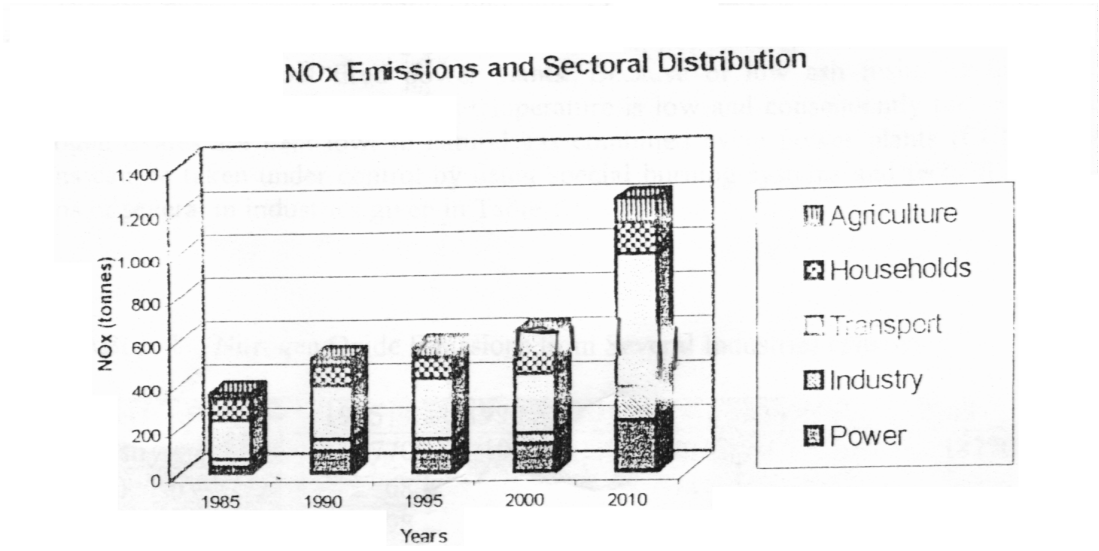

Figure 2 NO_x emissions and sectoral distributions in Turkey

The expected NO_x emission in Europe is 22 millions tons per year and NO_x emissions are spread throughout the continent. EU being highly sensitive to environmental protection set the emission limits for the poisonous gases. The permitted emission limits of the gases from light-duty vehicles in EU are given in Table 1 [5].

Table 1 EU emission limits for light-duty vehicles (g/km) (Directive 98/69/EEC)

	Stage 2000		**Stage 2005**	
	Petrol	***Diesel***	***Petrol***	***Diesel***
CO	2.30	0.64	1.00	0.50
HCs	0.2	-	0.1	-
NO_x	0.15	-	0.08	-
HCs+NO_x	-	0.56	-	0.30
Par	-	0.05	-	0.025

EU prepared the *"PROTOCOL TO THE 1979 CONVENTION ON LONG-RANGE TRANSBOUNDARY AIR POLLUTION CONCERNING THE CONTROL OF EMISSIONS OF NITROGEN OXIDES OR THEIR TRANBOUNDARY FLUXES'* in 1988 in Sofia. The EU identified the sources of NO_x emissions and the precautions and set desired the limits for the sources. In order to minimize the NO_x emissions several methods are studied and proposed [5]:

- Energy saving: Increasing the rational use of energy,
- Energy mix: Increasing the proportion of non-combustion energy sources,
- Fuel switching/cleaning: Switching from high-nitrogen fuel to low-nitrogen fuel, increasing the cracking technology in refineries,
- Process and combustion modifications,
- Catalytic removal of NO_x,

In compliance with sustainable development goals in Turkey, in order to control pollution caused by motor vehicles, Turkey aims to stay in touch with the developments in EU. Increasing the quality of petroleum to meet EU standard,

encouraging the consumption of unleaded gasoline and the stationary inspection of motor vehicles in cities regularly are done for minimizing the NO_x emissions in mobile sources in Turkey [4].

For effective pollution control, In 1983 The Environmental Act was passed in which general guidelines and principle of Turkish environmental policies were established. This Act required the preparation of Air Quality Control Regulation (AQRC) in which emission standards for the most important sources of air pollutant emissions have been defined which was issued in 1986 [4].

Table 2 NO emission limits for combustion plants in AQCR

Emission Standards (mg/m^3)						
	New Plants	***New Plants***	***New Plants***	***Old Plants***	***Old Plants***	***Old Plants***
	Solid Fuels	**Liquid Fuels**	**Gas**	**Solid Fuels**	**Liquid Fuels**	**Gas**
NO	>50MW: 800	>50MW: 800	>100MW: 500	>50MW: 1000	>50MW: 1000	>100MW: 500

1.4 Technologies to reduce NO_x emissions from vehicles

1.4.1 Non-catalytic removal of NO_x

In mobile sources initially, NO_x emissions were controlled by use of air/fuel mixtures within the bounds of HC and CO standards, retarded spark timing, and

exhaust gas recirculation (EGR). EGR returns a metered amount of exhaust gas to the engine cylinders, which lowers peak combustion temperatures. Reductions in combustion temperatures generally reduce NO_x formation. EGR was the primary NO_x emission control technique from 1971 until three-way catalyst technology came into wide spread use [1].

1.4.2 Catalytic removal of NO_x

1.4.2.1 NO reduction by CO

A catalytic converter is designed to maximize the conversion of exhaust gases into inert and less harmful compounds. A three-way catalytic converter typically consists of a cylindrical ceramic substrate with many small longitudinal channels. The channels are coated with metals of platinum, palladium, or a combination of these two metals. These two metals oxidize HC and CO to form carbon dioxide and water. The channels are also coated with metal rhodium, where NO_x are reduced by CO to form nitrogen and CO_2. Three-way catalysts are popular since they can eliminate more than 90% of the engine-out NO_x emissions while maintaining good fuel economy and performance. Three-way catalyst requires the use of an oxygen sensor, which is located upstream of the catalyst. The oxygen sensor maintains a precise required air/fuel ratio, which is near to stoichiometric ratio [1].

Rh/CeO_2-ZrO_2, Rh/TiO_2 catalyst prepared by sol-gel method are promising catalysts for reduction of NO_x by CO. CO is adsorbed on the deposited metal and NO_x oxidizes the support metal where CO is oxidized to CO_2 by the support metal. These catalysts require oxygen to CO ratio near to stoichiometric ratio [6,7,8].

1.4.2.2 Decomposition of NO

NO decomposition is the most attractive way to reduce NO_x from the point of the absence of the reductant. The suitable catalysts for this purpose are Cu- and Co-containing zeolites and Ba/MgO. Unfortunately, these catalysts are active in a limited interval of temperature and in the absence of oxygen. In addition water and sulfur-containing compounds cause rapid deactivation [9-12].

1.4.2.3 Selective catalytic reduction of NO_x

This type of reduction is called selective because in the presence of appropriate catalysts, NO_x has a higher oxidation potential than O_2 with respect to the reducer.

In stationary sources the SCR of NO_x is achieved by NH_3 on TiO_2 supported V_2O_5-WO_3 and/or V_2O_5-MoO_3 catalysts supported on TiO_2 (Anatase) [13,14].

The NH_3-SCR of NO_x is not suitable for automotive applications due to transient conditions and hazards related to the presence of an ammonia tank on-board [15].

The lean burn gasoline engines decrease the fuel consumption, which is the main approach for reducing CO_2 in air in the world. The use of this type of engines increases in Japan and also it will increase in Europe soon. This type of engines require higher air/fuel ratio. This requirement makes the use of three-way catalyst inapplicable in these engines.

This situation forces manufacturers to search for a suitable de-NO_x catalyst. Selective catalytic reduction of NO_x (SCR of NO_x) by hydrocarbons (HCs) in excess oxygen is an alternative technique for controlling NO_x emission from mobile sources. This process is target of research work since the time of pioneering investigations of Iwamato [16] and Held etal [17] on reduction of NO by HCs in the presence of oxygen using Cu-ZSM-5 as a catalyst. The interest in this study arises from two aspects:

1.Practical Aspects: Development of a suitable de-NO_x catalyst would lead to a highly efficient engine performance that will be achieved by using a higher air/fuel ratio than for the present 3-way catalyst.

2.Academic Aspects: It arises from the complex reaction mechanism and the nature of active sites involved.

1.5 Selective catalytic reduction of NO_x by hydrocarbons in the presence of oxygen

1.5.1 The main characteristics of SCR of NO_x by hydrocarbons in the presence of oxygen

1. *Influence of the type of the support*

In general, the transition metal-exchanged zeolites (ZSM-5, mordenite, ferrierite) are more active and selective than oxide (Al_2O_3, SiO_2 and Al_2O_3-SiO_2) based catalysts [2]. The effect of the zeolite structure could be associated with the environment provided to the exchanged metal ions. Microporosity also plays an important role. All zeolite-based catalysts are very sensitive to water and quickly deactivate the catalyst. At least two effects are responsible for this process [2]:

a) Changes in the coordination and position of the active metal ion in the zeolite structure,
b) Dealumination of the zeolite with the modification of the Brønsted acidity. This process is irreversible.

Many investigations have been devoted to non-zeolitic catalysts. The results are summarized by Iwamoto et al. [18-20], Bethke et al. [21,22], Tabata et al. [23] and Papp et al. [24]. In general, the structure of this type of catalysts is less sensitive to water and sulfur containing-compounds but the activity is lower than that of the zeolites. This leads to the conclusion that in order to develop durable de-NO_x

catalysts for lean-burn conditions a comprise must be found between activity and resistance to poisoning. Among the supports used (Al_2O_3, SiO_2, SiO_2- Al_2O_3, TiO_2, ZrO_2) titania (anatase) possesses a good thioresistance and is stable in SO_2 atmosphere.

2. The influence of the temperature

The optimal temperature for the SCR of NO_x is in the range 423-873 K and depends on the catalyst support, the active phase and the nature of the hydrocarbon [25-44].

The de-NO_x catalysts can be divided into three categories depending on the temperature range of their activity:

- Low temperature (423-573 K): this category catalysts consist mainly of platinum supported on oxides or zeolites [30,43],
- Medium temperature (573-723 K): To this category belong copper containing zeolites and other oxide supports [25,26,44],
- High temperature (>723 K): These catalysts usually contain metal oxides like cobalt, nickel, gallium, indium, tin and aluminum added on oxide (SiO_2, Al_2O_3) or zeolite supports [25-28,33,44].

3. *The role of the reducer*

Depending on their nature, the reducing gases are divided into two groups: selective and unselective [25,26]. In the case of Cu-ZSM-5 selective reducers are C_{2+}-hydrocarbons: ethylene [25,26,44,45], propylene [25,26,45-50], propane [39,50] and isobutene [40,51], whereas hydrogen, CO and methane are unselective [25,26].

In the presence of oxygen, NO_x can be reduced selectively by methane over cobalt-containing zeolites [40,42,52,53].

4. The role of oxygen

It is assumed that the role of oxygen is:

- To keep the surface clean [50,54] and oxidized [51,52]
- To convert NO to reactive surface compounds such as NO_2 [52,54], nitrites [54,55] or nitrates [54,55-59].

1.5.2 Mechanism of the SCR of NO_x by hydrocarbons in the presence of oxygen

It has been found that the reduction of NO with hydrocarbons is promoted by oxygen. Several reaction mechanisms have been proposed to explain this process [2]:

1. *Oxidation of NO to reactive NO_2 that is adsorbed on the catalyst surface ($NO_{2(ads)}$) and reacts with hydrocarbons [31,60-62]*

This mechanism is typical of the SCR of NO with CH_4. The adsorbed NO_2 interacts with CH_4 producing a reaction intermediate the nature of which is not yet known. Arguments supporting the formation of reactive NO_2 species are given by Li et al. [41,63] and Sachtler et al. [54].

2. *Oxidative conversion of hydrocarbons forming an intermediate by reaction with NO_x (e.g. isocyanate radical, oxygen-containing compounds etc.)*

This mechanism was first proposed by Ukusi et al. [65,66] for oxide non-zeolitic catalysts and C_{2+}-hyrocarbons as reducers. Later, other authors [30,67-69]

extended these ideas to metal zeolites.

The present knowledge on the mechanism of NO reduction on oxide non-zeolitic surfaces involves a reaction occurring through isocyanate [65,70] or oxygenated [67] intermediates. This suggestion seems to apply to all hydrocarbons. The formation of isocyanate species seems to depend on the chain length as well as on the type of hydrocarbon.

Several scientists [30,47,67] indicated that radical forms present in the carbon deposits can reduce NO to an intermediate species in the SCR. However, it is still unclear how carbon deposits can be generated. This hypothesis contradicts the zero order of SCR of NO_x by hydrocarbons with respect to NO and the higher order of the reaction towards the hydrocarbons.

In a large number of publications [48,70-78], formation of organic nitro-compounds is suggested. Hayes et al. [48,73] proposed a reduction of nitrate species to N_2 to occur via organic nitro-compound that further transforms to isocyanate. The interaction of the latter species with O_2 results in dinitrogen formation.

3.Redox mechanism

This mechanism involves reduction of the catalyst surface by the hydrocarbon and NO decomposition on the reduced sites [80,81]. However, there is no correlation between the activities of the catalysts in the SCR and NO decomposition.

It has been suggested that adsorbed NO_x species are essential for the activation of the HCs by H-abstraction [41,54,78,82-84]. This indicates that the knowledge of the nature and reactivity of the surface compounds formed on the

catalyst during NO/O_2 adsorption is of special importance for understanding the mechanism of the process.

The aims of this study are:

- To investigate the effect of the preparation of titania-supported manganese catalysts on the state and localization of the active phase,
- To study the nature of the active sites for adsorption of the SCR reactants and to identify the adsorbed compounds,
- To investigate the thermal stability and reactivity of the adsorbed species and their importance in the SCR of NO_x.

This information can help to elucidate the mechanism of SCR of NO_x by HCs and development of effective lean-burn de-NO_x catalysts.

1.6 Characterization of catalysts' surfaces by means of in situ-FTIR spectroscopy

The applicability of the IR technique is determined by the properties of the solid catalyst to be studied. Thus, catalysts that exhibit a weak bulk absorption and average particle size <d> which is smaller than the wavelength of the IR radiation in the region of interest are suitable for characterization by IR technique [85]. Most catalysts show a bulk absorption in the low wavenumber region (<1000 cm^{-1}). As a result, the accessible wavenumber range for IR spectroscopy is limited for surface studies to the mid-IR region (4000>ν>1000 cm^{-1}) [85].

IR spectroscopy is a bulk rather than a surface specific technique. It is therefore necessary to prove for any detected species that it is a surface group. This can be realized in many cases tracking the changes in band positions upon exposure of the solid adsorbent to a suitable adsorption or by isotopic exchange experiments [85].

The sensitivity of the technique is dependent on the extinction coefficients of surface groups, which may vary from $5x10^{-18}$ cm^2 $molecule^{-1}$ for the carbonyl stretching mode in CO ligands to between 10^{-20} and 10^{-19} cm^2 $molecule^{-1}$ for CH stretching modes in saturated HC chains [86].

The IR spectra can be obtained even at coverages below one tenth of monolayer [85]. With the application of data acquisition techniques the sensitivity of the technique can be increased further [85]. Quantitative measurements of surface group densities should be possible, provided that Beer-Lambert law is applicable [85].

1.6.1 Determination of the surface vibrational mode of CO_3^- and NO_x species

Identification of surface NO_x species by means of IR technique is very complicated due to the following reasons:

- The large number of compounds may coexist on the surface in which the formal charge of nitrogen atoms can vary from +1 to +5. Nitrogen-oxo

species can bind to surface via N atom or one or more O atom. The species can be bridged, mono-, bi-dentate, free-like bonded simultaneously by N and O ends.

- The interpretation of the NO_x species by means of the stretching frequencies of N-O and/or N-N can be difficult and contradictory. For example, N-O stretching mode is found around 1870 cm^{-1} for NO, $(NO)_2$ and N_2O_3 [86,87].

The assignments of the NO_x species on oxide surfaces are summarized as follows:

A. Oxo Compounds of Nitrogen in Oxidation State +1

1. N_2O; Nitrous oxide

The N_2O molecule has a linear N-N-O structure. N_2O has ν(NN) and ν(NO) stretching modes at 2224 and 1285 cm^{-1}, respectively [86,87]. N-N mode can be distinguished from N-O vibrations of N_xO_y species using ^{15}N substitution. Since N_2O has different origin and environment impact, it is not considered when one uses the term NO_x. N_2O has often been detected as a by product of surface reactions (usually NO decomposition). The observed ν(N-N) mode is between 2290 and 2210 cm^{-1} [87].

2. NO^-; Nitrosyl Anion

In case of electron donation to NO, the electron will occupy an antibonding orbital. Thus, it is difficult for NO to accept an electron and the NO^- anion is not well studied. NO^- has a bond order of 2 and as a result, the observed NO stretching modes

in M^+NO^- alkali salts lie in the 1374-1352 cm^{-1} region [86,87]. A reductive site, which is easily oxidized, should exist on the surface to produce NO^- from NO [88].

3. $N_2O_2^{2-}$; Hyponitrites

This anion can exist in cis- and trans- form where the latter being considered more stable. It is produced by a strong reduction of nitrates or nitrites [90] and is thus a candidate for an intermediate in SCR.

The trans-$N_2O_2^{2-}$ has ν(NN) stretching mode of at 1419 cm^{-1} whereas symmetric and antisymmetric N-O modes are at 1120 and 1030 cm^{-1} respectively [86,87]. For cis-$N_2O_2^{2-}$, the N-N vibrations are at 1314 cm^{-1}, whereas it has symmetric and antisymmetric N-O modes at 1057 and 857 cm^{-1} respectively [87].

The set of bands at 1350, 1015 and 954 cm^{-1} has been assigned to cis-$N_2O_2^{2-}$ after adsorption of NO on CeO_2 whereas trans- $N_2O_2^{2-}$ is characterized by the absorption band at 1105 cm^{-1} [90]. Two bands at 1176 and 1111 cm^{-1} are attributed to two forms of cis-$N_2O_2^{2-}$ on La_2O_3 [91]. Upon adsorption of NO on Mn/Al_2O_3 the band characterizing hyponitrites is observed at 1206 cm^{-1} [92].

B. Oxo Compounds of Nitrogen in oxidation State 2+

1. NO; Nitrogen Monoxide

The N-O bond order is 2.5 [89] and ν(N-O) stretching mode is at 1876 cm^{-1} [87]. The coordination of NO on a Lewis acid site is accomplished at the expense of

electron density of 3σ orbital, which is slightly antibonding. Thus, the bond order increases leading to a blue shift in the stretching frequency of the N-O bond. Formation of π-back bond by partial charge transfer from the metal center to $2\pi^*$ orbital is also possible and results in decrease in the bond order and ν(NO) stretching frequency of N-O bond. Observed ν(NO) stretching frequencies of mononitrosyl species on manganese containing surfaces are given in Table 3.

Table 3 Observed N-O stretching frequencies of mononitrosyl species on manganese containing surfaces

Site	**System**	**ν(N-O) (cm^{-1})**	**Notes**	**Ref.**
Mn^{2+}	Mn-ZSM-5	1894	Mn^{2+}(OH) site	93
Mn^{3+}	Mn-ZSM-5	1966	$Mn^{3+}(O^-)$ site	93
Mn^{3+}	Mn-ZSM-5	1935	$Mn^{2+}(O^-)(NO_2)$ site	93
Mn^{2+}	Mn/MgO	1760-1760	On isolated sites	94
Mn^{n+}	Mn/MgO	1900-1820	On associated Mn sites	94
Mn^{3+}	Mn/Al_2O_3	1833 1865	One coordinative vacancy Two coordinative vacancy	92

C. Oxo Compounds of Nitrogen in oxidation State 3+ and 5+

1. N_2O_3; Dinitrogen Trioxide

Although N_2O_3 is an unstable compound and decomposes easily into NO and NO_2, it can be expected to be the principal adsorption species during the NO+O_2 coadsorption [89].

It exists in two modifications, antisymmetric and symmetric forms [89]. Antisymmetric-N_2O_3 has the structure of O=N-NO_2. This structure has the modes of NO and NO_2 which hinders the spectral identification. The stretching vibrations, $\nu_s(NO_2)$, $\nu_{as}(NO_2)$ and ν(N=O) are at 1305, 1652 and 1832 cm^{-1} respectively [95].

The symmetric N_2O_3 is produced at low temperature condensation of ($NO+O_2$) or after irradiation of antisymmetric N_2O_3 (at 720 nm)[95]. It has the structure O=N-O-N=O. The ν_s(N=O), ν_{as}(N=O), ν_s(O-N) and ν_{as}(O-N) modes are observed at 1690, 1660 , 880 and 970 cm^{-1} respectively [86].

The adsorption of NO or $NO+O_2$ on zeolites usually give rise to adsorbed N_2O_3 [89]. It is easily removed by evacuation at room temperature. The observed regions for ν(N=O), $\nu_{as}(NO_2)$ and $\nu_s(NO_2)$ on zeolites are 1930-1880, 1590-1550 and 1305-1290 cm^{-1} respectively [88].

2. NO^+, Nitrosonium Ion

NO can easily lose its unpaired electron from 5σ orbital leading to the NO^+ formation. The bond order becomes ~3 and the N-O stretching mode is shifted to 2391-2102 cm^{-1} range [87,97].

3. NO_2^-, Nitrito or Nitro Compounds

Coordination of NO_2^- ion on oxide surface can occur in three ways [89]:

1) NO_2^- can replace another negative fragment (e.g., OH^-)

2) NO_2^- can be formed together with another counter pair ion (e.g., NO^+).

3) NO_2^- can be produced during the oxidation of a surface cation.

The free nitrite anion has a C_{2v} symmetry and the modes $\nu_{as}(NO_2)$ and $\nu_s(NO_2)$, are at 1260 and 1330 cm^{-1} respectively [86,87]. The coordination of NO_2^- ion on the surface causes drastic changes in its IR spectrum. The possible ways of coordination of NO_2^- are represented in Fig.3.

When NO_2^- is coordinated by one or two oxygen atoms, the corresponding species is called ***nitrito*** species. The monodentate ion has two distinct N-O modes, ν(N-O) and ν(N=O), because the symmetry of NO_2^- is reduced. The stronger the bond to the coordination site, the weaker the N-O bond and the stronger the N=O bond. Thus the bridging monodentate nitrito species are expected to manifest higher ν(N=O) stretching mode than those in the respective monodentate anions. However, on the basis of IR data, it is difficult to distinguish between both structures. In bulk monodentate nitrito complexes, ν(N-O) is observed in the 1206-1065 cm^{-1} spectral region, whereas the reported interval for ν(N=O) is 1470-1335 cm^{-1} [89].

In general, the chelating and bridging bidentate nitrito species have a C_{2v} symmetry. For that reason, their IR frequencies are similar to those of the free NO_2^- ion. For bulk species $\nu_{as}(NO_2)$ is shifted to 1314-1266 cm^{-1} and $\nu_s(NO_2)$ to 1203-1176 cm^{-1} [89].

When NO_2^- is coordinated via its N atom, the respective species are called ***nitro*** species. In this case the C_{2v} symmetry is also preserved, but N-O stretchings are observed at higher frequencies than the corresponding vibrations for bidentate

nitrito species, namely $\nu_{as}(NO_2)$ at 1650-1375 cm^{-1} and $\nu_s(NO_2)$ at 1350-1250 cm^{-1} [97].

When NO_2^- anion is bound simultaneously via one O and N atoms, the respective species are called ***nitro-nitrito*** species. Sometimes, they are denoted as chelated nitro species. The frequencies, reported for the bulk compounds, are at 1200 cm^{-1} (ν(N-O)) and at 1516-1435 cm^{-1} (ν(N=O)) [89]. Examples of various nitro and nitrito surface species are presented in Table 4.

Table 4 Assignment of various IR bands to different NO_2^- surface species

System	**Adsorbate**	**IR Bands**	**Coordination**	**Ref.**
TiO_2	NO_2	1550,1450	Monodentate Nitrito	100
MnO_x/Al_2O_3	NO	1466,1075 1136 1415,1322	Monodentate Nitrito Bridging Nitrito Nitro	101,102
Mn-ZSM-5	NO,NO+O_2	1516	Monodentate Nitrito	95

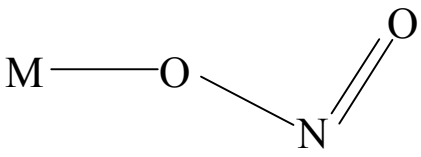

Monodentate nitrito

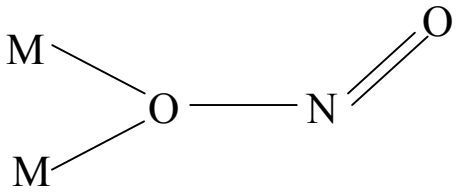

Bridging monodentate nitrito

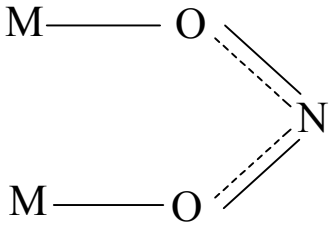

Bridging bidentate nitrito

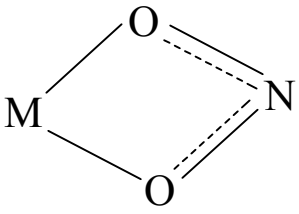

Chelating bidentate nitrito

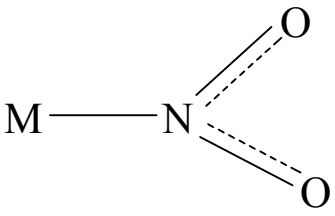

Nitro

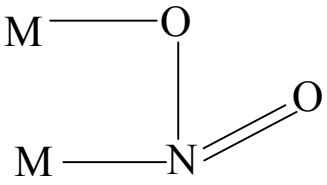

Bridging nitro-nitrito

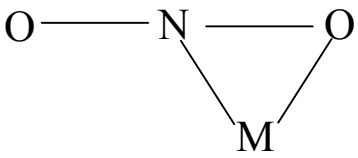

Chelating nitro-nitrito

Figure 3 Possible structures of surface NO_2^- species

3. CO_3^{2-} and NO_3^-, Carbonate and Nitrate Ions

The possible coordinations of nitrate and carbonate ions on the surface are presented in Fig.4. The NO_3^- and CO_3^{2-} ions have D_{3h} symmetry. The symmetry changes to C_{2v} or C_s, respectively. The changes in selection rules are shown in Table 5 [87]. The lowering of the symmetry due to the coordination causes the splitting of the doubly degenerate ν_3 and ν_4 vibrations, as well as the activation of ν_1. Despite the same number of IR active fundamentals for C_{2v} and C_s, the splitting of degenerate vibrations is larger for bidentate than for monodentate nitrate and carbonate ions [87]. The magnitude of $\Delta\nu_3$ splitting upon coordination of surface nitrates and carbonates is given in Table 6 [87,98]. The observed regions for the frequencies of ν_3 and ν_1 of surface NO_3^- and NO_2^- species are shown in Table 7 [88].

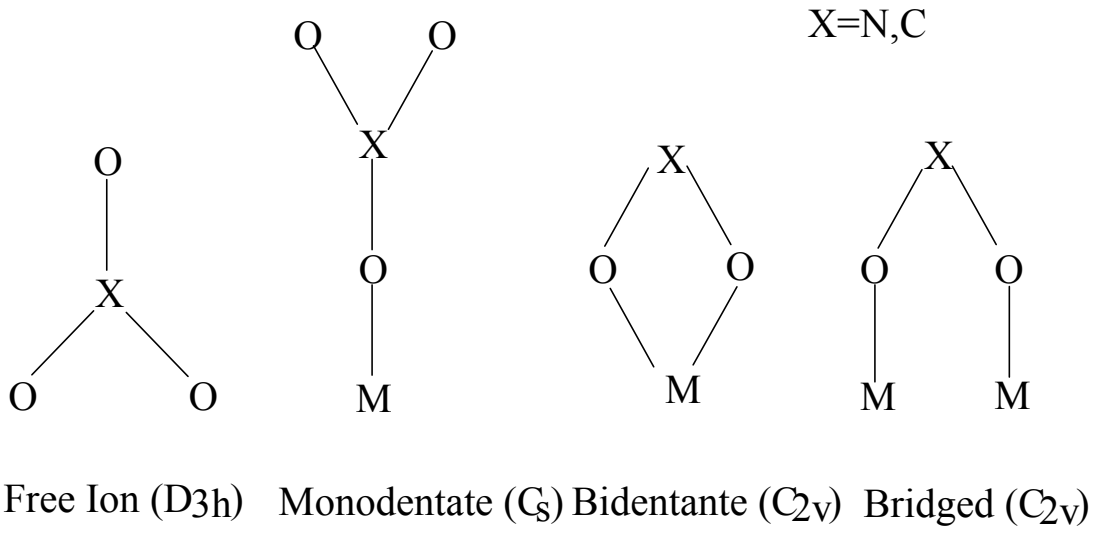

Figure 4 Possible structures of surface NO_3^- and CO_3^- species

Table 5 Correlation table for D_{3h}, D_3, C_{2v} and C_s point groups

Point Group	**ν_1**	**ν_2**	**ν_3**	**ν_4**
D_{3h}	$A_1'(R)$	$A_2''(I)$	$E'(I,R)$	$E'(I,R)$
C_{2v}	$A_1(I,R)$	$B_1(I,R)$	$A_1(I,R)+B_2(I,R)$	$A_1(I,R)+B_2(I,R)$
C_s	$A'(R)$	$A(I,R)$	$A'(I,R)+A'(I,R)$	$A'(I,R)+A'(I,R)$

Table 6 $\Delta\nu_3$ splitting of coordinated nitrates and carbonates

$\Delta\nu_3(cm^{-1})$	**Monodentate**	**Bidentate**	**Bridged**
NO_3^-	<300	>300	≥400
CO_3^-	~100	~300	≥400

Table 7 Observed regions of ν_3 and ν_1 stretching modes of surface NO_2^- and NO_3^- species

Structure	**$\nu_3(cm^{-1})$**	**$\nu_1(cm^{-1})$**
Free NO_3^- ion	1380	1050*
Monodentate Nitrate	1530-1480, 1290-1250	1035-970
Bidentate Nitrate	1565-1500, 1300-1260	1040-1010
Bridging Nitrate	1650-1600, 1225-1170	1030-1000
Free NO_2^- ion	1260	1330
Bridging Nitrite	1220-1205	
Nitro Compound	1440-1335	1350-1315
Monodentate Nitrite	1470-1450	1065-1050
Chelating Nitro Compound	1520-1390	1260-1180

E. Oxo Compounds of Nitrogen in Oxidation State 4+

1. NO_2, Nitrogen dioxide

NO_2 is easily formed from NO in the presence of O_2. It has C_{2v} symmetry and $\nu_{as}(NO_2)$ stretching mode at 1612 cm^{-1} with a Raman active $\nu_s(NO_2)$ mode at 1325 cm^{-1} [88]. The bands assigned to adsorbed NO_2 lie in 1642-1605 region and are found to disappear easily after evacuation [88].

2. N_2O_4, Dinitrogen Tetraoxide

N_2O_4 is easily formed by NO_2 dimerization. It has D_{2h} symmetry and $_2ON$-NO_2 structure. The characteristic bands for N_2O_4 in gas phase are at 1758-1730 cm^{-1} ($\nu_{as}(NO_2)$) with a shoulder at 1710 cm^{-1} (out-of-phase and in-phase modes, respectively) and at 1368-1359 cm^{-1} ($\nu_s(NO_2)$) [86].

Adsorbed N_2O_4 is observed after NO_2 or $NO+O_2$ coadsorption on oxides and zeolites [88]. Its spectral features do not differ considerably. N_2O_4 easily disappears upon evacuation at ambient temperature [88].

F. Carbon-Containing Oxo Compounds of Nitrogen

1. NCO^-, CN^-, Isocyanates and Nitriles

NCO^- usually absorb in the 2300-2160 cm^{-1} spectral region, whereas bands at 2270-2120 cm^{-1} have been attributed to nitriles [88].

1.7 X-ray photoelectron spectroscopy

XPS (X-Ray Photoelectron Spectroscopy) or ESCA (Electron Spectroscopy for Chemical Analysis) is a technique for measuring electron binding energy. Under high vacuum conditions (10^{-8} Torr) monoenergetic X-rays (Mg Kα at 1253.6 eV) strike the sample and cause ejection of electrons from valance and core levels of the atoms in the sample. The kinetic and binding energies of ejected electrons are measured with respect to Fermi level. Using data on binding energy, the elements in the sample can be identified. As binding energies depend on the kind of the atoms in the sample, their oxidation state and environment and penetration depth, a small shift usually in the order of a few eV, called chemical shift, is observed. This shift can be used for determining the chemical state of an element in the sample.

The oxidation state of manganese can not be elucidated from the binding energy of either of the manganese main peaks (2p or 3p). In order to determine the oxidation state of manganese by XPS, the best approach [102] is to use the magnitude of Mn 3s splitting due to the coupling of the unpaired valence electrons with the core hole. As an example, Mn^{2+} in the ground state has five 3d unpaired electrons (^6S state). After the ejection of 3s electron, an additional unpaired electron is produced with a spin which is parallel (^7S state) or antiparallel (^5S state) to 3d electrons. Due to the spin interactions between the unpaired valance electron and core hole following the Hund's rule, ^7S is lowered in energy by an amount of exchange energy. The magnitude of the lowering of the energy is proportional to 3s-

3d integral. The energy difference between these two states is formulated as shown below [103]:

$$\Delta E(3s)=(2S+1) \times G^2(3s\text{-}3d)/S$$

where G(3s-3d) is appropriate 3s-3d integral and S is the initial state spin. The equation above explains the proportionality of ΔE(3s) to the number of electrons in d orbitals. The values of ΔE(3s) for different Mn species in different oxidation states are given in Table 8 [104].

Table 8 ΔE(3s) values for Mn in different oxidation states

Compound	**ΔE(3s) (eV)**
Mn	4.1
MnO_2	4.5
Mn_2O_3	5.5
MnO	6.1

1.8 Flame atomic absorption spectroscopy

Flame atomic absorption is a useful technique for quantitative chemical analyses. In this technique, a solution of the sample is introduced into a flame in the form of a fine spray. The mechanism of obtaining atomic vapor is very complex, but it is basically illustrated in Fig.5 [105].

The solvent evaporates, leaving the dehydrated salt. The salt is dissociated into gaseous atoms. A certain fraction of these atoms can absorb energy from the

flame and be raised to an excited electronic state. These excited atoms, on returning to the ground state, emit photons of characteristic wavelength. These can be detected with a conventional monochromatic-detector setup.

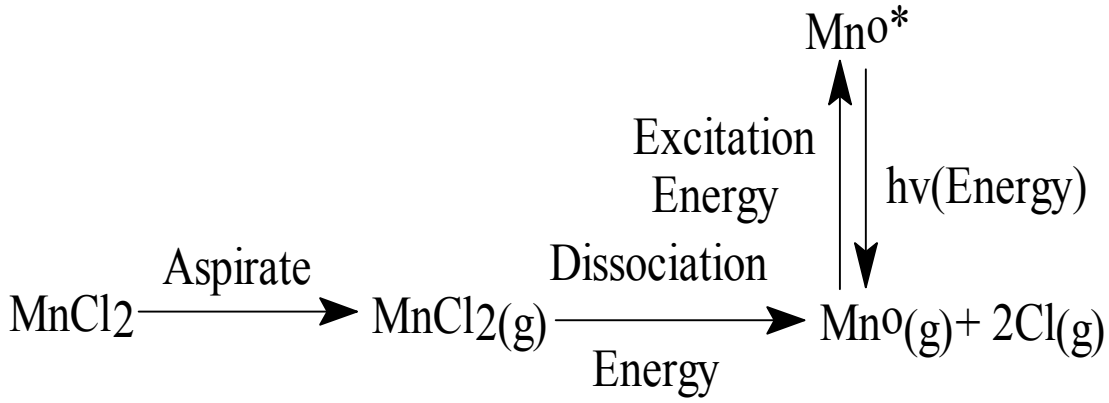

Figure 5 Mechanism of flame atomic absorption

The intensity of emissions is directly proportional to the concentration of the analyte in the solution being aspirated. By using the calibration curve of emission intensity as a function of concentration, the concentration of the desired analyte can be found.

2. EXPERIMENTAL

2.1 Catalyst preparation

The support TiO_2 (anatase) used is a commercial product (Degussa P 25, surface area 52 m^2/g) containing 90% anatase and 10% rutile.

The ion-exchanged sample was prepared by suspending the support (powder) in a 0.2 M aqueous solution of $MnCl_2$ for 2 h followed by alkalization (pH~13) of the mixture with aqueous ammonia (1:1) and immediate filtration. Then the sample was washed with deionised water, dried in air at 383 K and calcined for 1 h at 623 K and for 1 h at 723 K. This sample is denoted by MnTi-IE .

The impregnated sample was obtained by the incipient wetness technique (4% of nominal manganese content) using $MnCl_2$ solution which was alkalized with ammonia to pH~13 in the last stage of preparation procedure. The calcination procedure was the same as that used for the ion-exchanged catalyst. This sample is denoted as MnTi-I.

2.2. Chemical analysis

The sample was dissolved in a mixture (50 ml) containing 65% HNO_3 and 35% HCl (1:1). The solution was evaporated until 15 ml of the solution is left. This

procedure was repeated two times. After diluting to 50 ml with a mixture of (1:1) of HNO_3 and HCl, then the solution was filtered off and the filtrate was diluted to 100 ml. Then this solution of the sample was taken to Flame Atomic Absorption Spectrometer for analysis.

The flame atomic absorption spectroscopy was performed with Buck Scientific, Incorporated Model 200A Flame Atomic Absorption Spectrometer at the corresponding wavelength (for Mn λ=279.5 nm).

2.3 X-ray photoelectron spectroscopy measurements

XPS measurements were performed by using a Kratos ES300 spectrometer equipped with Mg Kα radiation source. The C1s line (B.E=285.0 eV) from residual hydrocarbons deposited on the surface of the sample was used as a reference. The pressure in the UHV chamber of the spectrometer was kept below 1.0×10^{-8} Torr.

The powdered catalyst was introduced into copper holder and pressed. It was attached to the probe of the spectrometer. The probe together with sample attachment was introduced into the UHV chamber of the spectrometer for analysis.

2.4 Visible absorption spectroscopy

The self-supporting discs of the MnTi-IE catalyst were prepared for the visible absorption studies. The visible absorption spectra of the self-supported disc of

the MnTi-IE catalyst were recorded with a Cary 5E UV-vis-NIR spectrometer where the reference substance was the catalyst support, titania.

2.5 Absorption measurements

2.5.1 Activation of the samples

Self-supporting discs were obtained by pressing the powdered catalysts under a pressure of 7 tons. The disc was cut to a pellet (9 mm x 15 mm) and placed in a pyrex glass sample holder and introduced into IR cell made of pyrex glass. The samples were activated in the evacuated IR cell at 673 K for 1 h, heating under 100 Torr of oxygen for 1 h at 673 K, and evacuation for 1 h at the same temperature.

2.5.2 Experimental setup for IR absorption Measurements

Specially designed IR cell equipped with NaCl windows was used in the absorption IR measurements (Fig.6(A)). The cell is 400 mm long with a diameter of 25 mm and is connected to a vacuum/adsorption apparatus. It has a sample introduction compartment. One end of the cell (IR-end) is specially designed allowing the installation of NaCl windows and ensuring a short path length of the IR beam. The other end of the cell (activation-end) was used for activation of the sample. This end can be placed in a small homemade furnace for heating of the

sample to desired activation temperature. The activation temperature was achieved by using a constant voltage supplier controlled manually. For reading the temperature a Thermocax chromel-alumel thermocouple was used. The transfer of the sample from one end of the cell to the other end was accomplished by tilting the cell and allowing the sample holder to slide along. The Pyrex cell is connected to the manifold by an on-off valve, which allows application of vacuum or introduction of gases.

The vacuum/adsorption apparatus is equipped with a manifold for introduction of various gases or mixtures of gases and contains 4 gas inlets (Fig.6(B)). The vacuum was achieved by a diffusion pump backed up with rotary pump. The pumps were isolated from adsorption system by a homemade liquid nitrogen trap, which also serves for purification of the applied gases.

(A)

(B)

Figure 6 (A) IR cell connected to vacuum/adsorption apparatus
(B) Vacuum/adsorption apparatus

2.5.3 Adsorption of carbon monoxide and formic acid on the catalysts

After the activation process and cooling down to room temperature, the sample is transferred to the IR end of the glass cell for IR measurements. The FTIR spectra were recorded with a BOMEM 102 with a DTGS 2 mm detector at a resolution of 4 cm^{-1} (256 scans).

Carbon monoxide adsorption was accomplished at room temperature under pressures of CO ranging from 0.5 Torr to 30 Torr to the catalysts. IR measurements were performed after reaching the equilibrium.

Partial deuteroxylation of MnTi-IE and MnTi-I was achieved by introduction to the evacuated IR cell of D_2O (99.9%) vapor at 3 Torr for 15 minutes at 673 K and evacuation for 30 minutes at the same temperature. This procedure was repeated two times.

After the same activation process described above, formic acid (0.5 Torr) was introduced to the catalyst and after the equilibrium was established IR measurement were performed.

2.5.4 Adsorption of NO_x and NO/O_2 coadsorption on the catalysts

NO adsorption was performed at room temperature introducing the respective NO under the given pressure and the time evaluation of the IR spectra with the time was followed.

Adsorption of NO_2 was accomplished by the introduction of NO_2 under 2 Torr pressure at room temperature and thermal stability of the adsorbed NO_2 was studied in the 373-673 K temperature range.

Coadsorption of NO and O_2 was accomplished at room temperature by introducing a gas mixture (52 Torr) of NO and O_2 (1:3.2) to the samples and the time evaluation of IR spectra was followed.

The thermal stability of the adsorbed NO_x species was studied by heating the sample for 10 min under vacuum in the temperature range 373-673 K.

2.5.5 Adsorption of n-decane on the MnTi-IE catalyst

Adsorption of n-decane on the MnTi-IE sample was achieved using 0.6 Torr of n-decane. The changes in the FTIR spectra after heating for 10 min in the temperature range 273-573 K were monitored.

2.5.6 Adsorption of n-decane on NO_x-precovered catalysts

The catalyst was in contact at room temperature with a gas mixture (52 Torr) of NO and O_2 (1:3.2). After achieving equilibrium (20 minutes) the system was evacuated for 10 minutes and then n-decane (0.6 Torr) was introduced to the catalysts.

The interaction between the adsorbed n-decane and NO_x species was studied by heating the closed IR cell in the temperature range 373-573 K for 10 min.

3. RESULTS AND DISCUSSION

3.1 Results

3.1.1 Chemical analysis

The chemical analysis was performed only for the ion-exchanged sample. The manganese content in the MnTi-IE catalyst is 1.9 wt%. The impregnated catalyst MnTi-I, has 4 wt% of nominal manganese content.

3.1.2 XPS measurements performed on the catalysts

The XPS spectra of the catalysts are shown in Fig.7. In order to differentiate between the different oxidation states of manganese, the magnitude of 3s multiplet splitting is used as already mentioned in the introduction part. The values for MnTi-I and MnTi-IE are 5.6 and 5.2 eV, respectively. Based on this we can conclude that a mixture of Mn^{2+} and Mn^{3+} ions is present on the impregnated catalyst and only Mn^{3+} ions are present on the ion-exchanged ones. The Mn $2p_{3/2}$ binding energy has a value of 642 eV for both catalysts, which is similar to those of bulk manganese oxides (640.5-643 eV) [103,104]. From this value it is difficult to estimate the degree of interaction of the deposited manganese ions with the surface of the support.

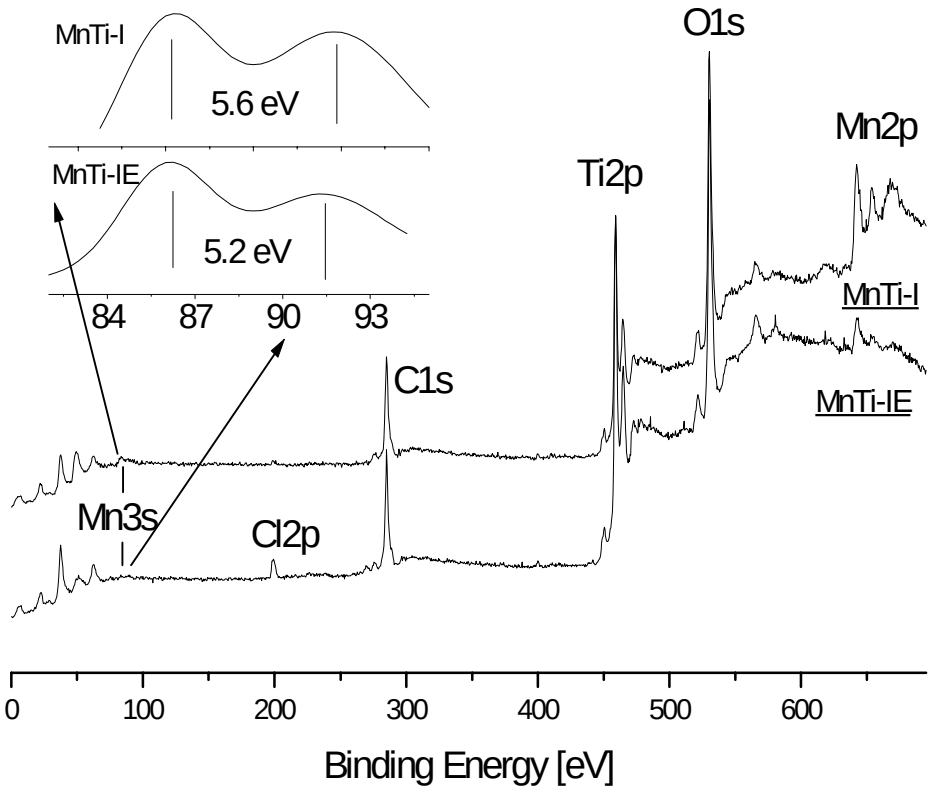

Figure 7 X-ray photoelectron spectra of the MnTi-IE and MnTi-I catalysts

3.1.3 Visible absorption spectroscopy

The visible absorption spectrum of the catalyst MnTi-IE taken in the 300-2000 nm region displays a broad absorption band due to the dark color of the sample (Fig.8). Two distinct maxima between 700-900 and at about 1025 nm are observed which correspond to different d-d transitions of Mn^{3+} ions [106].

It was not possible to obtain the visible absorption spectrum of the catalyst MnTi-I by application of the same technique because of the very strong absorption of this sample.

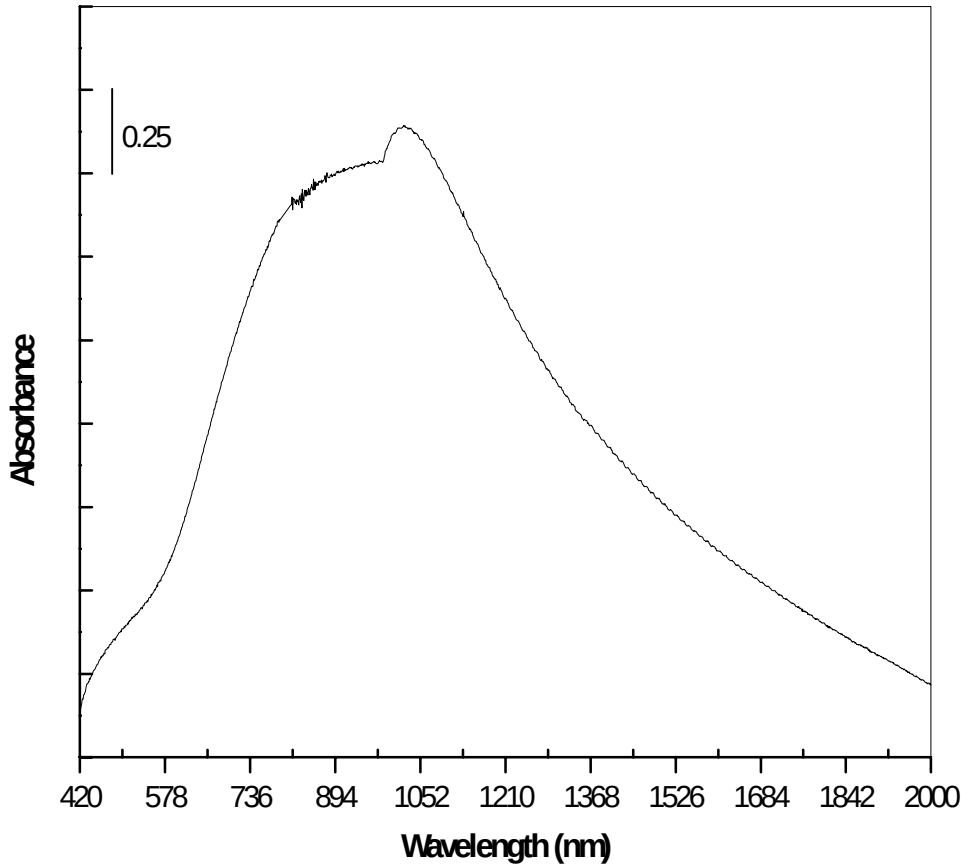

Figure 8 Absorption spectrum in the visible range of the catalyst MnTi-IE taken under ambient conditions

3.1.4 Adsorption of CO on the catalysts

3. 1.4.1 FTIR spectra of the activated samples

The FTIR spectra of TiO_2, MnTi-IE and MnTi-I catalysts in the OH stretching region are shown in Fig.9. A series of bands between 3735 and 3640 cm^{-1} characteristic for anatase [107] are observed in the spectrum of the support. The band at 3745 cm^{-1}, according to some authors [108,109], is due to presence of silicon. However, we are of the opinion that the band at 3745 cm^{-1} corresponds to the Ti-OH groups. The extent of participation of the surface OH groups of the support in the process of .manganese deposition depends on the method of preparation used. The low-frequency (i.e., the more acidic) OH groups of the support are involved to a larger extent in the impregnation process whereas the reverse is observed in the ion-exchange process. The MnTi-I catalyst exhibits a broad band between 3550-3200 cm^{-1}, which indicates the presence of H-bonded hydroxyl groups. A certain amount of H-bonded hydroxyls are also observed also on MnTi-IE sample. From these experimental data it is difficult to determine if residual OH groups of the manganese containing catalysts are of Ti^{4+}-OH type or coordinated to manganese ions. No other bands are detected at lower wavenumbers.

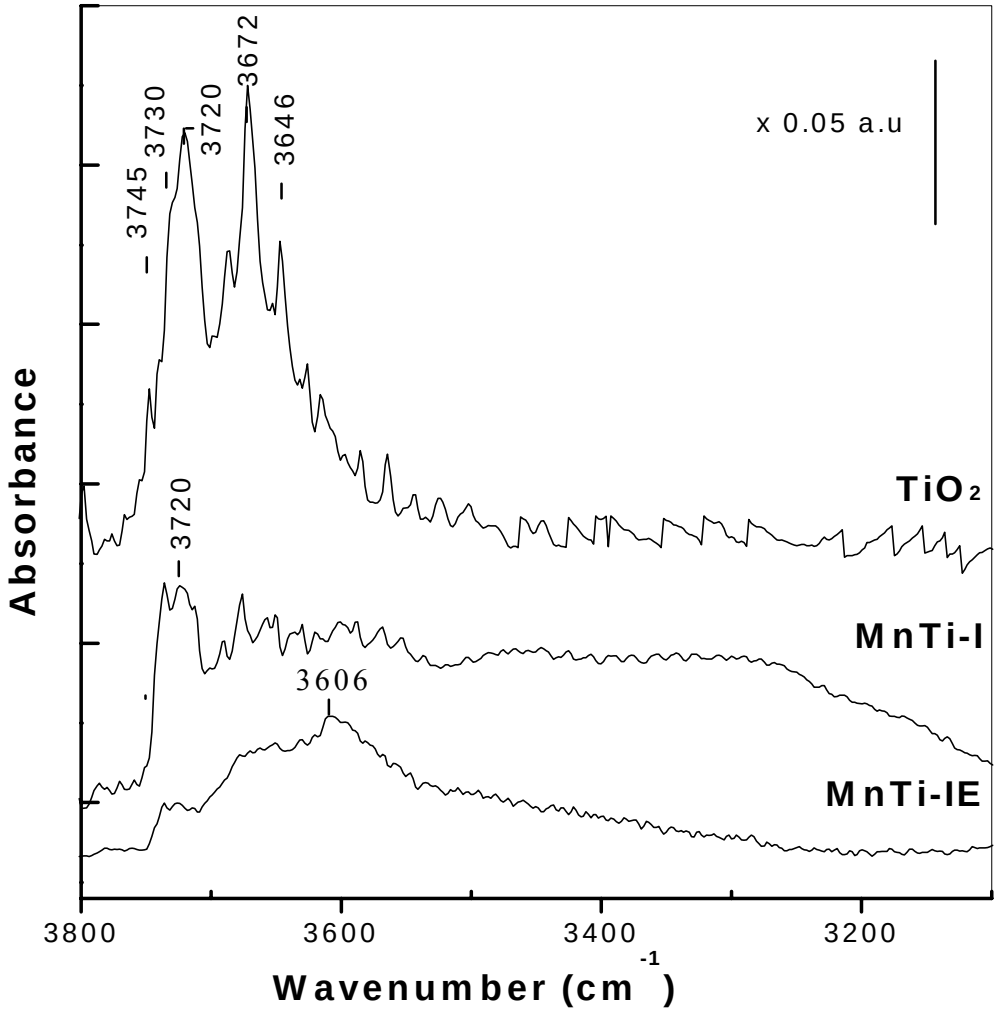

Figure 9 FTIR spectra of catalysts studied in the OH stretching region

3.1.4.2 FTIR spectroscopy of adsorbed CO

3.1.4.2.1 The support

The spectra of adsorbed CO (30 Torr) on activated TiO_2 and MnTi-IE at room temperature are shown in Fig.10. CO adsorption (30 Torr) at room temperature on the TiO_2 sample leads the appearance of two bands with maxima at 2206 and 2188 cm^{-1} (Fig.10). They are the characteristic of the CO stretching modes of two kinds of Ti^{4+}-CO surface carbonyls, formed with the participation of the strong (α) and weak (β') Lewis acid sites, respectively [107,110-112]. The intensities of these bands do not change with time at constant CO pressure and the surface Ti^{4+}-OH groups are not affected by the adsorbed CO. No other adsorbed species are observed under these conditions.

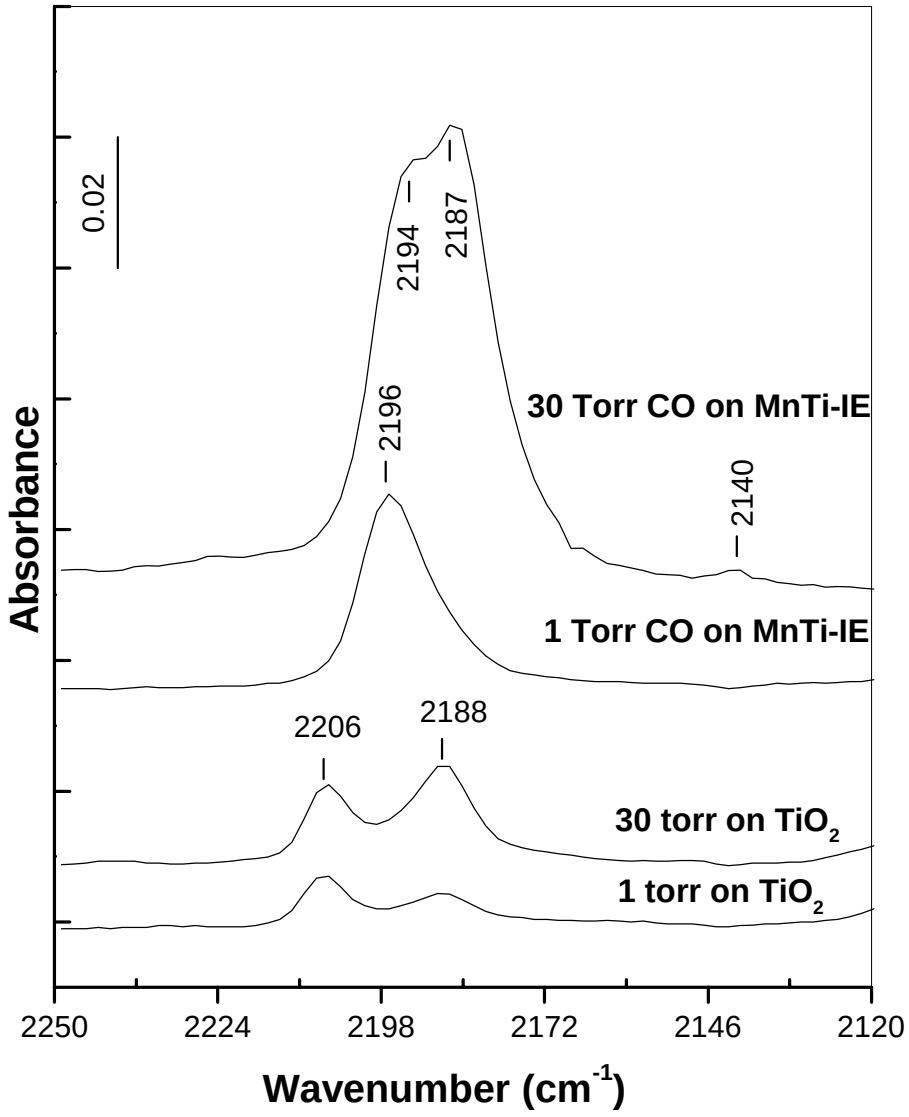

Figure 10 FTIR Spectra in the carbonyl region of adsorbed CO on TiO_2 and MnTi-IE catalyst at room temperature

3.1.4.2.2 The MnTi-IE catalyst

The adsorption of CO at 30 Torr (room temperature) on the activated MnTi-IE (Fig.10) leads the formation of Mn^{3+}-CO carbonyls (FTIR bands at 2194 and 2187 cm^{-1}). The higher frequency and the stability of the carbonyl manifesting at 2194 cm^{-1} (which is present in the spectrum taken at 1 Torr of CO) are indicative of greater acidity of the respective adsorption sites [113]. The ν(CO) stretching frequencies of the corresponding carbonyls are very close to those observed on the anatase surface. The assignment of the bands at 2194 and 2187 cm^{-1} to two different kinds of Mn^{3+}-CO are based on XPS results, the behavior of these species in a CO atmosphere (see below) and the band intensities (about 5 times more intense than Ti^{4+}-CO carbonyl bands-see Fig.10).

The spectrum of MnTi-IE catalyst in the carbonyl region is characterized by another weak absorption at 2140 cm^{-1}. This band can be associated with Mn^{2+} ions whose amount is low and below the XPS detection limits. Another possibility could be formation of Mn^{2+} ions during CO adsorption. All the carbonyls detected are unstable and disappear from the spectrum upon evacuation of CO at room temperature.

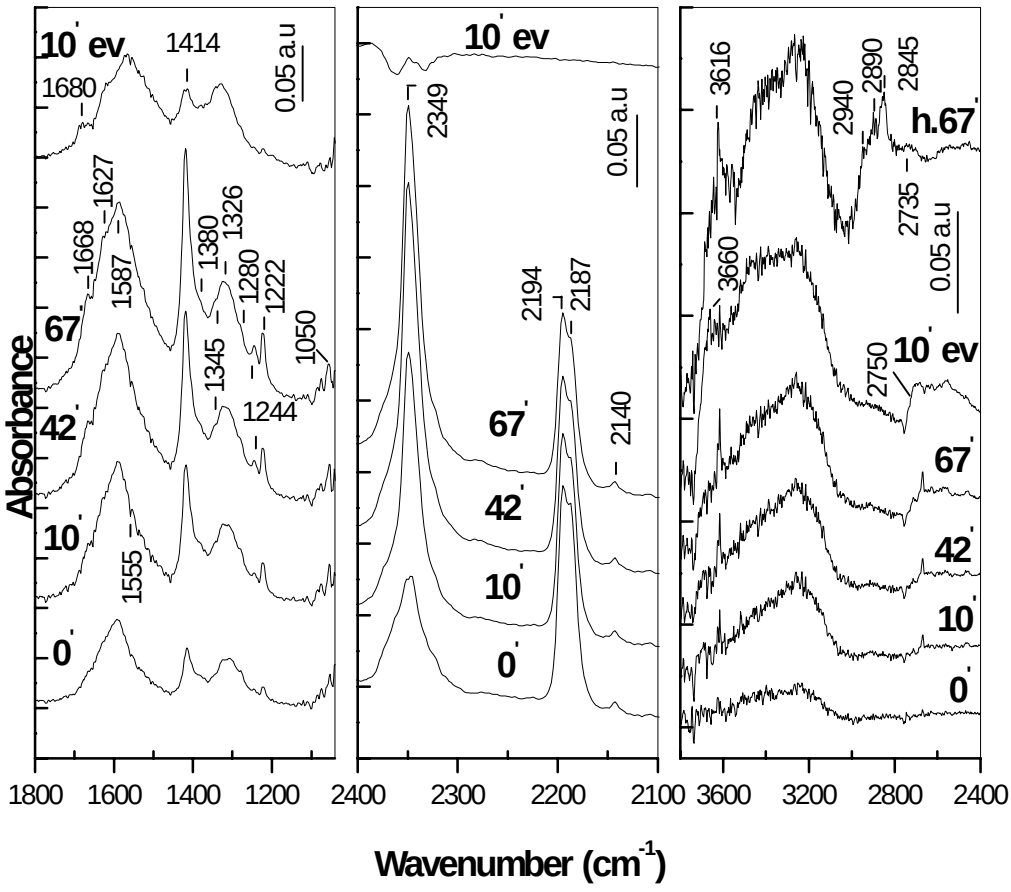

Figure 11 FTIR spectra of adsorbed CO (30 Torr) at room temperature on partially deuteroxylated MnTi-IE catalyst for the indicated times (After 10 min evacuation, (10' ev) and the spectrum of hydroxylated MnTi-IE in the OH stretching vibration region after 67 min in CO, (h.67'))

The adsorption of CO on the manganese-containing samples is a time dependent process. In order to follow better the behavior of the surface hydroxyl groups after admission of CO into the IR cell, a partially deuteroxylated MnTi-IE sample was used. The development of the spectra with time at constant CO pressure (30 Torr) is shown in Fig.11. The increase in the time of CO adsorption causes a gradual increase of the bands in the carbonate-carboxylate region (2000-1040 cm^{-1}). Simultaneously, the bands detected in the carbonyl region, at 2194 and 2187 cm^{-1}, decrease in intensity. It should be pointed out that the carbonyl bands of the partially deuteroxylated sample have a different intensity ratio compared to that of the hydroxylated sample. Obviously, the reason for this is the high-temperature treatment with D_2O vapor which causes some structural changes. The decrease in the intensity of the carbonyl bands is accompanied by a strong enhancement of the absorption in the 2400-2300 cm^{-1} region. The band at 2347 cm^{-1} is due to adsorbed CO_2 [87] and its growth with time indicates that oxidation of CO to CO_2 occurs. In the OH/OD stretching region (3650-3000/2740-2500 cm^{-1}), with the increase of CO contact time, the absorption due to H/D-bonded OH/OD groups rises in intensity. At the same time the negative band at 3730/2750 cm^{-1} due to isolated Ti^{4+}-OH/Ti^{4+}-OD groups gradually grows. The appearance of a positive absorption at 2668 and 3616 cm^{-1}, respectively, which is enhanced with time, is clearly observed. After 67 min of CO adsorption, the completely hydroxylated sample (spectrum (h.67') in Fig.11) displays the same bands detected in the partially deuteroxylated MnTi-IE sample in the OH portion of the spectrum. However, a group of bands at 2940, 2890 and 2845 cm^{-1}

together with the broad and weak at about 2735 cm^{-1} are detected in the CH region. The corresponding CD stretching vibrations are not observed because they fall in the region of strong carbonyl bands (2260-2160 cm^{-1}).

After evacuation for 10 min at room temperature the carbonyl bands due to adsorbed CO_2 disappears form the spectrum. The bands in the CH stretching and carbonate-carboxylate regions are observed with reduced intensities. Under these conditions new bands at about 1680 and 3660 cm^{-1} emerge in the spectrum.

The species in the carboxylate-carbonate region obtained after CO adsorption show low thermal stability: the intensities of the corresponding bands decrease strongly and almost simultaneously after evacuation for 5 min at 373 K. The heating at 473 K leads to complete desorption.

3.1.4.2.3 The MnTi-I catalyst

The adsorption of CO was also performed over a partially deuteroxylated sample. In this case, however, the establishment of the equilibrium between the gas phase and adsorbed species was slower. The complex band in the carbonyl region at 2186 cm^{-1} reached maximum intensity 10 min after admission (30 Torr) into the IR cell.

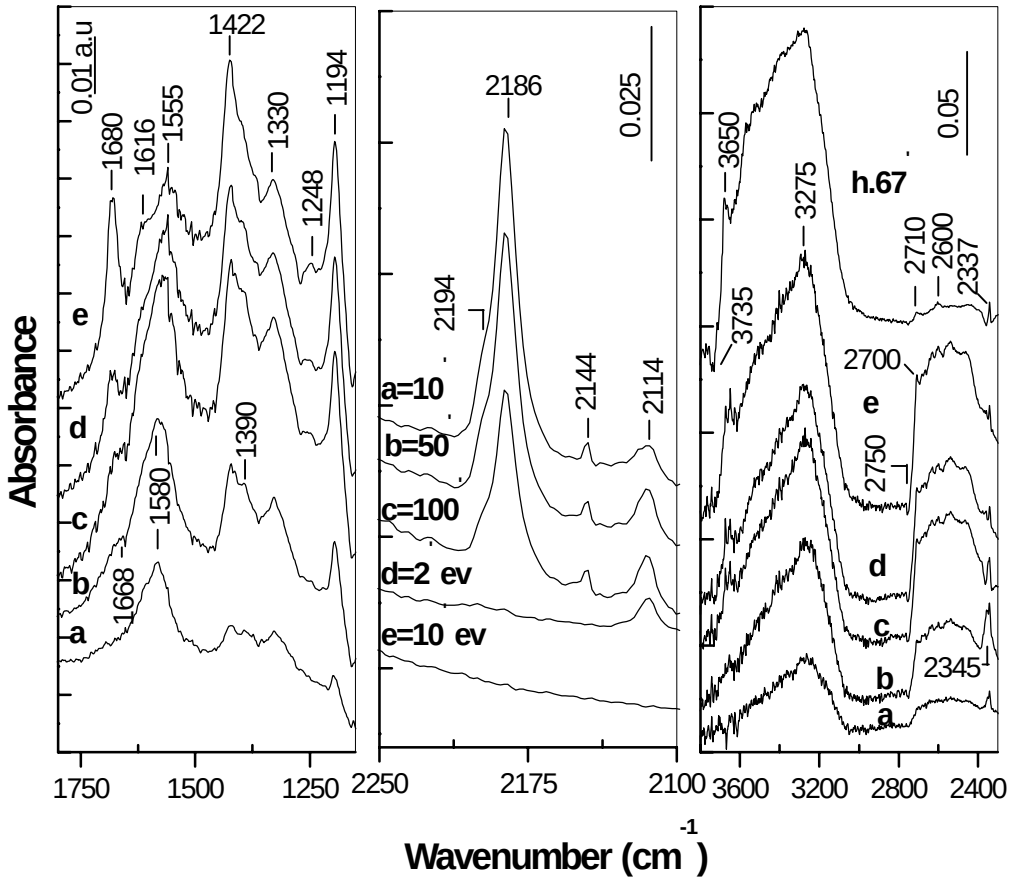

Figure 12 FTIR spectra of adsorbed CO (30 Torr) at room temperature on partially deuteroxylated MnTi-I catalyst for given times and after evacuation at room temperature for 2 min (residual pressure, $p=3.5\times10^{-1}$ Torr) (2' ev); and for 10 min ($p=3.3\times10^{-3}$ Torr)(10' ev), the spectrum of hydroxylated MnTi-I catalyst in the OH stretching region after 67 min in CO (30 Torr) (h.67')

Under the conditions described, together with the band at 2186 cm^{-1} (which has a shoulder at about 2194 cm^{-1}), two weak bands at 2144 and 2114 cm^{-1} are observed in the carbonyl region (Fig.12). The absorption at 2144 cm^{-1} can not be assigned to the ν(CD) stretching mode because it is detected also in the hydroxylated MnTi-IE and MnTi-I samples. Taking into account the XPS results on the MnTi-I catalyst and the FTIR data on the MnTi-IE sample, the complex absorption with the maximum at 2186 cm^{-1} can be attributed to the two types of Mn^{3+}-CO carbonyls, whereas the two weak bands at 2144 and 2114 cm^{-1} are assigned to different kinds of Mn^{2+}-CO species.

With increase in contact time, the intensity of the unresolved band due to the Mn^{3+}-CO carbonyls gradually decreases, whereas the population of Mn^{2+}-CO carbonyls showing absorption at 2114 cm^{-1} is enhanced almost twice after 100 min in CO atmosphere. The intensity of the band at 2144 cm^{-1} (corresponding to Mn^{2+}-CO carbonyls seems not to be affected by the time. In the carbonate-carboxylate region, with increase of exposure time numerous bands develop, which can be grouped as follows (see the arguments below): (i) the set of bands with maxima at 1650-1500 and 1400-1250 cm^{-1} and (ii) the bands at 1680, 1422 and 1194 cm^{-1}.

As in the case of the MnTi-IE catalyst the absorption due to H/D-bonded OH/OD groups (3800-2400 cm^{-1}) grows in intensity with the extent of contact time. This is accompanied by the appearance of a negative OD band at 2750 cm^{-1} indicating that consumption of isolated Ti^{4+}-OD groups takes place. The sharp bands at 2700 and 3650 cm^{-1}, respectively, corresponding to formation of isolated OD/OH

groups increase in intensity. Here again, evolution of CO_2 is observed, which is detected by the appearance of two bands between 2400 and 2300 cm^{-1} due to adsorbed CO_2. These bands reached maximum intensity after 30 minutes contact with CO (not shown in Fig.11) and started to decay at more prolonged (50 min and above) adsorption times. This is an indication that transformation of the adsorbed CO_2 into other surface forms occurs.

Figure 12 also shows the spectrum of hyroxylated MnTi-I catalyst in the OH stretching region taken after 67 minutes of CO adsorption (spectrum (h.67')). It is characterized by the same spectral features in the OH stretching observed for the deuteroxylated sample. In addition, it contains two weak bands at 2710 and 2600 cm^{-1} which corresponds to ν(CH) stretching modes.

The evacuation of the deuteroxylated sample at room temperature to different residual pressures (Fig.12, spectra (2' ev) and (10' ev)) causes the following changes in the IR spectra:

(i) Gradual increase is observed in the intensity of the H/D-bonded OH/OD groups and that of isolated OH/OD groups characterized by the absorption at 3650/2700 cm^{-1}.

(ii)The absorption corresponding to Mn^{3+}-CO and the band at 2144 cm^{-1} disappear form the spectrum at a residual pressure of $3.5x10^{-1}$ Torr. The carbonyl species characterized by the ν(CO) stretching frequency at 2144 cm^{-1} resist the short evacuation which is consistent with their assignment to Mn^{2+}-CO carbonyl.

(iii) In the carbonate-carboxylate region the set of the bands at 1680, 1422 and 1194 cm^{-1} increases in intensity. This increase is at the expense of the complex bands centered at 1580 and 1330 cm^{-1} and is more pronounced at a residual pressure of $3.3x10^{-3}$ Torr. This is an indication of that under these conditions transformation of some surface species into others take place.

The changes in the spectra are more clearly visible in the subtraction spectra (Fig.13) obtained from the spectra recorded after 10 min ($p=3.3x10^{-3}$ *Torr*) and 4 min of evacuation ($p=5.5x10^{-3}$ *Torr*), respectively, minus that taken after 2 min evacuation ($p=3.5x10^{-1}$ *Torr*). The constant intensity ratio between the bands at 1680, 1430 and 1194 cm^{-1} which is observed at different evacuation times and different residual pressures in the IR cell, respectively, indicates that these bands belongs to the same surface species. Similarly, it is concluded that the absorption in the 1650-1500 cm^{-1} region together with the complex band centered at 1330 cm^{-1} characterizes another species.

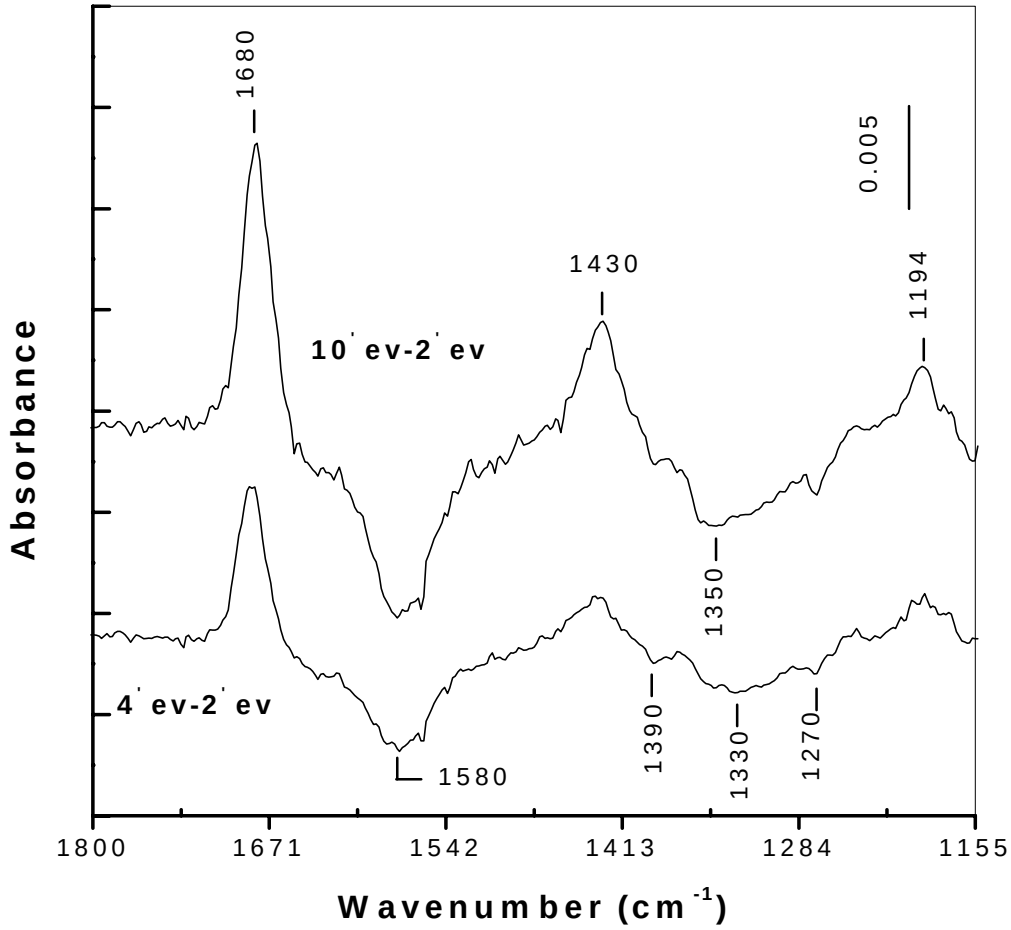

Figure 13 FTIR spectra of partially deuteroxylated MnTi-I catalyst in the carbonate-carboxylate region obtained by the subtraction of the spectrum of adsorbed CO (30 Torr) followed by evacuation for 2 min at room temperature ($p=3.5x10^{-1}$ *Torr*) from the spectrum after 4 min evacuation ($p=5.5x10^{-3}$ *Torr*) (4' ev-2' ev) and from the spectrum after 10 min of evacuation ($p=3.3x10^{-3}$ *Torr*) (10' ev-2' ev)

3.1.4.3 Room temperature adsorption of formic acid on the MnTi-IE sample

The FTIR spectrum of the formic acid used in the adsorption experiments is characterized by the following bands: a broad and intense absorption with a maximum at 3430 cm^{-1} due to ν(OH) of H-bonded OH groups, bands with maxima at 2947 (ν(CH)) and 1718 cm^{-1} (ν(C=O)), a group of bands at 1396 and 1380-1320 cm^{-1} both due to coupling between in-plane O-H bending and C-O stretching of the dimer, and absorption at 1190 cm^{-1} (ν(C-O)). The unresolved absorption at about 1630 cm^{-1} is due to the δ(HOH) mode of water used for stabilization of the formic acid. The two bands with maxima at about 2714 cm^{-1} and 2560 cm^{-1} are due to the presence of the formate moieties. This spectrum is consistent with the literature data [114,115] for the prevailing dimeric form of the acid.

The FTIR spectra HCOOH (0.5 Torr) adsorbed at room temperature on the surface of the MnTi-IE catalyst and after 10 min of evacuation are shown in Fig.14. The spectra differ from the spectrum of the free acid indicating an interaction of the latter with the catalyst surface. The bands typical for formate species [98,117,118] are detected at 2960 ($\nu_{as}(CO_2^-)$+ δ(CH)), 2874 (ν(CH)) and 2735 cm^{-1} ($\nu_s(CO_2^-)$+ δ(CH)). To these species belongs the group of bands with the maxima at 1582, 1573, and 1555 cm^{-1} due to $\nu_{as}(CO_2^-)$ and the absorptions at 1368 and 1315 cm^{-1} which correspond to the $\nu_s(CO_2^-)$ mode of the formate ions, respectively. The splitting in the CO_2^- stretching vibrations suggests different type of coordinations and/or different adsorption centers [98, 117,118]. The band at 1380 cm^{-1} can be attributed to the

deformation vibration, δ(CH). This experimental fact shows that the adsorption of formic acid on the surface of the MnTi-IE is mainly dissociative, leading the formation of H-bonded OH groups (an intense and broad band between 3500 and 3000 cm^{-1} in the IR spectrum). The water present in the acid contributes also to this absorption. The band at about 1620 cm^{-1} is attributed to the δ(HOH) mode of the adsorbed water molecules although the existence of the formate species with the same $\nu_{as}(CO_2^-)$ frequency can not be excluded. The weak band at 1690 cm^{-1} (ν(C=O)) together with the unresolved weaker absorption in the OH region at about 3620 cm^{-1} (ν(OH)) suggests the presence of some undissociated formic acid on the catalyst surface. The former band is red-shifted compared to its position in the spectrum of free acid which indicates that HCOOH is coordinated through the carbonyl oxygen to a Lewis acid site. The surface species formed are stable toward evacuation at room temperature for 10 min. The increased intensity of the bands in the 1580-1300 cm^{-1} region suggests formation of an additional amount of formate species. Finally, the weak negative bands at 3730-3670 cm^{-1} in the OH stretching region indicate that the isolated OH groups in the catalyst are altered during the adsorption of formic acid.

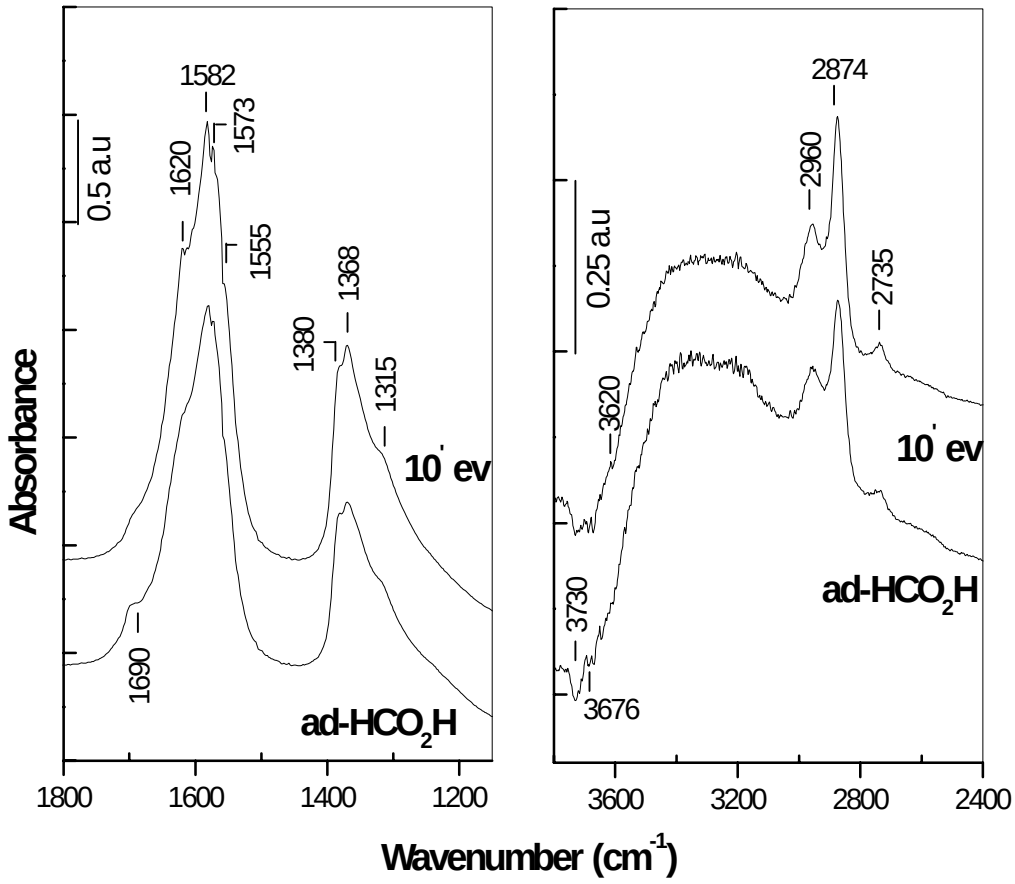

Figure 14 FTIR spectrum of adsorbed formic acid (0.5 Torr) on MnTi-IE catalyst (ad-HCO_2H) and after 10 min evacuation at room temperature (10' ev)

3.2 Discussion

3.2.1 Coordination number of deposited manganese ions

According to the XPS data the ion-exchanged catalyst, MnTi-IE, contains only Mn^{3+} ions. Manganese (III) usually forms six- and five-coordinated complexes [106]. The six-coordinated Mn^{3+} complexes are subject to Jahn-Teller effects [106,118,119] and the absorption spectra are difficult to interpret. The analysis of literature data [106] shows that five- and six-coordinated Mn^{3+} ions in the bulk coordination compounds have an overlapping region in the visible absorption spectra between 500 and 650 nm when the ligating atom is oxygen. However, they can be distinguished by the absorption at 1050-1100 nm ($^5A_{1g} \rightarrow {}^5B_{1g}$) for six-coordinate Mn^{3+} ions and by that at 730-830 nm for five-coordinated species. Based on this, it is possible to conclude that the catalyst MnTi-IE contains both five- and six-coordinate Mn^{3+} ions. The wide unresolved absorption with a maximum at about 850 nm is attributed to the d-d transition of five-coordinated Mn^{3+} ions whereas the band at about 1015 nm can be assigned to the transition $^5A_{1g} \rightarrow {}^5B_{1g}$ of six-coordinated species which are subject to Jahn-Teller distortion. Probably, the concentration of six-coordinated Mn^{3+} ions is higher. This conclusion is drawn by comparison of the molar absorptivities for the two transitions. The molar absorptivity for the transition $^5A_{1g} \rightarrow {}^5B_{1g}$ in the six-coordinated complexes is lower by approximately one order of

magnitude than that for the transition at 730-850 nm in the case of five-coordinated Mn^{3+} ions [106].

3.2.2 Localization of the manganese ions on the surface of the support

According to the chemical analysis the catalyst MnTi-IE contains 1.9 wt% of manganese which corresponds to a surface concentration of 4 Mn^{3+} ions/nm^2. On the anatase surface there are 4-7 Ti^{4+}/nm^2 and the concentration of the isolated Ti^{4+}-OH groups is not more than 0.5 OH groups/nm^2 [110,111]. If the anchoring sites are the hydroxyl groups and in the vicinity of the coordinatively unsaturated (cus) Ti^{4+} ions (assuming one Mn^{3+} ion per two Ti^{4+}), a monolayer coverage would be achieved at maximum 1.9 wt% of manganese. Hence, the experimentally determined manganese loading in the ion-exchanged catalyst corresponds to a monolayer coverage.

The adsorption of CO on activated MnTi-IE sample revealed the presence of two types of Mn^{3+} ions, which form two kinds of linear Mn^{3+}-CO carbonyls with ν(CO) stretching frequencies at 2194 and 2187 cm^{-1}, respectively. These two adsorption sites differ in their strength, the former being the stronger; i.e., they are characterized by a lower coordination saturation. Based on the loading determined by the chemical analysis, it is reasonable to assume that Mn^{3+} ions are localized mainly in the vicinity of cus Ti^{4+} ions. Several types of (cus) titanium ions exist on the surface of anatase but only α- and β'-Ti^{4+} centers can be detected by adsorption of CO at room temperature [107,110-112]. The so-called β''- and γ-Ti^{4+} ions possess

low electrophilicity and can be monitored only in low-temperature experiments [107,112]. The surface concentration of the α-sites is the lowest [111]. Consequently, a higher concentration of Mn^{3+}ions localized in the vicinity of β- and γ-Ti^{4+} ions than that of those ions situated in the proximity the α-Ti^{4+} sites can be expected. According to the results of visible absorption spectroscopy, the Mn^{3+} ions are five- and six-coordinate species, the latter being more abundant. The CO adsorption experiments show that only monocarbonyls are formed; i.e., the manganese species contain only one coordination vacancy. Since the electronic spectra are taken under ambient conditions, it is possible to conclude that after the catalyst activation four- and five-coordinated Mn^{3+} ions are formed. Hence, the following localization of the cus Mn^{3+} ions can be proposed:

- The vicinity of the of β- and γ-Lewis acid sites on anatase (which represent five-coordinated Ti^{4+} ions [[110,111]) is occupied by five-coordinated Mn^{3+} ions (type I). The carbonyls formed with their participation are characterized by absorption at 2187 cm^{-1}.
- Four-coordinated Mn^{3+} ions (type II) block the α-Lewis sites of the support (four-coordinated Ti^{4+} ions [[110,111]) and the form carbonyls with ν(CO) stretching frequency at 2194 cm^{-1}.

Finally, the existence of five-coordinate Mn^{3+} ions localized on the sites which correspond to surface Ti^{4+} to surface Ti^{4+}-OH groups participating in the deposition process should also be taken into account. It is believed [[110,111] that the Ti^{+4} ions, to which the residual OH groups are bound, are five coordinated.

No exposed Ti^{4+} ions are expected on the surface of MnTi-IE catalyst. However, this suggestion cannot be proved unambiguously by room-temperature adsorption of CO. In addition, the close frequencies and strong absorption of Mn^{3+}-CO carbonyls hinder the detection of Ti^{4+}-CO carbonyls eventually formed at room temperature.

According to the XPS data and FTIR Spectroscopy of adsorbed CO MnTi-I catalyst originally contains Mn^{2+} in addition to the two types of cus Mn^{3+} ions. Probably, the vicinity of the cus Ti^{4+} sites of the support is partially occupied by Mn^{2+} ions as well. The carbonyl band at 2114 cm^{-1} is assigned to these species. The presence of a high frequency shoulder to this band indicates that the Mn^{2+} ions are of two kinds, like the Mn^{3+} ions. The Mn^{2+} ions characterized by the carbonyl band at 2144 cm^{-1} are envisaged as products of the CO adsorption. The difference of 30 cm^{-1} in the stretching frequencies of the corresponding carbonyls is probably due to a difference in the σ components of the bond between Mn^{2+} and CO [120]. The carbonyl band at 2114 cm^{-1} present in the spectrum after short evacuation (i.e., the corresponding carbonyl is more stable) can be attributed to Mn^{2+} ions which form a bond with CO with a considerable π contribution. The behavior of the carbonyls characterized by the adsorption at 2144 cm^{-1} (not observed at low equilibrium pressures of CO) indicates that the adsorption centers are weak.

During the adsorption, CO is oxidized to CO_2 which further interacts with the basic surface sites, i.e. O^{2-} ions and OH groups producing surface carbonates and hydrogen carbonates (see below). The CO_3^{2-} and HCO_3^{2-} ions can attract electron

density via an inductive effect from the neighboring Mn^{2+} ion formed during the reaction. As a result the electrophilicity of the Mn^{2+} ions increases. This leads to an enhancement of the σ component of the bond between CO and the metal cation. As a result the C-O stretching frequency is increased. A similar effect was reported by Sussey et al [121]: the C-O stretching frequencies of CO adsorbed on ZnO before and after CO_2 adsorption differ by about 30 cm^{-1}.

Probably the MnTi-IE and MnTi-I catalysts have different morphologies which affect the rates of CO chemisorption. This process is much slower for the MnTi-I catalyst. The reason for this could be the preferential CO adsorption on sites near the surface of the pellet. This suggests the presence of MnO_x particles which are not covered by CO immediately after CO admission on MnTi-I catalyst.

3.2.3 CO chemisorption

The Mn^{3+}-CO carbonyls produced on the surface of the catalysts studied are not stable in a CO atmosphere. This is shown by the decrease in the intensity of the corresponding carbonyl bands and by the appearance of absorption typical for linearly bonded CO_2 and various carbonate-carboxylate structures. The formation of CO_2 from CO is associated with the oxidizing properties of Mn^{3+} ions [121]. The involvement of surface OH groups and the appearance of a series of bands in the carbonate-carboxylate region suggest formation of hydrogen carbonate or/and formate species.

The similarity of the FTIR spectra of adsorbed formic acid to the spectra in the carbonate-carboxylate region obtained during CO adsorption on the surface of MnTi-IE catalyst implies the existence of similar adsorption forms in both cases. The adsorption of formic acid on this catalyst is dissociative, resulting in the appearance of formate species characterized by the complex absorption bands in the 1630-1550 and 1400-1250 cm^{-1} regions. A similar set of bands, between 1630 and 1550 cm^{-1} and the complex absorption at 1350-1250 cm^{-1}, is observed upon CO absorption on the MnTi-IE catalyst. This allows us to attribute these bands to $\nu_{as}(CO_2^-)$ and $\nu_s(CO_2^-)$ stretching vibrations of formate species, respectively, which are formed during the reactive adsorption of CO. This assignment is supported by the appearance of weak bands at 2940, 2890, 2845 and 2750 cm^{-1} on the sample containing OH groups with the natural isotopic content of hydrogen, their absence in the spectra of a deuteroxylated sample, the appearance in the latter of a weak absorption at 1050 cm^{-1} in the latter. The bands at 2940 and 2750 cm^{-1} are typical of formate ions [87,117] and are due to the Fermi resonance between the ν(CH) fundamental (at 2890 cm^{-1}) and combinations or overtones of the bands in the carboxylated region (see Table 9). The band at 1050 cm^{-1} is characteristic for the δ(CD) mode of the DCO_2^- ion [87]. The pair of the bands at 1414 and 1222 cm^{-1} can be assigned to the splitting of the ν_3 vibration of monodentate carbonate ($\Delta\nu_3$<300 cm^{-1}) [87] whose ν_1 stretching mode is positioned at 1075 cm^{-1}. The bands at 1668 cm^{-1} (ν(C=O)) and 1244 cm^{-1} (ν(C-O)) together with the sharp band at 3616/2668 cm^{-1} (ν(OH)/ ν(OD)) are attribute to

formic acid formed on the surface of the catalyst MnTi-IE. The band assignment is presented in Table 9.

Similar arguments for the interpretation of the bands observed in the carbonate-carboxylate region are applied to the catalyst MnTi-I (see Table 9 and Fig.12). However, this sample displays different behavior during the evacuation at room temperature, allowing the bands at 1680 (ν_{as}(C=O)), 1422 (ν_{s}(C=O)) and 1194 cm^{-1} (δ(OH)) to be attributed to hydrogen carbonate species [87]. The absorption at 3600/2700 cm^{-1} (which increases simultaneously with the bands cited above during the evacuation) is also assigned to these species. The latter band corresponds to the ν(OH/OD) stretching frequency of the hydrogen carbonate ion.

The positive absorption due to H/D-bonded OH/OD groups which develops simultaneously with the bands in the carbonate-carboxylate region and which is observed on both catalysts is an indication of interaction of the adsorbed forms (formates, carbonates, and/or hydrogen carbonates) with the surface OH/OD groups originally present in the catalyst. However, the alteration of the latter can not be observed because the expected negative OH/OD bands fall in the same region of the strong positive band between 3700-3000 and 2700-2400 cm^{-1}, respectively.

The complex shape of the bands assigned to formate ions implies the existence of at least three kinds of formate species differing in their structure and type of coordination site, e.g., two types of Mn^{3+} ions and probably some exposed Ti^{4+} ions. However, exact determination of the coordination type and site(s) is difficult due to the simultaneous development of the corresponding bands during the

CO adsorption and the comparable stabilities of the formate structures toward evacuation at ambient and higher temperatures.

Table 9 Assignment of FTIR bands observed in the carbonate-carboxylate region during adsorption of 30 Torr CO at room temperature on MnTi-IE and MnTi-I catalysts

Catalyst	**Frequency (cm^{-1}) and the mode**	**Possible assignment**	**Refs.**
MnTi-IE	2940 ($\nu_{as}(CO_2^-)$+ δ(CH)) 2890,2845 (ν(CH)) 2735 ($\nu_s(CO_2^-)$+ δ(CH)) 1630-1550 ($\nu_{as}(CO_2^-)$) 1380(δ(CH)), 1350-1250 ($\nu_s(CO_2^-)$)	Formate species coordinated to Mn^{3+}	87, 116, 118
	3616(ν(OH)) 1668 (ν(C=O)), 1244 (ν(C-O))	Adsorbed formic acid	This work
	1414,1222(splitting of ν_3 mode)	Monodentate carbonate	87,116
MnTi-I	2710 ($\nu_s(CO_2^-)$+ δ(CH)) 2600 (comb, 1270+1330) 1630-1500 (($\nu_{as}(CO_2^-)$) 1390 (δ(CH)), 1350-1250 (ν(C-O))	Formate species coordinated to Mn^{3+}	87, 116, 118
	3616 (ν(OH)) 1668 (ν(C=O)), 1248 (ν(C-O))	Adsorbed formic acid	This work
	3650 (ν(OH)), 1860 (ν_{as}(C=O)) 1422 (ν_s(C=O)), 1194 (δ(OH))	Hydrogen carbonate species	87

The formation of formate species during CO adsorption can be described [117] as a nucleophilic attack of basic OH group on the carbonyl carbon of a coordinated CO molecule (Fig.15-A). The surface OH groups which are involved in this reaction are the Ti^{4+}-OH groups characterized by the absorption band at 3730 cm^{-1} (shifted to 2750 cm^{-1} after the deuteroxylation). The participation of hydroxyls with lower OH stretching frequencies is not excluded but it could not be monitored. The

observed decrease in the intensity of the bands corresponding to the Mn^{3+}-CO carbonyls and the respective Ti^{4+}-OH groups and the parallel growth of the bands due to the formate species support the proposed reaction scheme.

Some molecularly adsorbed formic acid is detected on the surface of the catalyst MnTi-IE. The formation of HCOOH can be explained by coordination of a proton from the acidic OH group with a formate species (Fig.15-B).

The experimental results show that the appearance of the formate species is associated only with the Mn^{3+} ions: the band at 2114 cm^{-1} due to Mn^{2+}-CO carbonyls (catalyst MnTi-I) does not decrease in intensity during the CO adsorption at constant pressure. In contrast, there is an enhancement of its intensity after prolonged (100 min) contact of the catalyst with CO; i.e., part of the Mn^{3+} ions is reduced to Mn^{2+} in the CO atmosphere. The CO_2 produced is coordinated on the surface and forms carbonates (MnTi-IE catalyst) and hydrogen carbonates (MnTi-I catalyst) during CO adsorption. The stabilization of the hydrogen carbonate species on the surface of the impregnated catalyst probably is favored by the Mn^{2+} ions. This suggestion is confirmed by the experimental fact that a similar process occurs to a much smaller extent on the surface of the MnTi-IE catalyst which contains originally Mn^{3+} ions.

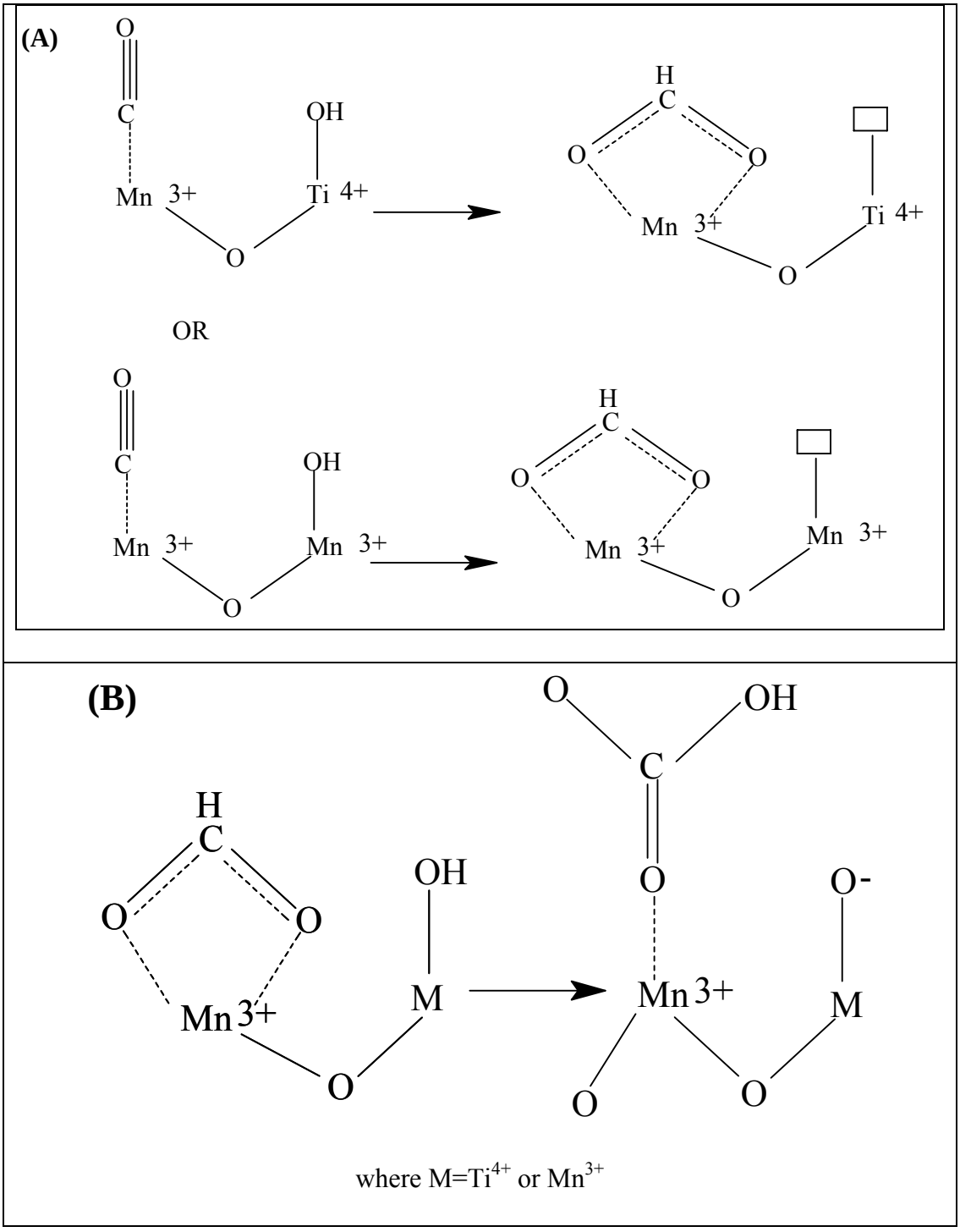

Figure 15 Mechanism of formation of formate species (A), and formic acid (B)

Finally, it should be noted that the frequencies of the formate species produced during CO adsorption differ slightly form those obtained from formic acid. The reason is the different mechanism of the formation of these surface forms which influences their structure. During the CO adsorption, the surface OH groups and Mn^{3+}-CO carbonyls are involved, whereas in the case of HCOOH the formation of HCO_2^- species is a result of dissociation of the acid. Variation of the frequencies of the formate ions produced by adsorption of formaldehyde, formic acid, or methanol oxidation on different oxide surfaces is reported also by other authors [117,123].

3.2.4 Conclusion

The results of the present investigation show that the application of the ion-exchange for deposition of manganese ions on titania (anatase) from manganese (II) chloride solution ensures a coverage by manganese oxide phase corresponding to a monolayer. The catalyst prepared by this method contains two kinds of Mn^{3+} ions differing in their coordinative saturation: five-coordinated Mn^{3+} ions located in the vicinity of the weaker Lewis acid sites and four-coordinated Mn^{3+} ions which block the stronger Lewis acid sites of the support. A small amount of the deposited manganese ions occupies part of the sites of the residual OH groups of the support participating in the synthesis process. This impregnated catalyst contains a mixture of Mn^{2+} and Mn^{3+} ions.

The adsorption of CO at room temperature on the catalyst studied results in the appearance of formate, carbonate and hydrogen carbonate structures. It is found that the formation of formate species is associated with the Mn^{3+} ions.

3.3 Adsorption of NO_X on the catalysts

3.3.1 Results and Discussion

3.3.1.1 The support

3.3.1.1.1 Adsorption of NO

The FTIR spectrum of adsorbed NO (10 Torr) on TiO_2 is shown in Fig.16. The adsorption of NO (10 Torr) on anatase at room temperature is a time dependent process (Fig.17). Immediately after the introduction of NO in the IR cell (spectrum (0')), a band at 1160 cm^{-1} and weak bands in the nitrosyl and nitrate-nitrite regions are detected. In the OH stretching region two negative bands between 3700 and 3600 cm^{-1} are observed together with a weak positive absorption with maximum at 3565 cm^{-1}. All these bands grow with the time, except the bands at 1160 and 1843 cm^{-1}: they reach saturation in 15 min (compare spectra (15') and (30') and see below). The evacuation for 10 min at room temperature causes decrease in the intensity of the

bands in the nitrosyl region (at 1913, 1843 and 1715 cm^{-1}) and that of the band at 1160 cm^{-1}. The bands in the 1625-1200 cm^{-1} region enhance their intensities. The negative band at 3718 cm^{-1} and positive absorption at 3565 cm^{-1} appear less intense. A broad absorption between 3600-3000 cm^{-1} is detected.

In order to assign the absorption bands, the subtraction spectra are considered (Fig.17). The spectrum (15'-0') shows that in the first period of 15 min, all of the bands in the 2000-1000 cm^{-1} region increase in intensity. In the next 15 min (spectrum 30'-0') the bands at 1625, 1610, 1580, 1550 and 1505 cm^{-1} grow simultaneously with the unresolved absorption in the 1300-1200 cm^{-1} region. The bands at 1843 and 1160 cm^{-1} do not change in intensity. This indicates that they belong to different species. Based on the sequence in the appearance of the IR bands and in accordance with the literature [99,124], the bands at 1625 and 1215 cm^{-1} are attributed to ν_3 splitting of bridged nitrates whereas the bands at 1505 and 1286 cm^{-1} characterize ν_3 splitting of monodendate ones. The bands due to ν_3 splitting of bidendate nitrates are at 1610, 1580, 1555 and 1215 cm^{-1}.

The formation of surface nitrates suggests that NO_2 is produced during the contact of NO with anatase surface. Since TiO_2 is considered non-reducible with NO at room temperature, the following interaction can be proposed as a source of NO_2:

$$2NO + OH^- \rightarrow NO_2 + NOH \quad (13) \text{ or}$$

$$3NO + OH^- \rightarrow NO_2 + 2NO^- + H^+ \quad (14)$$

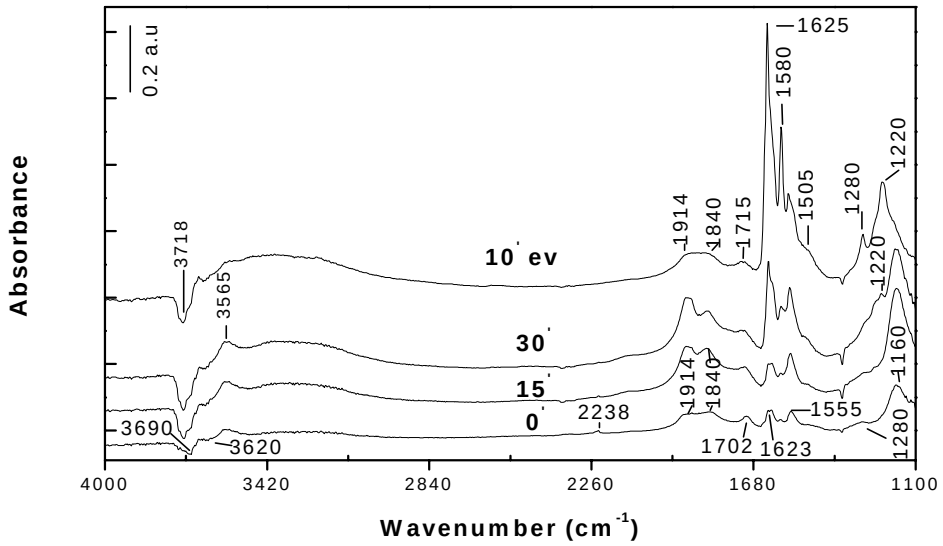

Figure 16 Time evolution of the FTIR Spectra of adsorbed NO (10 Torr) on TiO_2 and after 10 min evacuation (10' ev) at room temperature

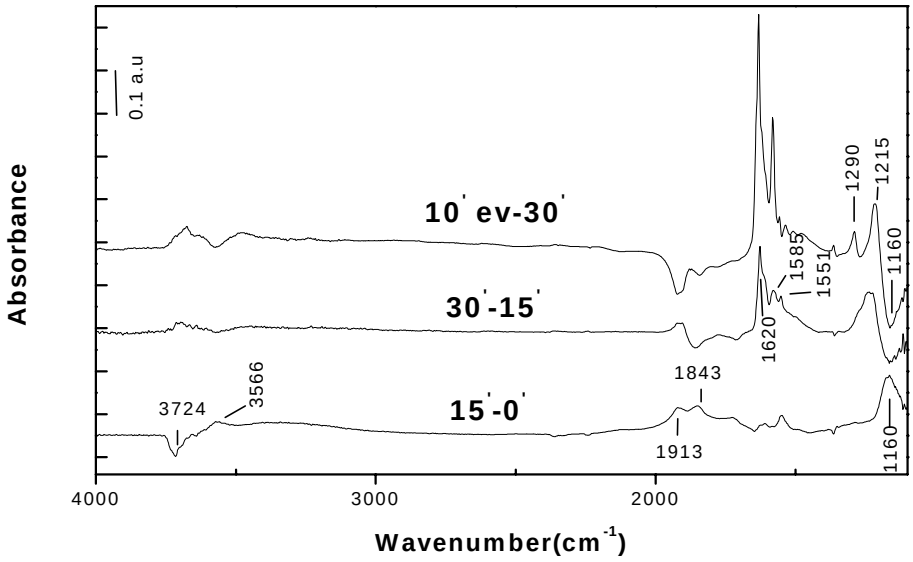

Figure 17 Subtraction FTIR spectra of adsorbed NO (10 Torr) obtained from Fig.16: by subtracting the spectrum '0'' from spectrum '15'' (15'-0'), and from spectrum '30'' (30'-0') and by subtracting the spectrum '30'' from spectrum '10' ev' (10' ev-30')

The band at 1160 cm^{-1} is attributed to ν(NO) of NOH species. This assignment is supported by the fact that the appearance of the band at 1160 cm^{-1} is accompanied by a negative absorption band in the 3690-3620 region due to less basic Ti^{4+}-OH groups (Fig.16 and Fig.17). The positive absorption at 3565 cm^{-1} suggests the existence of protonated NO^- species, i.e. NOH. The intensity of the band at 3565 cm^{-1} changes in parallel with that at 1160 cm^{-1} (see Fig.17, spectra (15'-0') and (30'-15')) which confirms the existence of NOH species. Anionic NO^- species are observed on La_2O_3 [91,125,126], and CeO_2 [90] giving respective bands at 1170, 1195 and 1174 cm^{-1}. Formation of NO^- during the adsorption of NO on TiO_2 (anatase) has been reported also in [127] assuming disproportination of NO to NO^-, nitrates and hyponitrite ion, $N_2O_2^{2-}$. Under the conditions of our experiments, we do not observe the latter species, which can be formed by dimerization of NO^-.

The appearance of the surface nitrates is accompanied by a negative complex band with maximum at 3718 cm^{-1}, which grows with time (Fig.17) due to consumption of the corresponding Ti^{4+}-OH groups according to the reaction [99,124]:

$$2\ Ti^{4+}\text{-}OH + 2NO_2 \rightarrow 2Ti^{4+}\text{-}NO_3^- + H_2O + NO \quad (15)$$

The occurrence of this process has been confirmed by adsorption of NO_2 on deuteroxylated TiO_2 (Anatase) [124].

This means that portion of the absorption at 1625 cm^{-1} is due to bending modes of adsorbed water molecules. The existence of adsorbed water molecules causes the appearance of a wide positive absorption band in the 3500-3000 cm^{-1}

region. Another possibility for H_2O formation is by recombination of surface OH groups with protons formed in reactions (13) and (14).

The broad bands at 1913 and 1840 cm^{-1} fall in the nitrosyl region. However, their interpretation as nitrosyls of the type α- and β-Ti^{4+}-NO would be incorrect for two reasons: (i) In general, the nitrosyl bands are more narrow and (ii) The concentration of more energetic (cus) Ti^{4+} ions (α-Ti^{4+} sites) is lower than that of β-Ti^{4+} ions [112]. The intensities of the nitrosyl bands shown in Fig.16 are reverse (assuming similar absorptivities).

The subtraction spectra in Fig.17 show that the bands at 1913 and 1840 cm^{-1} increase in intensity within the period of 15 min. However, with the extent of the contact time up to 30 min, only the former band continues to grow in parallel with the bands due to nitrate species. For that reason, we assign the band at 1913 cm^{-1} to NO adsorbed on Ti^{4+} ion to which a nitrate ion is coordinated, probably bridged or monodentate, i.e. ($^{-}O_2NO$-Ti^{4+}-NO). The development of the band at 1840 cm^{-1} follows the behavior of the band at 1160 cm^{-1} due to NO^{-} species. For that reason, we assign the absorption at 1840 cm^{-1} to the complex ON-Ti^{4+}-NO^{-}. The NO_3^{-} and NO^{-} species differ in their electronegativity, the nitrate ion having stronger electron accepting abilities than NO^{-}. This results in a stronger N-O bond in the O_2NO-Ti^{4+}-NO nitrosyl complex. The proposed interpretation is in agreement with the conclusion made by Hadjiivanov and Knozinger [127] that Ti^{4+} ions alone do not form nitrosyls. However, it contradicts the assignment of the bands at 1913 and 1840 cm^{-1} proposed by them. According to these authors the absorption at 1913 and 1840

cm^{-1} is due to Fermi resonance of N-O stretching vibration with M-N mode at about 900 cm^{-1}. This assignment requires constancy of the ratio of relative intensities of the bands at 1913 and 1843 cm^{-1} with increase in the surface concentration of the nitrosyl species which is not the case observed by us. In addition, the M-N stretching vibrations in nitrosyl complexes are at lower frequencies [87] (below 650 cm^{-1}).

The evacuation for 10 min at room temperature causes disappearance of the NO^- species and increase in the intensities of the bands corresponding to the nitrates, especially to those due to bridged and bidentate species. This indicates that under these conditions, the population of the corresponding adsorption forms has increased. This experimental fact can be explained by the assumption of the following process:

$$NO^- + 2NO_2 \rightarrow NO_3^- + 2NO \qquad (16)$$

Obviously, in the static experimental conditions, the NO^- species are stabilized on Ti^{4+} ions, but NO_2 can oxidize them during the dynamic evacuation.

The weak band at 1715 cm^{-1}, which resists the evacuation, can be associated with Ti^{3+}-NO. Reduced titanium ions can arise from the thermo-vacuum activation. Finally, the weak negative band at 1360 cm^{-1} is due to nitrate ions adsorbed on the IR windows.

3.3.1.1.2 Coadsorption of NO and O_2

The time evolution of the IR spectra during the coadsorption of NO and O_2 (28 Torr) on TiO_2 is shown in Fig.18. Immediately after the introduction of the gas

mixture to the IR cell, the bands at 1913 and 1840 cm^{-1} are detected which correspond to Ti^{4+}-NO nitrosyls of two types. These two bands disappear with time indicating that adsorbed NO is oxidized by the oxygen. At the same time massive absorption develops in the nitrate region. The assignment of the nitrate bands is the same as described in the previous section (Table 10, Section 3.3.1.4). The following difference should be noted:

- Absence of the band at 1160 cm^{-1} due to NO^- species. This indicates that the source of NO_2 leading to formation of surface nitrate species, is the oxidation of NO by oxygen:

$$2NO + O_2 \rightarrow 2NO_2 \quad (17)$$

- Development of a band at 2210 cm^{-1} due to NO^+ ion [87,99,123].

It should be pointed out that the spectra obtained upon NO/O_2 coadsorption on TiO_2 are practically identical to those obtained during the adsorption of NO_2 [99,123]. The nitrate species formed posses high thermal stability and they can not be removed completely by thermo-vacuum treatment. A band at 1550 cm^{-1} is detected after heating at 673 K and is interpreted as a bridged nitro-nitrito compound [123].

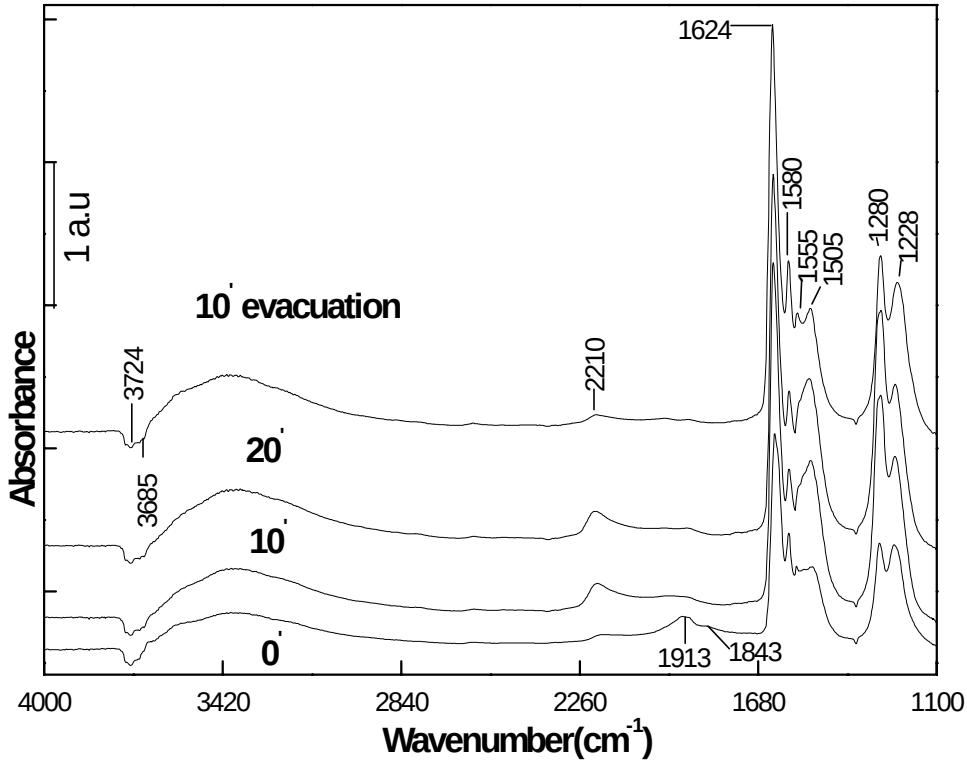

Figure 18 Time evolution of the FTIR Spectra of adsorbed NO/O_2 mixture (28 Torr, (1:3.2)) on TiO_2 and after 10 min evacuation at room temperature

3.3.1.2 The MnTi-IE catalyst

3.3.1.2.1 Adsorption of NO

The FTIR spectrum of adsorbed NO (10 Torr) on MnTi-IE is shown in Fig.19. The introduction of NO (10 Torr, room temperature) into the IR cell (Fig.19) causes the appearance of two bands in the nitrosyl region at 1880 and 1865 cm^{-1} corresponding to two types of Mn^{3+}-NO species in accordance with the existence of two types of Mn^{3+} ions in the catalyst studied (Section 3.2.3). In the low frequency region, weak bands at 1645, 1612 and 1487 cm^{-1} and the complex absorption with maximum at 1200 cm^{-1} and shoulder at 1132 cm^{-1} are detected. The intensities of the nitrosyl bands decrease slightly after 50 min whereas those of the bands in the 1700-1100 cm^{-1} region increase. With the extent of the contact time, a strong absorption develops in the OH stretching region with simultaneous increase in the intensities of the negative bands at 3725 and 3690 cm^{-1}. It is possible that the altered OH groups are of Mn^{3+}-OH type.

The evacuation for 10 min at room temperature (Fig.19, (10' ev)) leads to almost complete disappearance of the Mn^{3+}-NO nitrosyls (very weak band at 1860 cm^{-1}). The spectrum contains strong absorption in the ν(OH) stretching region with maximum at 3290 cm^{-1}, two bands of moderate intensity at 1612 and 1200 cm^{-1} and shoulder at 1645 cm^{-1}, weaker band at 1478 cm^{-1}, and unresolved absorption at about 1130 cm^{-1}. The species characterized by the band at 1555 cm^{-1} are not observed.

Based on the sequence of appearance/disappearance of the surface species, we assign the bands at 1645 and 1555 cm^{-1} to bridged and bidentate nitrates respectively (Table 10, Section 3.3.1.4). The low-frequency component of the split ν_3 mode is at 1200 cm^{-1}. The bands at 1487 (shifted to 1478 after evacuation) and 1130 cm^{-1} are assigned to nitro-nitrito (bridging NO_2^-) species [87,99,127]. The strong absorption with the maximum at 3290 cm^{-1} and the band at 1612 cm^{-1} are due to ν(OH) and $\delta(H_2O)$, respectively, of adsorbed water molecules. The water molecules are formed by recombination of the surface OH groups (negative band at 3725 cm^{-1}) with protons released in analogous process already observed in the case of pure TiO_2 (see reaction 14) i.e. through disproportionation of NO to NO^- and NO_2 with the participation of less basic OH groups (unresolved negative band at 3690 cm^{-1}). The assignment of the band at 1612 cm^{-1} to adsorbed water molecules is supported by the fact that the behavior of this band parallels that of the broad, intense absorption at 3290 cm^{-1} (Fig.19). Compared to the pure TiO_2, the concentration of the surface nitrates is lower and portion of NO_2 is adsorbed as N_2O_4 (weak band at approximately 1720 cm^{-1} [87], which disappears after evacuation).

The NO^- species are probably coordinated to Mn^{3+} ions. The corresponding ν(NO) mode is superimposed to the nitrate band at 1200 cm^{-1} and has a major contribution to the band intensity. The existence of the protonated NO^- species can not be excluded. No bands, which can be assigned to adsorbed NO on Ti^{4+} sites are observed.

The surface nitrates are formed by adsorption of the NO_2 produced *in situ* and oxidation of NO by the Mn^{3+} ions: the intensities of the corresponding nitrosyl bands decrease slightly during the contact with NO (Fig.19). The assignment of the absorption bands is presented in Table 10, Section 3.3.1.4.

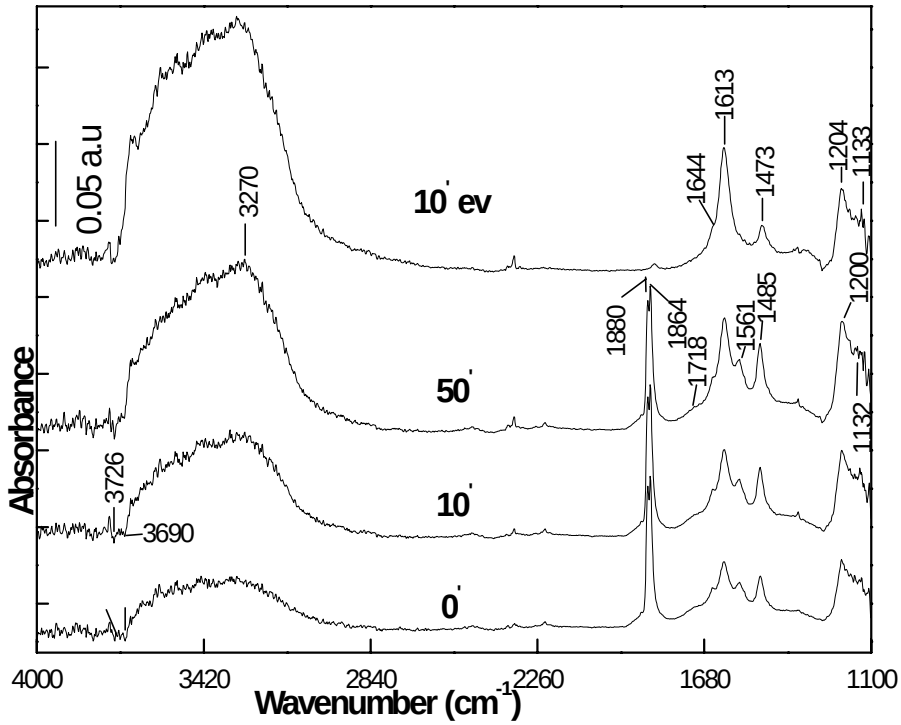

Figure 19 Time evolution of the FTIR spectra of adsorbed NO (10 Torr) on MnTi-IE after 10 min evacuation (10' ev) at room temperature

3.3.1.2.2 Coadsorption of NO and O_2

The evolution of the spectra obtained during the contact of mixture of NO and oxygen (28 Torr, NO:O_2=1:3.2) with MnTi-IE catalyst is shown in Fig.20. Immediately after the introduction of the gaseous mixture, weak bands in the nitrate region (1650-1200 cm^{-1}) are detected. These bands grow fast with the extent of the contact time and correspond to different kinds of nitrate species. Based on the sequence of their appearance and thermal stability (see Fig.21), the absorption bands are grouped as follows: 1619,1610 and 1248 cm^{-1} (bridged nitrates), 1552 and 1276 cm^{-1} (bidendate nitrates) and 1514 and 1320 cm^{-1} (monodentate nitrates) [99]. The presence of nitrate species indicates that NO_2 is involved in their formation, i.e. NO is oxidized to NO_2. The bands in the nitrosyl region require special attention. Immediately after introduction of the reaction mixture in the IR cell, weak bands in the 2100-1850 cm^{-1} region are observed. The bands at 1870 and 1902 cm^{-1} are due to Mn^{3+}-NO species (two types). In the spectrum, taken 10 min later, (spectrum 10'), these bands are masked by the broad absorption with maximum at 1957 cm^{-1} and shoulder at 2034 cm^{-1}. Since the latter absorption develops together with the nitrate bands, it is assigned to two types of Mn^{3+}-NO nitrosyl, which have NO_3^- ions in their coordination spheres, i.e. (ON)-Mn^{3+}-(ONO_2^-) complexes. The electron withdrawing NO_3^- group induces partial positive charge on the Mn^{3+} ions. This results in a shift of the N-O stretching frequency to a higher wavenumber. The weak band at 2155 cm^{-1} (which disappears after evacuation at room temperature for 10 min) is interpreted as

adsorbed NO^+ ion [89,100]. The formation of NO^+ species indicates that Lewis acid-base pairs together with the OH groups at 3275 cm^{-1} (negative band) are involved in the process of the formation of surface nitrates. As already explained, the band at 1610 cm^{-1} can have some contribution from bending modes of adsorbed water. This assumption is supported by the appearance of absorption in the region of H-bonded OH groups. The intensities of the nitrate bands display slight decrease after evacuation at room temperature for 10 min.

The thermal stability of the absorption forms is followed by heating in vacuum for 10 min at a given temperature (Fig.21). The least stable are the NO^+ ion and the nitrosyls at 2034 and 1965 cm^{-1}. They are not observed after evacuation at 398 K. The nitrate species disappear after heating at 533 K. The assignment of the absorption bands is summarized in Table 10, Section 3.3.1.4.

The adsorption of NO_2 (2 Torr) at room temperature on the catalyst MnTi-IE leads to identical surface species observed during the NO/O_2 coadsorption. No differences in their behavior upon desorption at room and higher temperatures are observed (Fig.22). This experimental fact confirms the conclusion that in the presence of the oxygen the predominant adsorbed species are the surface nitrates.

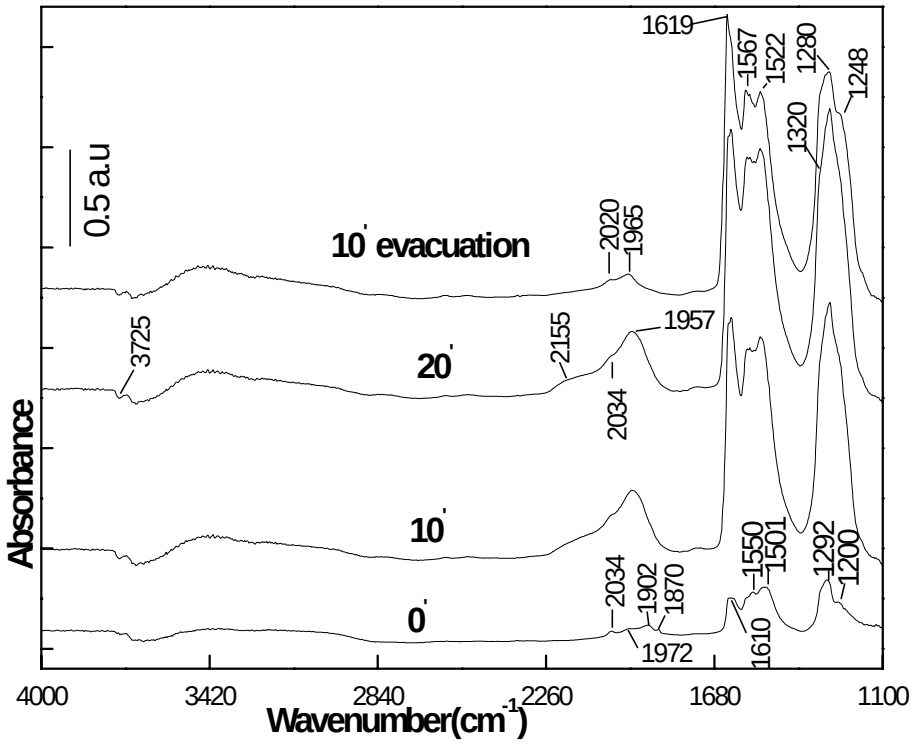

Figure 20 Time evolution of the FTIR Spectra of adsorbed NO/O_2 (28 Torr, (1:3.2)) on MnTi-IE after 10 min evacuation (10' ev) at room temperature

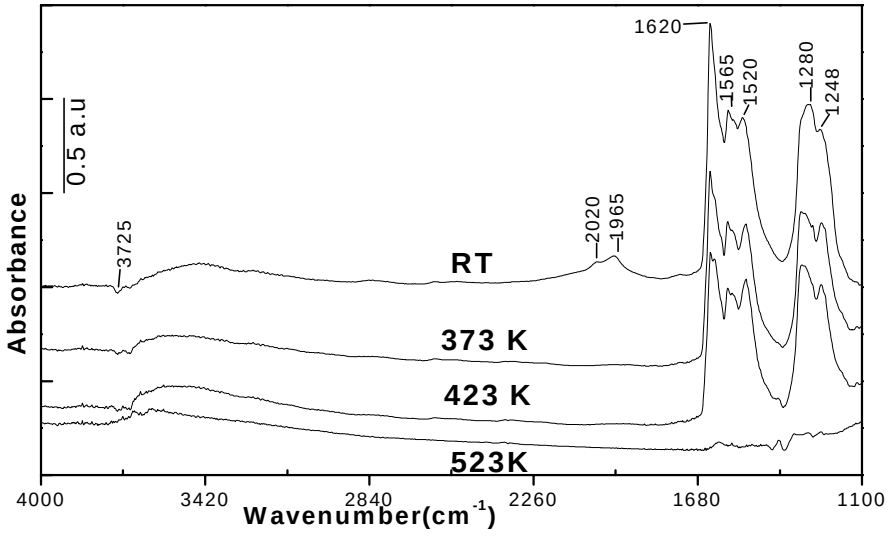

Figure 21 FTIR Spectra of coadsorbed NO and O_2 (39 Torr, (1:3.6)) on MnTi-IE after 10 min evacuation at given temperatures

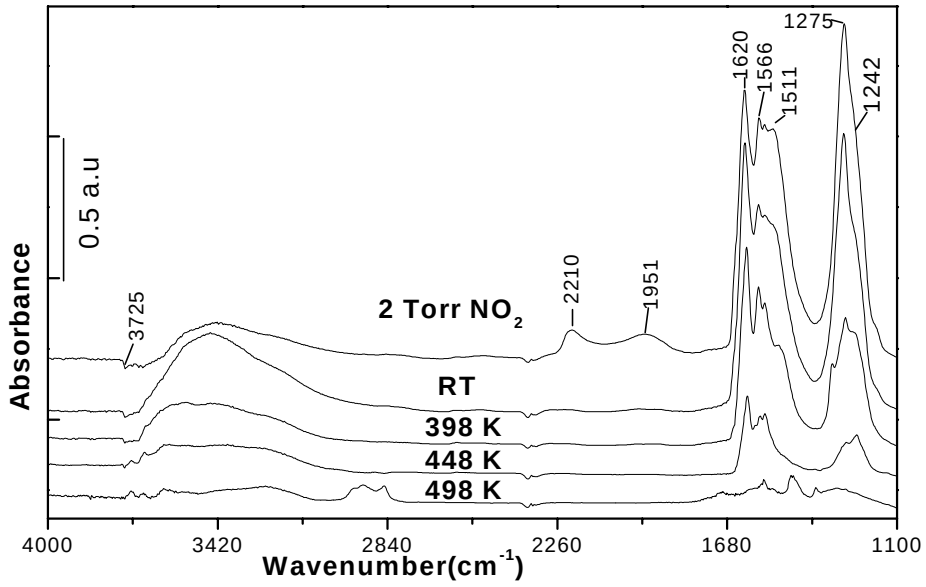

Figure 22 FTIR Spectra of adsorbed NO_2 (2 Torr) on MnTi-IE catalyst at room temperature and after evacuation for 10 min at various temperatures

3.3.1.3 The MnTi-I catalyst

3.3.1.3.1 Adsorption of NO

The spectra of adsorbed NO (10 Torr) at room temperature on the catalyst MnTi-I taken at increasing contact time and after evacuation are shown in Fig.23. The interpretation of the absorption bands is analogous to that proposed already in Section 3.3.1.2.1. The assignment of the bands is presented in Table 10, Section 3.3.1.4.

The band at 1612 cm^{-1}, as in the case of MnTi-IE sample, is due mainly to adsorbed water (strong absorption between 3600 and 3000 cm^{-1} in the OH stretching region). The following features are noticed for the impregnated catalyst which have not been observed in the case of the ion-exchanged sample, MnTi-IE:

- Existence of Mn^{2+}-NO nitrosyls on the MnTi-I catalyst; this is in agreement with the results from CO adsorption (Section 3.2.2).
- Formation of Ti^{4+}-NO^{-}, respectively ON- Ti^{4+}-NO^{-} species which indicates that there are Ti^{4+} ions exposed on the surface of MnTi-I catalyst, i.e. the distribution of the active phase is inhomogeneous.
- The NO^{-} species coordinated to Mn^{3+} ions display higher resistance toward evacuation at room temperature than those located on Ti^{4+} sites; this behavior indicates stronger Mn^{3+}- NO^{-} bond which is due to difference in the electronic configuration of the adsorption sites ($Mn^{3+}(d^4)$ is a π donor but $Ti^{4+}(d^0)$ is not).

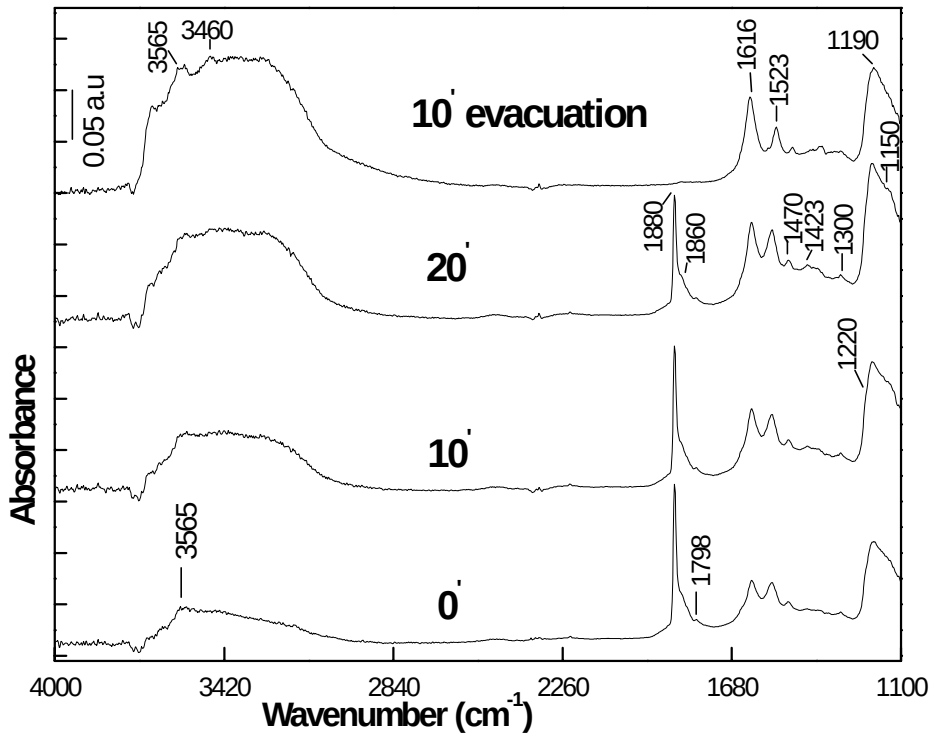

Figure 23 Time evolution of the FTIR spectra of adsorbed NO (10 Torr) on MnTi-I after 10 min evacuation (10' ev) at room temperature

3.3.1.3.2 Coadsorption of NO and O_2

Time evolution FTIR spectra of NO/O_2 adsorption (28 Torr, (1:3.2)) at room temperature is shown in Fig.24. The bands detected on the MnTi-I catalyst (Fig.24) in the nitrate region are practically identical to those already observed for the MnTi-IE sample. Noticeable difference is the presence of a very weak absorption band at about 1920 cm^{-1} which (similar to the TiO_2) is associated with (ON)-Ti^{4+}-ONO_2^- complex. This experimental fact shows that nitrate species are coordinated mainly to the Ti^{4+} ions.

The thermal stability of the nitrate species obtained during the NO/O_2 coadsorption seems to be lower for the impregnated catalyst (compare Fig.25 and Fig.22). Based on the sequences of the nitrate for formation and desorption, they are identified as bridged (1625 and 1275 cm^{-1}), bidentate (1570 and 1240 cm^{-1} and 1540 and 1240 cm^{-1}) and monodentate species (1505 and 1320 cm^{-1}).

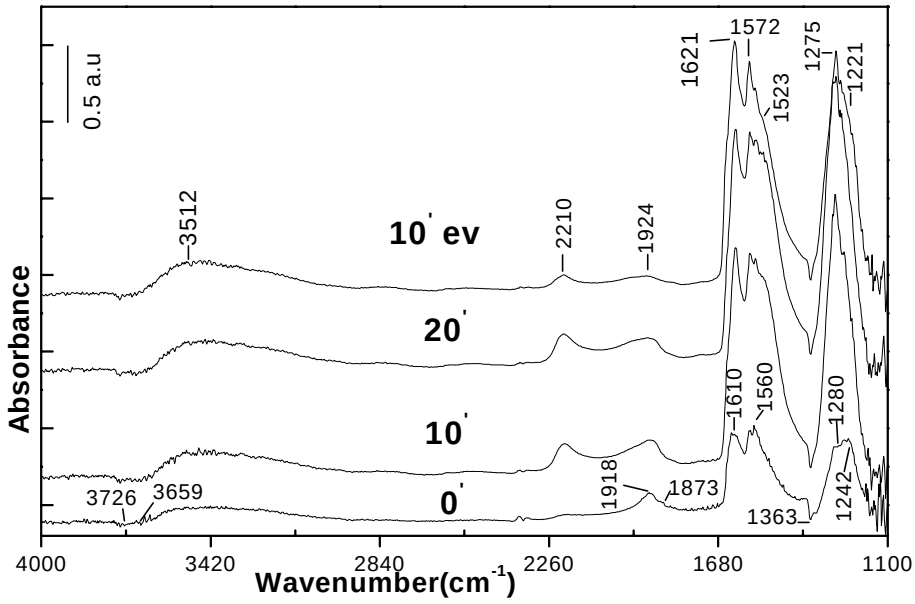

Figure 24 Time evolution of the FTIR Spectrum of coadsorbed NO/O_2 (28 Torr, (1:3.2)) on MnTi-I after 10 min evacuation (10' ev) at room temperature

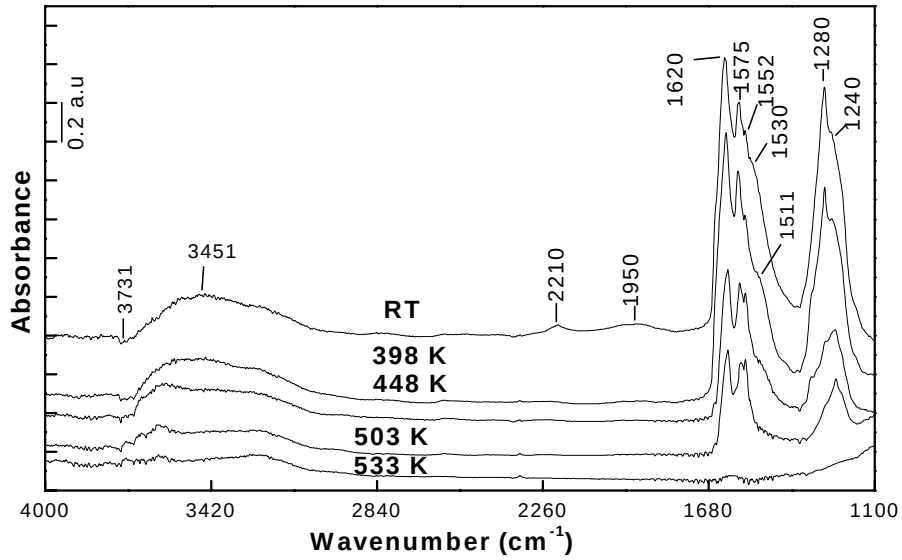

Figure 25 FTIR Spectra of coadsorbed NO/O_2 (48 Torr, (1:2.7)) on MnTi-I after 10 min evacuation at the indicated temperatures

3.3.1.4 Summary of the results on NO adsorption and NO/O_2 coadsorption on the catalysts studied

The proposed assignment of the NO_x species observed during the adsorption of NO and its coadsorption with O_2 is summarized in Table 10.

The common feature observed during the adsorption of NO on the support TiO_2 and the catalysts MnTi-IE and MnTi-I is the formation of the anionic nitrosyl NO^-. This species arises by interaction of adsorbed NO with the surface OH groups of lower acidity characterized by absorption bands in the 3690-3610 cm^{-1} region. This process leads the appearance of NO_2 and protons. The released H^+ ions coordinate to the NO^- ion giving NOH species and/or recombine with more basic surface OH groups (3730-3720 cm^{-1}) producing water molecules. The Mn^{3+} ions posses greater ability for stabilization of the NO^- species than the Ti^{4+} species. The absence of Ti^{4+}-NO^- species on the surface of MnTi-IE catalyst upon NO adsorption indicates better dispersion of Mn^{3+} ions on the support than in the case of MnTi-I catalyst, in agreement with the results of CO adsorption.

The second product of disproportionation of NO is the NO_2, which gives raise to surface nitrates. The concentration of the nitrate species is higher on titania than on manganese containing samples. This difference probably is due to different amounts of NO_2 produced *in situ* and leads to the conclusion that titania surface favors the disproportionation of NO more than the manganese containing samples. Another important finding is that Ti^{4+} ions alone do not form nitrosyls in the presence of NO

and only adsorbed NO on Ti^{4+} ions which have NO_3^- or NO^- group in the coordination sphere is observed.

Upon coadsorption of NO/O_2 at room temperature on the samples studied, various kinds of surface nitrates are observed differing in the mode of their coordination. No anionic nitrosyls are present. The nitrates on the manganese containing samples are characterized by significantly low thermal stability than that in the case of the pure support, TiO_2.

Table 10 Assignment of the FTIR bands observed during the adsorption of NO and NO/O_2 coadsorption at room temperature on the catalysts studied

Catalyst	**Frequency [cm^{-1}] and Mode**	**Possible Assignment**	**Reference**
TiO_2 (NO and NO/O_2 adsorption)	1913 (ν(NO)) 1843 (ν(NO))	ON-Ti^{4+}-ONO_2^- ON-Ti^{4+}-NO^-	This work
	1715 (ν(NO))	Ti^{3+}-NO	127
	1630-25,1215 (split ν_3) 1610,1215 (split ν_3) 1580,1215 (split ν_3) 1555,1215 (split ν_3) 1508-05,1286-80 (split ν_3)	NO_3^- (bridged) NO_3^- (bridged) NO_3^- (bidendate) NO_3^- (bidendate) NO_3^- (monodendate)	99,111,124
	1160 (ν(NO)) 3565 (ν(OH))	Ti^{4+}-NO^- Ti^{4+}-NOH	This work
	2210 (ν(NO))	NO^+	99,111,124
MnTi-IE (NO adsorption)	1880 (ν(NO)) 1865 (ν(NO))	Mn^{3+}-NO Mn^{3+}-NO	This work
	~1720 ($\nu_{as}(NO_2)$)	N_2O_4	87
	1612 ($\delta(H_2O)$) 3600-3000 (ν(OH))	H_2O	87
	1645,1200 (split ν_3) 1555,1200 (split ν_3)	NO_3^- (bridged) NO_3^- (bidendate)	This work
	1487 ($\nu_{as}(NO_2^-)$) 1130 ($\nu_s(NO_2^-)$)	NO_2^- (bridging nitro-nitrito)	87,127

Table 10. Continuation

Catalyst	Frequency [cm^{-1}] and Mode	Possible Assignment	Reference
	1200 (ν(NO)) 3565,3510 (ν(OH))	Mn^{3+}-NO^- Mn^{3+}-NOH	This work
MnTi-IE (NO/O_2 adsorption)	2155 (ν(NO))	NO^+	100,112,125
	2033 (ν(NO)) 1957 (ν(NO))	ON-Mn^{3+}-ONO_2^- ON-Mn^{3+}-ONO_2^-	This work
	1905 (ν(NO)) 1870 (ν(NO))	Mn^{3+}-NO Mn^{3+}-NO	This work
	1619, 1248 (split ν_3) 1610, 1248 (split ν_3) 1560-50, 1276 (split ν_3) 1514, 1320 (split ν_3)	NO_3^- (bridged) NO_3^- (bridged) NO_3^- (bidentate) NO_3^- (monodentate)	
MnTi-I (NO adsorption)	1875 (ν(NO)) 1798 (ν(NO))	Mn^{3+}-NO Mn^{2+}-NO	This work
	~1850 (ν(NO))	ON-Ti^{4+}-NO^-	This work
	1645, 1220 1523, 1220	NO_3^- (bridged) NO_3^- (bidendate)	This work
	1612 (δ(H_2O)) 3600-3000 (ν(OH))	H_2O	87
	1470,1423,1300 ($\nu_{as}(NO_2^-)$)	NO_2^- (nitro-nitrito)	87,127
	1190 (ν(NO)) 3565 (ν(OH))	Mn^{n+}-NO^- (n=2 or 3) Mn^{n+}-NOH	This work
	1150 (ν(NO)) 3565 (ν(OH))	Ti^{4+}-NO^- Ti^{4+}-NOH	This work
MnTi-I (NO/O_2 adsorption)	2213 (ν(NO))	NO^+	99,111,124
	1896 (ν(NO))	ON-Ti^{4+}-ONO_2^-	This work
	1620, 1250 (split ν_3) 1610, 1250 (split ν_3) 1570, 1275 (split ν_3) 1515, 1320 (split ν_3)	NO_3^- (bridged) NO_3^- (bridged) NO_3^- (bidentate) NO_3^- (monodentate)	This work

3.3.2 Adsorption of n-decane on NO_x-precovered catalysts

3.3.2.1 The MnTi-IE catalyst

The interaction of n-decane (0.6 Torr) at different temperatures (Fig. 26) with the stable NO_x species obtained on the surface of MnTi-IE catalyst during the coadsorption of NO and O_2 (40 Torr, NO:O_2 = 1:4) followed by evacuation for 10 min at room temperature has been studied. The introduction of the hydrocarbon to the catalyst at room temperature does not lead to changes in the NO_x bands. Absorption typical for the hydrocarbon is observed in the ν(OH) stretching region: bands at 2961 ($\nu_{as}(CH_3)$), 2924 ($\nu_{as}(CH_2)$) and 2852 cm^{-1} ($\nu_s(CH_3)$). The bands at 1467 and 1380 cm^{-1} are due to CH_2 scissoring vibration ($\beta_s(CH_2)$) and symmetric CH_3 deformation vibration ($\delta_s(CH_3)$), respectively [128]. The raise of the temperature of the closed cell from 373 to 573 K, leads to gradual decrease in the intensities of the bands corresponding to the adsorbed hydrocarbon and NO_3^- species (the spectra are taken after cooling the cell down to room temperature). This result indicates that interaction between the n-decane and the nitrate species adsorbed on the surface of the catalyst occurs. The spectrum detected after heating at 373 K contains strong absorption in the ν(OH) stretching region with maximum at 3600 cm^{-1}. Obviously, the oxidation of the hydrocarbon starts already at that temperature leading to appearance of adsorbed water and oxygenated hydrocarbon compounds (e.g. aliphatic acids). Indeed, there is a weak absorption at approximately 1700 cm^{-1} which is typical for ν(C=O) in

carboxylic acids [128]. However, due to the heavy overlapping bands in the 1700-1350 cm^{-1} it is difficult to propose more detailed assignment. The treatment at 473 K causes strong decrease in the intensity of the band at 3600 cm^{-1} and weaker, broad band at about 3400 cm^{-1} is detected which can be assigned to adsorbed water. This suggests that decomposition of the oxygenated species has occurred. The only species, which appears with significant intensity in the 1700-1100 cm^{-1} region after the interaction at 473 K, is the one characterized by a band at 1575 cm^{-1}. This could be associated with a carbonate-carboxylate structure and/or less reactive bidentate nitrate which low-frequency component is not resolved in the full spectra but appears in the subtraction spectrum at 1280 cm^{-1} (see Fig. 27, spectrum (573 K-473 K)). After heating at 573 K (Fig.26) the bands characteristic for the adsorbed hydrocarbon appear with strongly reduced intensity and the band at 1575 cm^{-1} is not observed. This behaviour suggests that the absorption at 1575 cm^{-1} is associated with nitrate species. Under these conditions, new bands at 1640, 1550 and 1365 cm^{-1} are detected. The former absorption (together with the bands at 3660 and 3400 cm^{-1}) is attributed to adsorbed water whereas the band at 1540 and 1365 are assigned to bidentate carbonate species [87].

Fig. 27 presents the spectra obtained by subtraction from the spectrum taken after heating at a given temperature the spectrum obtained after the preceding thermal treatment. The spectra contain strong negative bands indicating decrease in the surface concentrations of the hydrocarbon and the nitrate species. The following important observations should be noted:

- The reactivity of the surface nitrates depends on the temperature (Fig. 27A). At 373 K the bridged nitrates (1625 and 1233 cm^{-1}) are altered in larger extent than the monodentate nitrates (1550 and 1270 cm^{-1} and 1512 and 1318 cm^{-1}). This means that the former species are the most reactive. At 473 K mainly the monodentate nitrates (1505 and 1300 cm^{-1}) are involved in the interaction with the hydrocarbon. The bidentate nitrates giving raise of the negative bands at 1580 and 1280 cm^{-1} possess the lowest reactivity – they disappear after heating at 573 K.
- In the 2800-2100 cm^{-1} region, the bands at 2380 and 2345 cm^{-1} detected after heating at 373 K (Fig. 27B, spectrum (373 K-RT)) are due to adsorbed CO_2 [see section 3.1.4.2.2]. The bands at 2740 and at 2560-2500 cm^{-1} are typical for formate ions adsorbed on MnTi-IE catalyst [see section 3.2.3, Table 9] and are due to Fermi resonance between the ν(CH) fundamental and combinations or overtones of the bands in the carboxylate region. The spectrum in the OH region contains the positive band at 3600 cm^{-1}. Based on the data of adsorbed formic acid on the MnTi-IE catalyst [see section 3.2.3, Table 9], we assign the band at 3600 cm^{-1} to ν(OH) stretching modes of adsorbed formic acid. The ν(C=O) stretching frequency is positioned at 1666 cm^{-1} and is partially masked by the strong negative band at 1625 cm^{-1}. After heating at 473 K, the band at 3600 cm^{-1} decreases in intensity (negative band at 3600 cm^{-1}). Under these conditions, the concentration of the formate species increases slightly (weak positive band at 2765 cm^{-1}). Two distinct

bands at 2630 and 2385 cm^{-1} are detected. The former absorption is assigned to combination or overtone modes of carbonate species. This assignment is supported by the fact that the band at 2630 cm^{-1} is present in the spectrum taken after heating at 573 K which contains bands attributed to carbonate species (1530 and 1365 cm^{-1}). The increased intensity of the band at 2385 cm^{-1} indicates that after heating at 473 K the concentration of the adsorbed CO_2 is enhanced. These experimental facts suggest that the formic acids produced during the oxidation of the hydrocarbon by the surface nitrates undergoes decomposition (negative bands at 3600 and about 1670 cm^{-1} (Fig. 27A, spectrum (473 K-373 K)). This process leads to formation of adsorbed H_2O (weak positive band at 3277 cm^{-1}), CO_2 and carbonate species. The further increase of the temperature (to 573 K) causes involvement of the least reactive surface nitrates in interaction with the hydrocarbon and fast decomposition of the oxygenated hydrocarbon products. As a result, positive bands due to adsorbed water (3660 (ν_{as}(OH)), 3400 (ν_s(OH) and 1640 cm^{-1} ($\delta(H_2O)$) and carbonate species (2630 (overtone or combination), 1530 and 1365 cm^{-1} (split ν_3 mode)) are observed. Homogeneous interaction between the hydrocarbon and NO_2 (which could arise from the thermal decomposition of the nitrates) should be excluded because the interaction of alkanes and NO_2 in gas phase occurs at about 673 K [129,130]. The facts reported present unambiguous evidence that the n-decane is activated and oxidized by the surface nitrate species.

- The weak band at 2283 cm^{-1}, which decreases in intensity with increase in the reaction temperature (Fig. 27B, spectra (373 K-RT) and (473 K-373 K)), is attributed to isocyanate, NCO^-, species. The literature data [128] on organic isocyanates show that the ν_{as}(N=C=O) band normally occurs in the range 2290-2255 cm^{-1}. In the complex $[Mn(NCO)_4]^{2-}$ the isocyanate group is characterized by a band at 2222 cm^{-1} [87]. The position of the NCO^- band depends strongly on the nature of the ion to which the NCO^- ion is coordinated [87,131]. For example, Al^{3+}–NCO species absorb in the region 2274-2256 cm^{-1} [132-136] and Co^{2+}–NCO^- species are identified by absorption at 2205-2178 cm^{-1} [131, 132,138,139]. To the best of our knowledge, no data are available for surface NCO^- species coordinated to manganese or titanium ions. It is possible that the band at 2283 cm^{-1} is due to organic isocyanate.

It should be pointed out that the heating of the MnTi-IE catalyst pre-covered by n-decane (0.6 Torr, 10 min evacuation) causes some oxidation of the adsorbed hydrocarbon (Fig. 28). However, the decrease in the intensities of the absorption bands in the ν(CH) stretching region is considerably smaller compared to that observed in the presence of adsorbed nitrates (compare Figures 26 and 28). The nitrates on titania start to interact with the n-decane at small extent at 573 K.

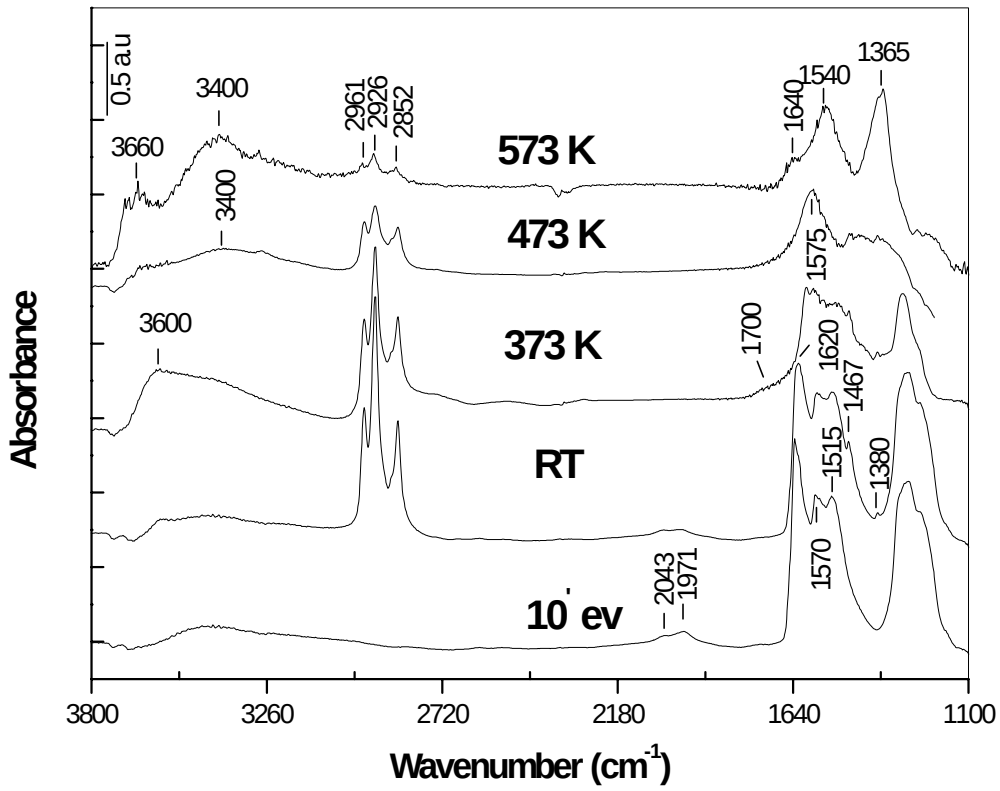

Figure 26 FTIR spectra obtained from the interaction of (0.6 Torr) n-decane at different temperatures with NO_x species on MnTi-IE catalyst formed during the coadsorption of NO/O_2 (28 Torr, (1:3.2)) followed by 10 min evacuation at room temperature

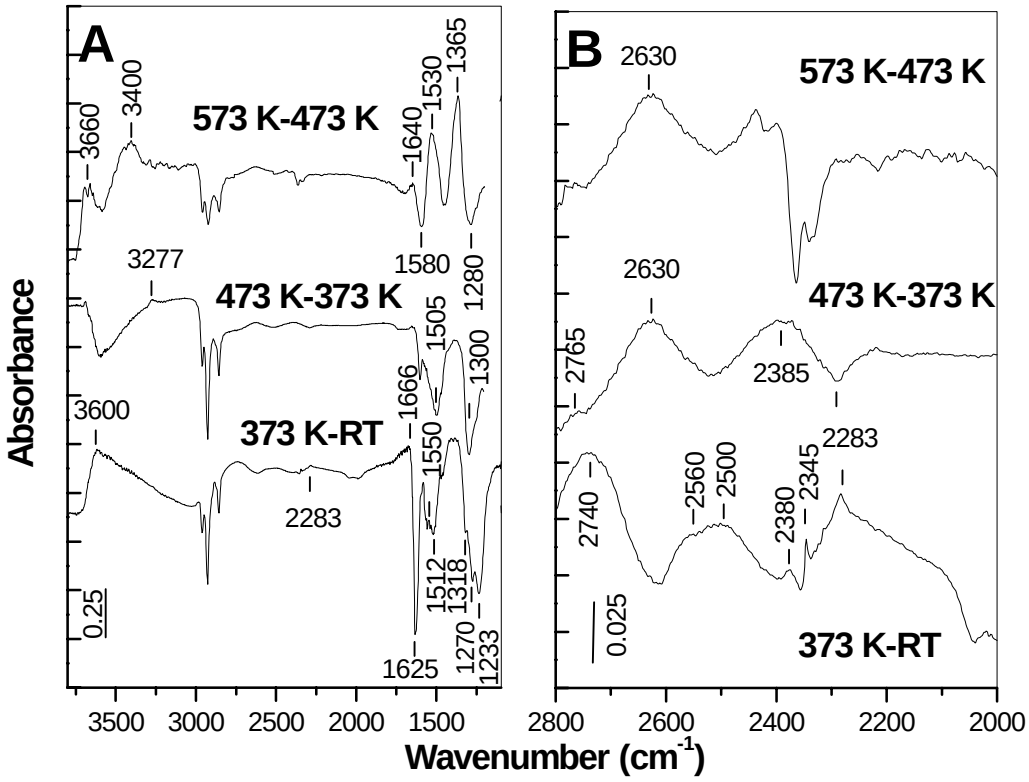

Figure 27 FTIR spectra obtained from Fig.26 by subtracting spectrum ‘RT’ from the spectrum ‘373 K’ (373 K-RT), spectrum ‘373 K’ from spectrum ‘473 K’ (473 K-373 K), and spectrum ‘473 K’ from spectrum ‘573 K’ (573 K-473 K)

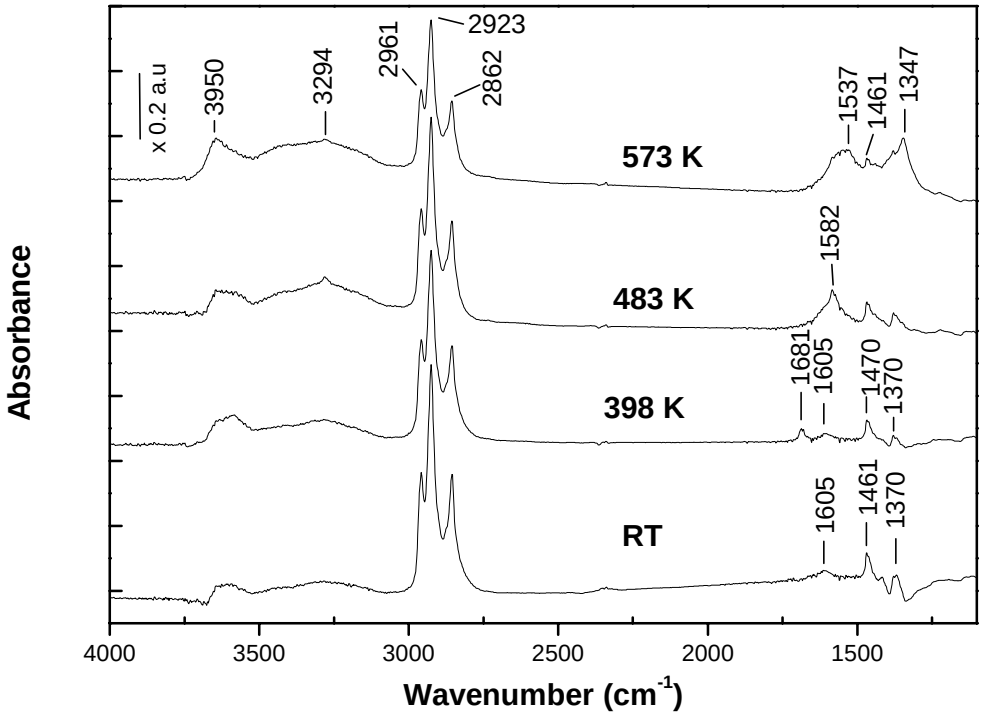

Figure 28 FTIR spectrum of MnTi-IE catalyst pre-covered by n-decane (0.6 Torr, 10 min evacuation) at indicated temperatures

3.3.2.2 The MnTi-I catalyst

The reactivity of the nitrate species toward the hydrocarbon is followed by identical experiment described above and the results are shown in Fig. 29. As in the case of the ion-exchanged sample, the concentration of the surface nitrates and that of the adsorbed hydrocarbon decrease with increase in the temperature. A noticeable difference is that, compared to MnTi-IE catalyst, the relative changes in the intensities of the bands in the 3000-2850 cm^{-1} region associated with the n-decane, are considerably lower for the MnTi-I catalyst (temperature interval 373-473 K). The reason for this can be the lower concentration of the reactive surface nitrates on the latter sample.

The behavior of the absorption bands (consumed and produced) in the whole region is similar to that already observed for the MnTi-IE catalyst, which is illustrated by the subtraction spectra (Fig. 30). The same sequence in the interaction of the surface nitrates with n-decane is observed. After the interaction at 373 K (Fig. 29A, spectrum (373 K-RT))) bands typical for adsorbed formic acid are detected on the MnTi-I catalyst: 3625 (ν(OH)), 3394 (hydrogen bonded hydroxyls) and 1680 cm^{-1} (ν(C=O)). The heating at 473 K causes decomposition of the formic acid (negative bands at 3625 and 1690 cm^{-1}) and additional oxidation of the hydrocarbon (small decrease in the intensity of the n-decane bands). The latter process results in increase in the concentration of the formate species: broad band in the 2800-2500 cm^{-1} region (Fig. 29B, spectrum (473 K-373 K)) and positive bands at 1588 (ν_{as} (CO_2^-)) and

1375 cm^{-1} (δ(CH) (Fig.29, spectrum (473 K-373 K)). The appearance of a band at 2360 cm^{-1} indicates that CO_2 is formed also under these conditions which gives raise to carbonate or bicarbonate species (band at 1433 cm^{-1}). Another possibility for the interpretation of the bands at 1585 and 1433 cm^{-1} is to attribute them to acetate species, CH_3COO^- ($\nu_{as}(CO_2^-)$ and $\nu_s(CO_2^-)$), respectively [84]).

As in the case of the ion-exchanged sample the band at 2284 cm^{-1} is associated with NCO^- species. Here again, the intensity of this band decreases with increase in the temperature.

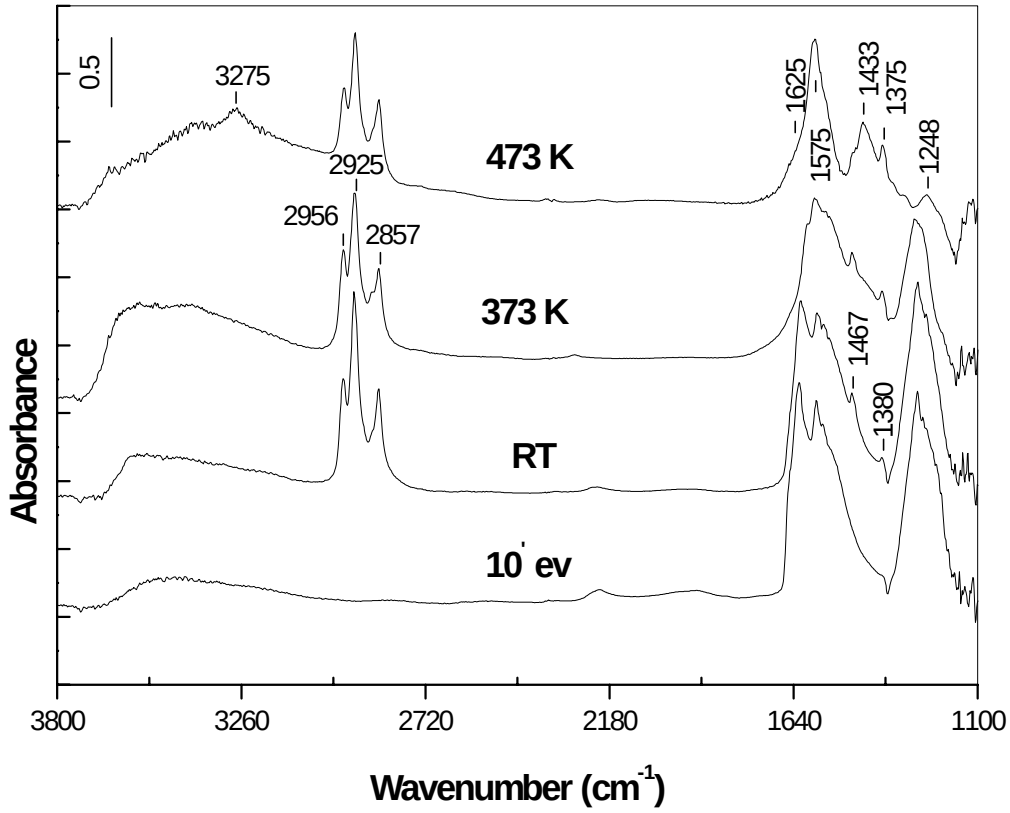

Figure 29 FTIR spectra obtained from the interaction of (0.6 Torr) n-decane at different temperatures with NO_x species on MnTi-I catalyst formed during the coadsorption of NO/O_2 (28 Torr, (1:3.2)) followed by 10 min evacuation at room temperature

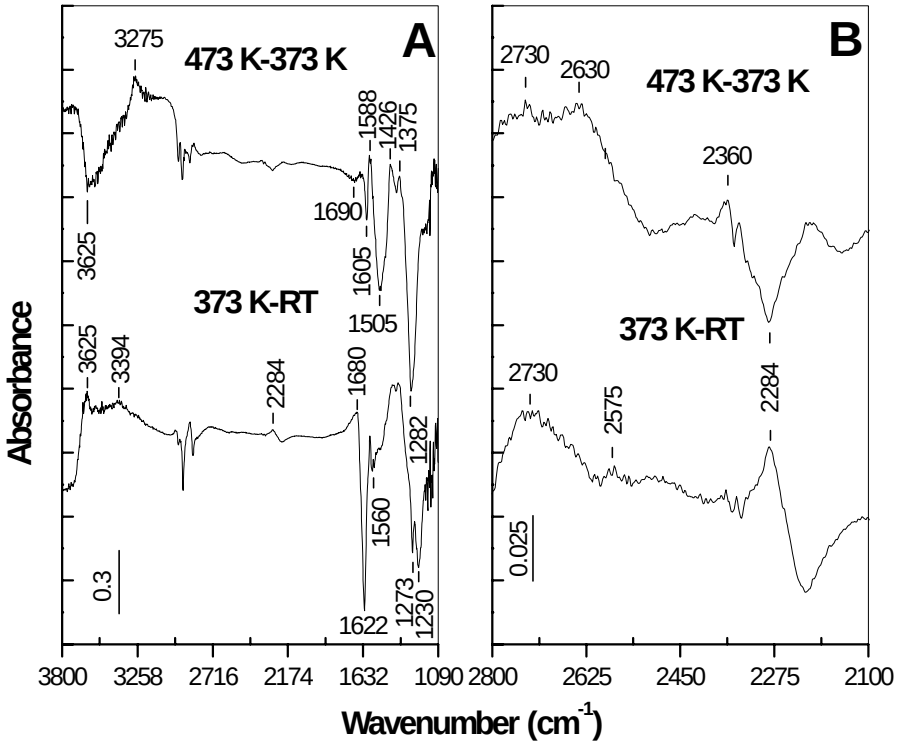

Figure 30 FTIR spectra obtained from Fig.26 by subtracting spectrum ‘RT’ from the spectrum ‘373 K’ (373 K-RT), and spectrum ‘373 K’ from spectrum ‘473 K’ (473 K-373 K)

3.3.2.3 Summary of the results on the reactivity of the adsorbed nitrate species

The experimental results clearly show that the nitrate species formed upon NO/O_2 adsorption on the manganese-containing catalysts are able to oxidize the adsorbed n-decane at temperature as low as 373 K. The reactivity of the nitrates depends on the nature of the coordination site(s) – Mn^{3+} or Ti^{4+}. This conclusion is supported by the fact that the NO_3^- species formed on titania interact with the hydrocarbon at temperatures considerably higher than for the manganese-containing catalysts. Another important factor is the mode of the coordination of the NO_3^- species: the bridged and monodentate nitrates are more reactive than the bidentate ones.

During the interaction of the adsorbed hydrocarbon with the nitrates, various oxygenated hydrocarbon products (formic acid, formate species, NCO^-), CO_2 and carbonates are observed. The formation of HCOOH suggests that prior the oxidation cracking of the n-decane takes place. It should be pointed out that no nitrosyl species are detected in the spectra of the catalysts studied taken after the NO_3^--C_9H_{20} interaction. This can serve as an evidence that the nitrates are reduced to dinitrogen. The reaction path for the latter process has to include the pairing of the nitrogen atoms. The subsequent steps of this process are not clear. Ukizu et al. [65] suggested that the reduction of NO on oxide catalysts occurs through isocyanate species. Aylor et al. [93] have proposed similar reaction mechanism of the NO reduction by methane on Mn-ZSM5 catalysts, involving cyanide and nitrite species. Our

experimental results show formation of NCO^- species on the surface of the catalysts studied after heating at lower temperature. The fact that the concentration of the NCO^- species decreases with the increase in the temperature indicates that they interact further and they can be considered as possible intermediates in the dinitrogen formation.

The above results can be summarized in Fig.31, which shows the possible pathways of the SCR of NO by n-decane on the manganese-titania catalysts.

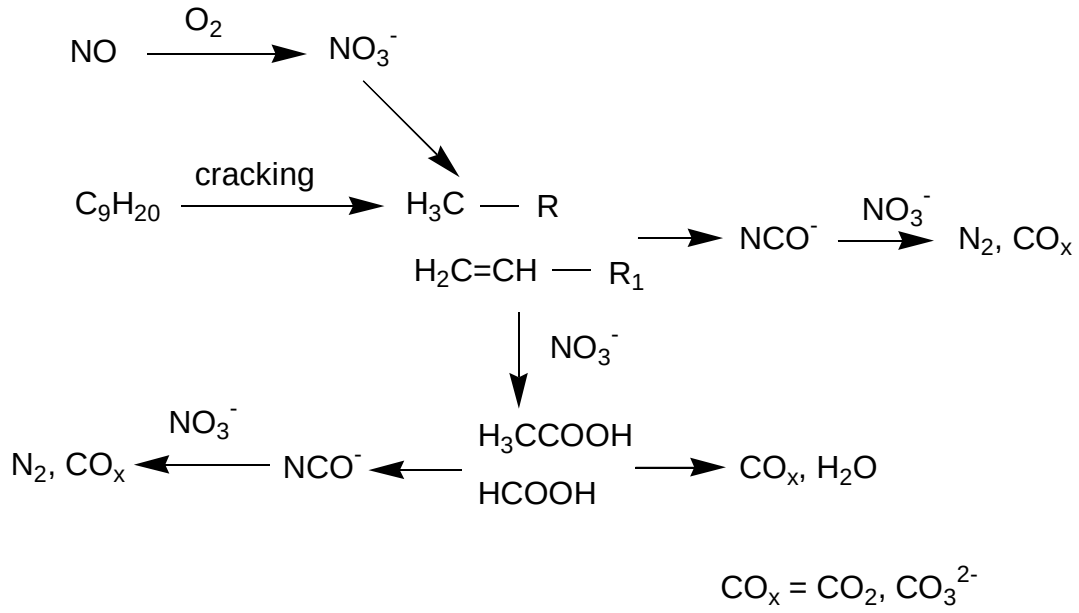

Figure 31 Possible reaction pathways of the SCR of NO by n-decane on the manganese-titania catalysts

The reaction starts with the cracking of n-decane, which is followed by partial oxidation of the cracking products by the surface nitrates to formic and acetic acids and isocyanates. The latter species can be produced also in the reduction of the

nitrates by the formate and acetate ions. The coupling of the NCO^- species with the nitrates leads to dinitrogen formation. The reaction pathway proposed assumes that the NO_3^- species participate in at least three different reaction steps. This means that a good de-NO_x catalyst should contain a high concentration of reactive NO_x species able to oxidize the hydrocarbon(s), respective oxygenated compounds and the NCO^- intermediate. This can explain the considerably lower relative changes in the concentration of the adsorbed hydrocarbon on the catalyst MnTi-I in the 373-473 K temperature interval compared to that on the ion-exchanged one. The MnTi-IE catalyst contains dispersed manganese ions and unreactive NO_x compounds coordinated to the Ti^{4+} ions are not formed. This catalyst can be promising in the selective catalytic reduction of NO by longer-chain saturated hydrocarbons.

4.CONCLUSIONS

1. A method using ion exchange for stabilization of Mn^{3+} ions on the surface of titania (anatase) has been proposed. The alkalization of manganese(II) solutions in the last stage of the ion-exchange ensures coverage by manganese(III) oxide phase, which corresponds to a monolayer. The localization of the Mn^{3+} ions deposited on the surface of titania and their coordination has been determined. The adsorption of CO at room temperature reveals that there are no exposed coordinatively unsaturated Ti^{4+} sites on the surface of the catalyst.
2. The nature of the NO_x species, their stability and the mechanisms of their formation on the catalysts studied have been investigated. The adsorption of NO is reactive leading to disproportionation of NO to anionic nitrosyl, NO^- and NO_2. The absence of Ti^{4+}–NO^- species on the surface of the ion-exchanged catalyst confirms the high dispersion of the Mn(III) on the support in agreement with the results of CO adsorption.
3. Upon coadsorption of NO and O_2 at room temperature on the samples studied, various kinds of surface nitrates are observed differing in the mode of their coordination. No anionic nitrosyls are present. The nitrates on the manganese-containing samples are characterized by significantly lower thermal stability than that in the case of the pure support, anatase.
4. The difference in the thermal stability of the nitrates affects their reactivity toward the reducer (n-decane) in the reaction of SCR of NO. A direct

evidence is obtained for the importance of the bridged and monodentate nitrates for the activation of the adsorbed hydrocarbon. The monodentate and bridged nitrates formed on the catalysts studied are able to oxidize the adsorbed hydrocarbon at temperature as low as 373 K.

5. Formic acid, formate species, carbonates and adsorbed CO_2 are identified as products of the interaction between the adsorbed n-decane and the nitrates on the surface of manganese-titania catalysts and mechanism for their formation is proposed.
6. Formation of isocyanate species on the surface of manganese-titania catalysts is detected. It is proposed that the surface NCO^- and NO_3^- species couple leading to production of CO_2 and N_2.
7. The concentration of the reactive surface nitrates on the catalyst prepared by ion exchange is considerably higher than that on the impregnated sample. The former catalyst could be promising in the selective catalytic reduction of NO by long-chain saturated hydrocarbons.

5. REFERENCES

[1] "Sources and Control of Oxides of Nitrogen Emissions," Stationary Source Division and Motor Source Control Division, State of California, California Environmental Protection Agency Air Resources Board, August 1997

[2] V.I. Parvulescu, P.Grange, B.Delmon, "Catalytic removal of NO," *Catal. Today*, vol.46, pp.233-316, 1998

[3] http://www.suton.ac.uk/~engenvir/environment/air/acid.fomation.html

[4] Environmental Pollution Prevention Fund Regulation, Official Gazette, 18757, 17.5.1985

[5] UNITED NATIONS, "PROTOCOL TO THE 1979 CONVENTION ON LONG-RANGE TRANSBOUNDARY AIR POLLUTION CONCERNING THE CONTROL OF EMISSIONS OF NITROGEN OXIDES OR THEIR TRANSBOUNDARY FLUXES", New York and Geneva, 1995

[6] P. Fornasiero, G. Ranga Rao, J. Kaspar, F. L'Erario, and M. Graziani, "Reduction of NO by CO over Rh/CeO_2-ZrO_2 catalysts," *J. Catal*., vol.172, pp. 269-279, 1998

[7] S. Castillo, M. Moran-Pineda, R. Gomez, and T. Lopez, "RESEARCH NOTE Nonselective reduction of NO by CO under oxidizing conditions on supported rhodium sol-gel catalysts," *J.Catal*., vol.172, pp. 263-266, 1997

[8] T.Chafik, D.I.Kondarides, X.E.Verykos, "Catalytic reduction of NO by CO over rhodium catalysts 1. Adsorption and displacement characteristics investigated by *in situ* FTIR and transient-MS techniques," *J.Catal.,* vol.190, pp.446-459, 2000

[9] S. Xie, M. P. Rosynek, and J. H. Lunsford, "Catalytic reactions of NO over 0-7 mol% Ba/MgO Catalysts, I. The Direct Decomposition of NO," *J.Catal*, vol.188, pp.24-31, 1999

[10] Yun-feng Chang and Jon G. McCarty, "Decomposition of NO over [Co]-ZSM-5 zeolite: Effect of Co-adsorbed O_2," *J.Catal.*, vol.178, pp.408-413, 1998

[11] Z.Schay, L. Guczi, Zs. Koppany, I. Nagy, A. Beck, V. Samuel, M. K. Dongare, D. P. Sabde, S. G. Hegde, A.V. Ramaswamy, "Decomposition of NO over Cu-AITS-1 zeolites," *Catal.Today*, vol.54, pp.569-574, 1999

[12] V. I. Parvulescu, M. A. Centeno, P. Grange, and B. Delmon, "NO decomposition over Cu-Sm-ZSM-5 zeolites containing low-exchanged copper," *J.Catal.*, vol.191, pp.445-455, 2000

[13] E.Hums, "Is advanced SCR technology at a standstill? A provacation for the academic community and catalyst manufacturers," *Catal.Today*, vol.42, pp.23-35, 1998

[14] G.Busca, L.Lietti, G.Ramis, F.Berti, "Chemical and mechanistic aspects of the selective catalytic reduction of NO_x by ammonia over oxide catalysts: a review," *Appl.Catal. B*:, vol.18, pp.1-36, 1998

[15] T.Tabata, H. Ohtsuka, L. M. F. Sabatino, G. Bellussi, "Selective catalytic reduction of NO_x by propane on Co-loaded zeolites", *Microporous and Mesoporous Materials*, vol.21, pp. 517-524, 1998

[16] M.Iwamoto, *Proc. of Meeting Catalytic Removal Of Nitrogen Oxide, Tokyo*, 1990, p.1

[17] N.Held, A. Koning, T. Richter, L. Puppo, *SAE paper 900496,* 1990

[18] S.Sato, H.Hirabayashi, H.Yahiro, N.Mizuno, M.Iwamoto, "Iron ion-exchanged zeolite: the most active catalyst at 473 K for the selective reduction of nitrogen monoxide by ethene in oxidizing atmoshere," *Catal. Lett.,* vol.12, pp.193-200, 1992

[19] T.Torikai, H.Yahiro, N.Mizuno, M.Iwamoto, "Enhancement of catalytic activity of alumina by copper addition for selective reduction of nitrogen monoxide by ethane in oxidizing atmosphere," *Catal .Lett.*, vol.9, pp.91-96, 1991

[20] H.Hosose, H.Yahiro, N.Mizuno, M.Iwamoto, "A remarkable increment in catalytic activity of SiO_2-Al_2O_3 by copper addition for selective catalytic reduction of nitrogen monoxide by ethane in oxidizing atmosphere," *Chem. Lett.,* vol., pp.1859-1860, 1991

[21] K.A.Bethke, D.Alt, M.C.Kung, "NO reduction by hydrocarbons in an oxidizing atmosphere over transition metal-zirconium mixed oxides," *Catal .Lett., vol.25, pp.37-48, 1994*

[22] K.A.Bethke, M.C.Kung, B.Yang, M.Slah, D.Alt, C.Li, H.H.Kung, "Metal-oxide catalysts for lean NO_x reduction," *Catal. Today*, vol.26, pp.169-183, 1995

[23] M.Tabata, H.Hamada, F.Suganuma, T.Yoshinari, H.Tsushida, Y.Kintiachi, M.Sasaki, T.Yto, "Promotive effect of Sn on the catalytic activity of Al_2O_3 for the selective reduction of NO by methanol," *Catal .Lett.,* vol.25, pp.55-60, 1994

[24] J.Pasel, V.Speer, Ch.Albrecht, F.Richter, H.Papp, "Metal doped sulfated ZrO_2 as catalyst for the selective catalytic reduction (SCR) of NO with propane," *Appl.Cata.l B:,* vol. 25 (2-3), pp.105-113, 2000

[25] M.Iwamoto, *Stud. Surf. Sci. Catal*., vol.84, p.51, 1990

[26] M.Iwamoto, N. Mizuno, H. Yakiro, Proc. 10th Int. Cong. Catal. 1992, Editors: L. Guczi, F. Solymosi, P.Tetenyi, Akademia Kiado, Budapest, , part B., p.1285, 1993

[27] M. Iwamoto, M. Hamada, *Catal.Today*, vol.10, p.57, 1991

[28] Y. Li, J.N. Armor, *Appl.Catal. B:*, vol.2, p. 239, 1993

[29] Y. Li, J.N. Armor, *J.Catal*., vol.154, 1991

[30] F. Witzel, G. A. Sill, W.K. Hall, "Reaction studies of the selective catalytic reduction of NO by various hydrocarbons," *J.Catal*., vol.149, p.229-237, 1994

[31] K.Yogo, S.Tanake, M. Ihare., T .Hishiki, E. Kikuchi, *Chem.Lett*., p.1052 , 1992

[32] K. Yogo, M. Ihare, I. Terasaki, K. Kikuchi, "Selective catalytic reduction of nitric-oxide by ethene on gallium ion-exchanged ZSM-5 under oxygen rich conditions," Appl. Catal. B:, vol.2(1), pp.L1-L5,1993

[33] H. Hamada, Y. Kintaichi, M. Sasaki, T. Ito, "Selective reduction of nitrogen monoxide with propane over alumina and H-ZSM-5 zeolite-Effect of oxygen and nitrogen dioxide intermediate," *Appl.Catal*., vol.70, p. L15-L20, 1991

[34] M.Iwamoto, M. Yahiro, Y. Mine, "Excessively copper ion-exchanged ZSM-5 zeolites as highly-active catalysts for direct decomposition of nitrogen monoxide," *Chem. Lett.*, pp.213-26, 1989

[35] Y.Li, J.N.Armor, *Appl.Catal.B:,* vol.1, p. L31 , 1992

[36] H.Hamada, Y.Kintaichi, M.Sasaki, T.Ito, *Appl. Catal*., vol.64, p.L1, 1990

[37] R.Burch, S.Scire, "An investigation of the mechanism if the selective catalytic reduction of NO on various metal/ZSM-5 catalysts-reactions of H_2/NO mixtures," *Catal. Lett*., vol.27, pp.177-186, 1994

[38] Y.Kintaichi, H.Hamada, M.Sasaki, M.Tabata, T.Ito, "Selective reduction of nitrogen-oxides with hydrocarbons over solid acid catalysts in oxygen-rich atmospheres," *Catal. Lett*., vol.6, p.239-244, 1990

[39] M.Sasaki, H.Hamada, Y.Kintaichi, T.Ito, "Role of oxygen in the selective reduction of nitrogen monoxide by propane over zeolite and alumina-based catalysts," *Catal.Lett*., vol.15 p.297-304, 1992

[40] J.O.Petunchi, W.K.Hall, *Appl. Catal.,B:,* vol.2, p. L17 , 1993

[41] Y.Li, J.N.Armor, "Selective reduction of NO_x by methane on Co-ferrierites," *J.Catal*., vol.150, pp.376-387, 1994

[42] Y.Li, W.K.Hall, "Catalytic decomposition of nitric oxide over Cu-zeolites," *J.Catal*., vol.129, p. 202-215 ,1991

[43] H.Hirabayashi, H.Yakiro, N.Mizuno, M.Iwamoto, "High catalytic activity of platinium-ZSM-5 zeolite below 500 K in water-vapour for reduction of nitrogen monoxide," *Chem. Lett*., pp. 2235-2236 1992

[44] M.Shelef, "Selective catalytic reduction of NO_x with N-free reductants," *Chem.Rev*., vol.95, p.209-225, 1995

[45] B.K.Cho, "Nitric oxide reduction by hydrocarbons over Cu-ZSM-5 monolith catalysts under lean burn conditions: Steady-state kinetics," *J.Catal*., vol.142, pp.418-429, 1993

[46] C.J.Bennet, P.S.Bennet, S.E.Golunski, J.W.Hayes, R.R.Rajaram, T.J.Truex, A.P.Walker, *Appl. Catal,A:,* vol.86, pp.L1-, 1992

[47] G.P.Ansell, A.F.Diwell, S.E.Golunski, J.W.Hayes, R.R.Rajaram, T.J.Truex, A.P.Walker, "Mechanism of the lean NO_x reaction over Cu/ZSM-5," *Appl. Catal.B:*, vol.2, pp.81-100, 1993

[48] N.W.Hayes, R.W.Joyner, E.S.Shpiro, "Infrared spectroscopy studies of the mechanism of the selective reduction of NO_x over Cu-ZSM-5 catalysts," *Appl.Catal.B:*, vol.8, pp.343-363, 1996

[49] R.Burch, P.J.Millington, "Role of propene in the selective catalytic reduction of nitrogen monoxide in copper-exchanged zeolite," *Appl.Catal.B:* vol.2, pp.101-116, 1993

[50] J.L.d'Itri, W.M.H.Sachtler, "Selective reduction of nitric-oxide over Cu/ZSM-5 – The role of oxygen in suppressing catalyst deactivation by carbonaceous deposites," *Appl.Catal.B:,* vol.2, pp.L7-L15, 1993

[51] J.O.Petunchi, G.A.Sill, W.K.Hall, "Effects of selective reduction of nitric-oxide on zeolite structure," *Appl. Catal., B*: vol.2, pp.239-257, 1993

[52] Y.Li, J.N.Armor, *Appl.Catal.B:,* vol.2, p. L30, 1992

[53] Y.Li, P.J.Battavio, J.N.Armor, "Effect of water vapor on the selective reduction of NO by methane over Cobalt-exchanged ZSM-5," *J.Catal*., vol. 142, pp.561-571, 1993

[54] B.J.Adelman, T. Beutel, G.D. Lei, and W. M. H., "Mechanistic Cause of Hydrocarbon Specifity over Cu/ZSM-5 and Co/ZSM-5 Catalysts in the Selective Catalytic Reduction of NO_x", *J. Catal*., vol.158, pp. 327-335, 1996

[55] V.A.Sadykov, S.L.Baron, V.A.Mathyshak, G.M.Alibina, R.V.Bunime, A.Y.Rozovski, V.V.Lunin, E.V.Lunina, A.N.Kharlanov, A.S.Ivanova, S.A.Veniaminov, *Catal. Lett.,* vol 37, pp.157-, 1996

[56] K.I.Hadjiivanov, D.Klissurski, G.Ramis, G.Busca, "Fourier transform IR study of NO_x adsorption on a CUZSM-5 $DeNO_x$ catalyst," *Appl.Catal.B*: vol.7, pp.251, 1996

[57] M.Kantcheva, V.Bushev, D.Klissurski, "Study of the NO_2-NH_3 on a Titania (Anatase) supported vanadia catalyst," *J. Catal*., vol.145, pp.96-106, 1994

[58] M.Kantcheva, K.Hadjiivanov, D.Klissurski, *Proc. 8th Int. Symp. Heterogeneous Catal*., Varna 1996, Edited by A.Andrew etal., Sofia, 1996, p.371

[59] B.Dojonev, D.Klissurski, B.Tsyntsarski, K.Hadjiivanov, "IR spectroscopic study of NO_x adsorption and NO_x-O_2 coadsorption on Co^{2+}/SiO_2 catalysts," *J. Chem .Soc. Faraday Trans*., vol.93, pp.4055, 1997

[60] K.Yogo, S.Tanaka, M. Ihare., T .Hishiki, E. Kikuchi, "Selective reduction of NO with propane on gallium ion-exchanged zeolites," *Chem.Lett*., pp.1025-1028, 1992

[61] M.Sasaki, H.Hamada, Y.Kintaichi, T.Ito, "Role of oxygen in selective reduction of nitrogen monoxide by propane over zeolite and alumina-based catalysts," *Catal.Lett*., vol.15, pp.297-304, 1992

[62] M.Shelef, C.N.Montreuil, H.W.Jen, "NO_2 formation over Cu-ZSM-5 and the selective catalytic reduction of NO," *Catal.Lett*., vol.26, pp.277-284, 1994

[63] Y.Li, T.L.Slager, J.N.Armor, "Selective reduction of NO_x by methane on Co-ferrierites II. Catalyst characterisation," *J.Catal.,* vol.150, pp.388-399, 1994

[64] J.O.Petunchi, G.A.Sill, W.K.Hall, "Studies of the selective reduction of nitric-oxide by hydrocarbons," *Appl. Catal., B*: vol.2, pp.303-321, 1993

[65] Y.Ukisi, S.Sato, A.Abe, K.Yoshida, "Possible role of isocyanate species in NO_x reduction by hydrocarbons over copper-containing catalysts," *Appl. Catal.*., vol.2, pp.147-152, 1993

[66] Y.Ukisi, S.Sato, G.Muramatsu, K.Yoshida, "Surface isocyanate intermediate formed during the catalytic reduction of nitrogen oxide in the presence of oxygen and propylene," *Catal. Lett*., vol.11, pp.177-182, 1991

[67] A.Obuchi, A.Ogata, K.Mizuno, A.Ohi, M.Nakamura, H.Ohuchi, "Mechanism of the selective catalytic reduction of nitrogen monoxide by organic-compounds," *J. Chem. Soc., Chem. Commun.,* vol., pp.247-248, 1992

[68] R.Burch, S.Scire, "An investigation of the mechanism of the selective catalytic reduction of NO on various metal/ZSM-5 catalysts-Reactions of H_2/NO mixtures," *Catal. Lett*., vol.27 (1-2), p.177-186, 1994

[69] R.Burch, J.A.Sullivan, T.C.Walting, "Mechanistic considerations for the reduction of NO_x over Pt/Al_2O_3 and Al_2O_3 catalysts under lean-burn conditions," *Catal. Today,* vol.42, pp.13-23, 1998

[70] Y.Li, J.N.Armor, "Metal exchanged ferrierites as catalyst for the selective catalytic reduction of NO(x) with methane," *Appl.Catal.,B:* vol.3 (1), p. L1-L11, 1993

[71] C.Yokoyama, M.Misono, "Catalytic reduction of nitrogen oxides by propene in the presence of oxygen over cerium ion-exchanged zeolites 2. Mechanistic study of roles of oxygen doped metals," *J.Catal*., vol.150 (1), pp.9-17, 1994

[72] K.C.C.Khars, "Performance, selective, and mechanism in Cu-ZSM-5 lean-burn catalysts," *Appl. Catal.,B:* vol.2, pp.207-224,1993

[73] N.W.Hayes, W.Grunert, G.J.Huchings, R.W.Joiner, E.S.Shpiro, "Formation, storage and reactivity of nitrile species during the lean NO_x reaction over CU/ZSM-5 catalysts" *J.Chem. Soc., Chem. Commun.,* vol.4, pp.531-532, 1994

[74] T.Beutel, B.J.Adelman, W.M.H.Sachtler, "Potential reaction paths in NO_x reduction over Cu/ZSM-5," *Catal.Lett*., vol. 37, pp.125-130, 1996

[75] M.Iwamoto, H.Takeda, "Pulse study on reactivity of ethane adsorbed on Cu-MFI with nitrogen oxides and oxygen," *Catal. Today,* vol.27, pp.71-78, 1996

[76] M.Iwamoto, H.Yahiro, N.Mizuno, *Procedings of the Ninth International Zeolite Conference,* vol.II, pp.397-, 1992

[77] F.Witzel, G.A.Sill, W.K.Hall, in: J.Weitkam, H.G.Karge, H.Pfeifer, W.Hoderich (Eds.). Zeolites and Related Microporous Materials: State of the Art 1994, Studies in Surface Science and Catalysis, vol.84, part C, Elsevier, Amsterdam, pp. 1531-, 1994

[78] D.B.Lukyanov, G.Sill, J.L.d'Itri, W.K.Hall, "Comparison of catalyzed and homogeneous reactions of hydrocarbons for selective catalytic reduction of NO_x," *J.Catal*., vol.153, pp.265-274, 1995

[79] F.Pognant, J.Saussey, L.C.Lavalley, G.Mabillon, "In situ FT-IR study of NH_3 formation during the reduction of NO_x with propane on H/Cu-ZSM-5 in excess oxygen," *Catal. Today*, vol.29, pp.93-97, 1996

[80] T.Inui, S.Iwamoto. S.Koja, S.Shimizu, T.Hirabayshi, "Removal of nitric oxide on metallosillicate catalysts," *Catal. Today,* vol.22 (1), pp.41-57, 1994

[81] T.Inui,, in: L.Bonnevoit, S.Kaliaguin (Eds.), Zeolites: A refined Tool for Designing Catalytic sites, Studies in Surface Science and Catalysis, vol.95, Elsevier, Amsterdam, p.1523-, 1995

[82] T. Beutel , B.J.Adelman, G.D. Lei, and W. M. H. Sachtler, "Potential reaction intermediates of NO_x reduction with propane over Cu/ZSM-5," *Catal. Lett.* vol.32 (1-2), pp.83-92, 1995

[83] D.B.Lukyanov, E.A.Lombardo, G.Sill, J.L.d'Itri, W.K.Hall, *J.Catal*., vol.163, pp.447-, 1996

[84] K.Shimizu, H.Kawabata, A.Satsuma, T.Hattori, "Role of Acetate and Nitrates in the Selective Catalytic Reduction of NO by Propene over Alumina Catalyst as investigated by FTIR," *J. Phys. Chem. B*, vol.103, pp.5240-5245, 1999

[85] H.Knozinger, "Fundamental aspects of heterogeneous catalysis studied by particle beams," H.H.Brongersma and R.A.van santum (Editors), Plenum press, New York, PP.167-189, 1991

[86] J.Laane, J.R.Ohlsen, "Characterization of Nitrogen oxides by vibrational spectroscopy," *Prog.Inorganic Chem*., vol.L3, pp.465-510, 1978

[87] K.Nakamoto, *Infrared and Raman spectra of inorganic and coordination compounds*, John Wiley & Sons, New York, 1986

[88] K. I. Hadjiivanov, "Identification of Neutral and Charged N_xO_y Surface Species by IR Spectroscopy," *Catal. Rev.-Sci.Eng.,* vol.42 (1&2), pp.71-144, 2000

[89] N.Ahmetov, *Inorganic Chemsitry*, Vyshaya Schola, Moscow, 1985

[90] A.Martinez-Arias, J.Soria, J.C.Conesa, X.L.Secane, A.Arcoya, R.Cartulana, "NO reaction at the surface oxygen vacancies generated in cerium oxide," *Chem.Soc.FaradayTrans.,* vol.91(11), pp.1679-1687, 1995

[91] B.Klingerberg, M.A.Vannice, "NO adsorption and decomposition on La_2O_3 studied by DRIFTS", *Appl.Catal.B:*, vol.21, pp.19-33, 1999

[92] F.Kapteijn, L.Singoredio, M. van Drill, A.Andreini, J.Moulijn, G.Ramis, G.Busca, "Alumina-Supported Manganese Oxide Catalysts II. Surface Characterization and adsorption of ammonia and nitric oxide," *J. Catal.,* vol.150, pp.105-116, 1994

[93] A.Aylor, L.Lobree, J.Reimer, A.T.Bell, " NO adsorption, desorption, and reduction by CH_4 over Mn-ZSM-5," *J. Catal.,* vol.170, pp.390-401, 1997

[94] A.Kuznetzov, I.Vorontzov, I.Miheilkin, "v," *Russ. J. Phys. Chem.*, vol.55, pp.652-, 1981

[95] T.Ohno, F.Hatayama, Y.Toda, S.Konishi, H.Miyata, "Fourier-transform infrared studies of reduction of nitric oxide by ethylene over V_2O_5 layered on ZrO_2," 89-101 DEC 31 1994," *Appl. Catal.,B:,* vol. 5(1-2), pp.89-101, 1994

[96] A.Givan, A.Loewenschuss, "Fourier transform infrared and Raman studies on solid nitrogen dioxide: Temperature cycling of ordered, disordered, and multicomponent layers," *J. Chem. Phys.,* vol.90, pp.6135-6145, 1989

[97] T.Tanaka, T.Okuhara, M.Misono, "Intermediacy of organic nitro and nitrite surface species in selective reduction of nitrogen monoxide by propene in the presence of excess oxygen over silica-supported platinum ," *Appl. Catal.,B:,* vol.4(1), pp. L1-L91994

[98] G.Busca, V.Lorencelli, "Infrared spectroscopic identification of the species arising from reactive adsorption of carbon oxides on metal-oxide surfaces," *Mater.Chem.*, vol.7, pp.89-126, 1982

[99] K.Hadjiivanov, M.Kantcheva, V.Bushev, D.Klissurski, "Infrared spectroscopy study of the species arising during NO_2 adsorption on TiO_2 (Anatase)," *Lanqmuir,* vol.10, pp.464-471, 1994

[100] W.S.Kijlstra, D.S.Brands, E.K.Poels, A.Bliek, "Mechanism of the selective catalytic reduction of NO by NH_3 over MnO_x-Al_2O_3 I. Adsorption and desorption of the single reaction components," *J. Catal.*, vol.171, pp.208-218, 1997

[101] W.S.Kijlstra, D.S.Brands, H.I.Smit, E.K.Poels, A.Bliek, "Mechanism of the selective catalytic reduction of NO by NH_3 over MnO_x-Al_2O_3 II. Reactivity of adsorbed NH_3 and NO complexes," *J. Catal.*, vol.171, pp.219-230, 1997

[102] T.Gryzberk, J.Klinik, M.Rogoz, H.Papp, "Manganese supported catalysts for selective catalytic reduction of nitrogen oxides with ammonia Part 1 Characterization," *J. Chem. Soc. Faraday Trans.,* vol.94, pp.2843-2850, 1998

[103] A.B.Mandale, S.Badrinarayanan, "X-ray photoelectron spectroscopic studies of the semimagnetic semiconductor system $Pb_{1-x}Mn_xTe$," *J. Electr. Spec. and Rel. Phenom.,* vol.53, pp.87-95, 1990

[104] J.S.Foord, R.B.Jackman, G.C.Allen, "An X-ray photoelectron spectroscopic investigation of the oxidation of manganese," *Philosphical Mag. A,* vol.49 No.5, pp.657-663, 1984

[105] G.D.Christian, *Analytical chemistry*, PP.464-466, John Wiley & Sons, New York, 1994

[106] A.B.P.Lever, *Inorganic electronic spectroscopy (second edt.),* pp.440-451, Elsevier, Amsterdam, 1984

[107] K.I.Hadjiivanov, D.G,Klissurski, "Surface chemistry of titania (anatase) and titania-supported catalysts," *Chem.Soc.Rev.*, vol.25(1), 61-70, 1996

[108] G.Busca, J.Saussey , O.Saur, J.Lamotte, J.C.Lavalley, V.Lorencelli, "FT-IR characterization of the surface-acidity of different titanium-dioxide anatase preparations," Appl. Catal., vol.14, pp.245-260, 1985

[109] K.I.Hadjiivanov, D.G,Klissurski, G.Busca, V.Lorencelli, "Benzene ammonia coadsorption on TiO_2 (Anatase)," *J. Chem. Soc. Faraday Trans.*, vol.87, pp.175-178, 1991

[110] K.I.Hadjiivanov, A.A.Davydov, D.G,Klissurski, *Kine. Katal.*, vol.29, pp.161,1998

[111] K.I.Hadjiivanov, O.Saur, J.Lamotte, J.C.Lavalley, "FT-IR spectroscopic study of NH_3 and CO adsorption and coadsorption on TiO_2 (Anatase)," *Z.Phys.Chem.*, vol.187, pp.281-300, 1994

[112] K.I.Hadjiivanov, O.Saur, J.Lamotte, J.C.Lavalley, "FT-IR study of low-temperature CO adsorption on pure and ammonia-precovered TiO_2 (Anatase)," *Langmuir*, vol.13, pp.3374, 1997

[113] G.Busca, "The surface acidity of solid oxides and its characterization by IR spectroscopic methods," *Phys.Chem.Chem.Phys*., vol.1, pp.723-736, 1999

[114] B.Scrader, "Raman/Infrared Atlas of organic compounds," p.B3-04.VCH, Weinheim, 1989

[115] S.Holly, P.Sohar, "Absorption spectra in the infrared region," (L.Lang and W.H.Prchard, Edts), p.105, Akademiai Kiado, Budapest, 1975

[116] M.Kantcheva, E.Albano, G.Ertl, H.Knozinger, "Infrared and X-ray photoelectron-spectroscopy study of K_2CO_3/Gamma-Al_2O_3," *Appl.Catal.,* vol.8, pp.71-84, 1983

[117] G.Busca, J.Lamotte, J.C.Lavalley, V.Lorencelli, "FT-IR study of the adsorption and transformation of formaldhyde on oxide surfaces," *J. Am. Chem. Soc. Faraday Trans.*, vol.109, pp.5197-5202, 1987

[118] J.B.Goodenough, A.L.Loeb, *Phys. Rev.*, vol.98, pp.391-, 1955

[119] D.Jarosch, "Crystal-structure refinement and reflectance measurements of hausmannite, Mn_3O_4," *Miner.Petrol.*, vol.37, pp.15-23, 1987

[120] K.I.Hadjiivanov, M.M.Kantcheva, D.G. Klissurski, "IR study of CO adsorption on Cu-ZSM-5 and CuO/SiO_2 catalysts: σ and π components of the Cu^+-CO bond," *J. Chem. Soc., Faraday Trans.*, vol.92, pp.4595-4605, 1996

[121] J.Saussey, J.C.Lavalley, J.C.Bovet, *J.Chem.Soc.Faraday Trans.1*, vol.78, pp.1457, 1992

[122] J.E.Huheey, E.A.Keiter, R.L.Keiter, *Inorganic chemistry,* (Fourth Edition), p.584, Harper Collins, New York, 1993

[123] A.Glisenti, "Interaction of formic acid with Fe_2O_3 powders under different atmosphere: an XPS and FTIR study," *J.Chem.Soc.Faraday Trans.,* vol.94, p.3671-3676, 1998

[124] M.Kantcheva, V.P.Bushev, K.I.Hadjiivanov, "Nitrogen dioxide adsorption on deuteroxylated titania (Anatase)," *J. Chem. Soc. Faraday Trans.,* vol.88(20), pp.3087-3089, 1992

[125] S.J.Huang, A.B.Walters, M.A.Vannice, "Adsorption and decomposition of NO on lanthanum oxide," *J. Catal.*, vol.192, pp.29-47, 2000

[126] S.J.Huang, A.B.Walters, M.A.Vannice, "NO reduction by CH_4 over La_2O_3: temperature programmed reaction and *in situ* DRIFTS studies," *Catal. Lett.,* vol.64, pp.77-83, 2000

[127] K.Hadjiivanov, H.Knozinger, "Species Formed After NO adsorption and $NO+O_2$ Coadsorption on TiO_2: an FTIR Spectroscopic Study," *Phys. Chem. Chem. Phys*., vol.2, pp.2803-2806, 2000

[128] S.Holly, P.Sohar, "Absorption spectra in the infrared region," (L.Lang and W.H.Prchard, Edts), p.105, Akademiai Kiado, Budapest, 1975

[129] J.March, "Advanced Organic Chemistry," J.Wiley&Sons, New York, 1992, p.711

[130] C.C.Cheung, M.C.Kung, " Influence of homogeneous decane oxidation on the catalytic performance of lean NO_x catalysts," *Catal. Lett.,* vol.61, pp.131-138, 1999

[131] F.Solimosi, T.Bansagi, "Infrared spectroscopic study of the isocyanate surface complex over Cu-ZSM-5 catalysts," *J. Catal*, vol.156, pp.75-84, 1995

[132] B.Djonev, B.Tsyntsarski, D.Klissurski, K.Hadjiivanov, "IR spectroscopic study of NO_x adsorption and NO_x-O_2 coadsorption on Co^{2+}/SiO_2 catalyts ," *J.Chem. Soc. Faraday Trans.*, vol.93, pp.4055-4063, 1997

[133] S.Sumiya, H.Hong, A.Abe, N.Takezawa, K.Yoshida, "Formation and reactivity of isocyanate (NCO) species on Ag/Al_2O_3," *J.Chem. Soc. Faraday Trans.*, vol.94 (15), pp.2217-2219, 1998

[134] Y.Ukisu, T.Miyadera, A.Abe, K.Yoshida, "Infrared study of catalytic reduction of lean NO_x with alcohols over alumina-supported silver catalyst," *Catal. Lett.*, vol.39, pp.265-267, 1996

[135] T.Chafic, S.Kameoka, Y.Ukisu, T.Miyadera, "In *situ* diffuse reflectance infrared Fourier transform spectroscopy study of surface species involved in NOx reduction by ethanol over alumina-supported silver catalyst," *J. Mol. Catal. A: Chem.,* vol.136(2), pp.203-211, 1998

[136] S.Kameoka, T.Chafic, Y.Ukisu, T.Miyadera, "Role of organic nitro compounds in the selective catalytic reduction of NO_x with ethanol over different supported silver catalysts," *Catal. Lett.*, vol.51 (1-2), pp.11-14, 1998

[137] K.Hadjiivanov, H.Knozinger, B.Tsyntsarski, L.Dimitrov, "Effect of water on the reduction of NO_x with propane on Fe-ZSM-5. An FTIR mechanistic study," *Catal. Lett.*, vol.62, pp.35-40, 1999

[138] A.Satsuma, A.D.Cowan, N.W.Cant, D.L.Trimm, "FTIR studies of the origin of the deactivation during the decomposition of nitromethane on Co-ZSM-5," *J. Catal.,* vol.181, pp.165-169, 1999

[139] S.De Rossi, G.Ferrais, S.Frmoitti, E.Garone, G.Ghiotti, M.Campa, V.Indovina, "Propane dehydrogenation on Chromia/Silica and Chromia/Alumina catalyst," *J. Catal.,* vol.148, pp.36-46, 1994